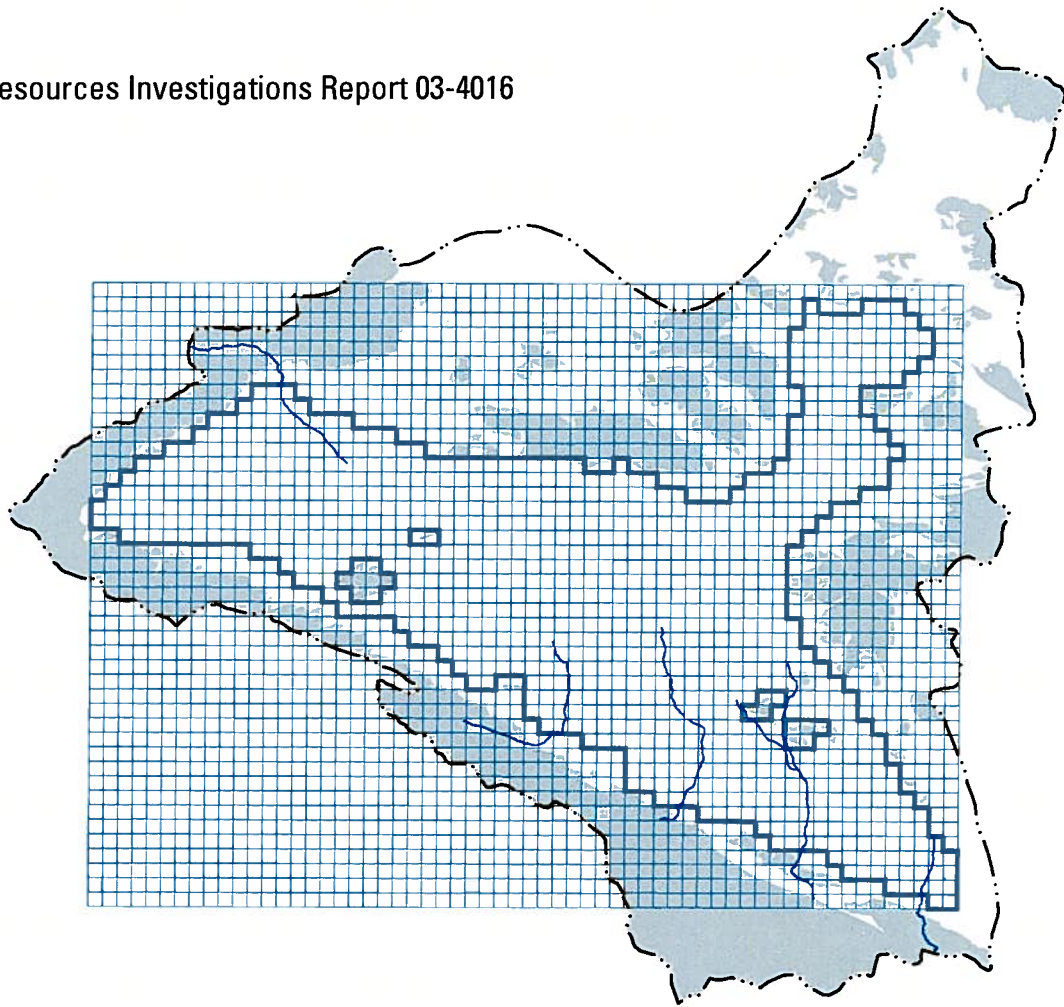


**PART 4 OF 4  
TO EXHIBIT “B”**

## Appendix C

# Simulation of Ground-Water Flow and Land Subsidence, Antelope Valley Ground-Water Basin, California

Water-Resources Investigations Report 03-4016



*Prepared in cooperation with the* **Antelope Valley Water Group**

# **Simulation of Ground-Water Flow and Land Subsidence in the Antelope Valley Ground-Water Basin, California**

By David A. Leighton and Steven P. Phillips

---

U.S. GEOLOGICAL SURVEY

Water-Resources Investigations Report 03-4016

Prepared in cooperation with the

ANTELOPE VALLEY WATER GROUP

7212-53

Sacramento, California  
2003

**U.S. DEPARTMENT OF THE INTERIOR**

GALE A. NORTON, *Secretary*

**U.S. GEOLOGICAL SURVEY**

Charles G. Groat, *Director*

Any use of trade, product, or firm names in this publication is for descriptive purposes only and does not imply endorsement by the U.S. Government.

---

For additional information write to:

District Chief  
U.S. Geological Survey  
Placer Hall—Suite 2012  
6000 J Street  
Sacramento, California 95819-6129  
<http://ca.water.usgs.gov>

Copies of this report can be purchased from:

U.S. Geological Survey  
Information Services  
Building 810  
Box 25286, Federal Center  
Denver, CO 80225-0286

# CONTENTS

Abstract .....	1
Introduction .....	2
Purpose and Scope .....	3
Description of Study Area.....	3
Acknowledgments.....	6
Geohydrology .....	6
Geologic Setting.....	6
Aquifer System and Boundaries.....	7
Pre-Development Conditions.....	8
Recharge.....	9
Discharge .....	11
Post-Development Conditions .....	11
Recharge.....	11
Discharge .....	13
Ground-Water Levels and Movement.....	17
Land Subsidence And Aquifer-system Compaction .....	22
Simulation Of Ground-Water Flow.....	25
Model Discretization and Boundaries.....	25
Model Parameters.....	27
Hydraulic Conductivity and Transmissivity .....	27
Vertical Leakance .....	28
Storage Coefficient .....	29
Preconsolidation Head .....	31
Horizontal-Flow Barriers .....	32
Model Stresses .....	32
Natural Recharge.....	32
Artificial Recharge.....	34
Irrigation-Return Flow .....	34
Treated Wastewater .....	36
Natural Discharge .....	36
Pumpage.....	36
Model Calibration .....	40
Steady-State Simulation.....	40
Transient-State Simulation.....	44
Model Results.....	52
Water Levels .....	52
Land Subsidence .....	64
Water Budget .....	67
Model Sensitivity Analysis .....	72
Limitations of the Model.....	74
Simulation of Aquifer-System Response to Pumping Scenarios .....	82
Summary .....	88
References Cited .....	89
Appendix: Water use 1992–95 .....	93

Ground Water..... 94

Surface Water..... 95

    Local Surface Water..... 95

    Imported Water ..... 95

Reclaimed Wastewater..... 95

## FIGURES

Figure 1.	Map showing location of study area, Antelope Valley, California.....	4
Figure 2.	Map showing location of faults, ground-water subbasins, line of geologic section, and approximate areal extent of lacustrine deposits in the Antelope Valley ground-water subbasin, California .....	5
Figure 3.	Generalized geologic section showing relation of lacustrine deposits to aquifers in the Lancaster and the North Muroc subbasins in the Antelope Valley ground-water basin, California.....	9
Figure 4.	Map showing ground-water levels in 1915 and location of areas of potential natural recharge, natural discharge as ground-water underflow, and alkali soils in the Antelope Valley ground-water basin, California.....	10
Figure 5.	Graph showing estimated ground-water pumpage in Antelope Valley, California, 1915–95.....	14
Figure 6.	Map showing distribution of pumpage in Antelope Valley, California.....	18
Figure 7.	Map showing ground-water levels in spring 1996 and location of area of natural discharge as ground-water underflow in the Antelope Valley ground-water basin, California .....	21
Figure 8.	Map showing measured subsidence in the Antelope Valley ground-water basin, California, 1930–92.....	23
Figure 9.	Graph showing paired water-level and land-subsidence data for sites near and east of Lancaster, Antelope Valley, California.....	24
Figure 10.	Map showing model grid and boundaries of model layers in the ground-water flow model of the Antelope Valley ground-water basin, California.....	26
Figure 11.	Map showing location of barriers to horizontal ground-water flow simulated in the ground-water flow model of the Antelope Valley ground-water basin, California.....	33
Figure 12.	Map showing location of model cells used to simulate natural recharge, recharge of imported water used for irrigation, and recharge of treated wastewater in the ground-water flow model of the Antelope Valley ground-water basin, California.....	35
Figure 13.	Map showing location of model cells used to simulate natural ground-water discharge in the ground-water flow model of the Antelope Valley ground-water basin, California.....	37
Figure 14.	Graph showing time-varying specified hydraulic head used for the north boundary of the ground-water flow model of the Antelope Valley ground-water basin, California.....	38
Figure 15.	Map showing location of wells and bench marks used to calibrate the transient-state model of the Antelope Valley ground-water basin, California.....	39
Figure 16.	Map showing location of wells used to calibrate the steady-state simulation and measured and simulated steady-state water levels from the ground-water flow model of the Antelope Valley ground-water basin, California .....	41
Figure 17.	Map showing areal distribution of natural recharge specified in the ground-water flow model of the Antelope Valley ground-water basin, California.....	43
Figure 18.	Map showing areal distribution of hydraulic conductivity for layer 1 and transmissivity for layer 2 and layer 3 in the ground-water flow model of the Antelope Valley ground-water basin, California .....	45
Figure 19.	Map showing areal distribution of vertical leakance between layers 1 and 2 and layers 2 and 3 in the ground-water flow model of the Antelope Valley ground-water basin, California.....	49
Figure 20.	Map showing areal distribution of specific yield in layer 1 of the ground-water flow model in the Antelope Valley ground-water basin, California .....	52



Figure 21. Map showing areal distribution of the storage coefficient representing the compressibility of water for layer 1 and layer 2 in the ground-water flow model of the Antelope Valley ground-water basin, California .....	54
Figure 22. Map showing areal distribution of the elastic skeletal storage coefficient for layer 1 and layer 2 in the ground-water flow model of the Antelope Valley ground-water basin, California.....	55
Figure 23. Map showing areal distribution of the inelastic skeletal storage coefficient for layer 1 and layer 2 in the ground-water flow model of the Antelope Valley ground-water basin, California.....	57
Figure 24. Map showing difference between steady-state water levels and preconsolidation head in the ground-water flow model of the Antelope Valley ground-water basin, California.....	59
Figure 25. Graphs showing measured and simulated water levels at selected wells in the Antelope Valley ground-water basin, California, 1915–95 .....	60
Figure 26. Map showing measured (1996) and simulated (1995) water levels from the ground-water flow model of the Antelope Valley ground-water basin, California.....	65
Figure 27. Graphs showing measured and simulated total land subsidence at selected bench marks in the Antelope Valley ground-water basin, California, 1915–95.....	66
Figure 28. Graphs showing simulated annual volumes of recharge, discharge, and recharge in relation to discharge in the Antelope Valley ground-water basin, California, 1915–95.....	71
Figure 29. Graph showing cumulative change in simulated ground-water storage in the Antelope Valley ground-water basin, California, 1915–95 .....	72
Figure 30. Diagram showing components of the simulated water budget for selected periods from the ground-water flow model of the Antelope Valley ground-water basin, California.....	73
Figure 31. Graphs showing simulated water levels for two pumping scenarios for the Antelope Valley ground-water basin, California, 1995–2025 .....	86
Figure 32. Graphs showing simulated land subsidence near indicated bench marks for two pumping scenarios for the Antelope Valley ground-water basin, California, 1995–2025.....	89
Figure A1. Graph showing sources of water supply in the Antelope Valley ground-water basin, California, 1947–95 .....	96
Figure A3. Graph showing wastewater use in Antelope Valley ground-water basin, California, 1975–95 .....	99

## TABLES

Table 1.	Annual treated wastewater discharged to ponds and spreading grounds, and potential annual infiltration of the treated wastewater in the Antelope Valley ground-water basin 1975–95 .....	12
Table 2.	Unit consumptive use of crops grown in Antelope Valley, California, 1952–95 .....	14
Table 3.	Crop area acreage, annual crop consumptive use, and total applied water used for irrigation in the Los Angeles County part of Antelope Valley, California, 1952–95 .....	16
Table 4.	Specific storage values used in calculating storage coefficients for layers 1 and 2 in the ground-water flow model of the Antelope Valley ground-water basin, California .....	31
Table 5.	Hydraulic characteristics of the horizontal-flow barriers simulated in the ground-water flow model of the Antelope Valley ground-water basin, California .....	34
Table 6.	Measured and simulated (layer 1) water levels for wells used to calibrate the steady-state simulation of the ground-water flow model of the Antelope Valley ground-water basin, California .....	42
Table 7.	Measured and simulated water levels at two sites with nested piezometers completed at multiple depths in the Lancaster subbasin of the Antelope Valley ground-water basin, California .....	63
Table 8.	Simulated recharge, discharge, and change in storage for the Antelope Valley ground-water basin, California, 1915–95 .....	68
Table 9.	Change in simulated water levels at the end of the transient period (1995) resulting from the sensitivity analysis of the ground-water flow model of the Antelope Valley ground-water basin, California .....	75
Table 10.	Change in simulated land subsidence at the end of the transient period (1995) resulting from changes in selected model input parameters and stresses during the sensitivity analysis of the ground-water flow model of the Antelope Valley ground-water basin, California .....	80
Table A1.	Water-use information for public water suppliers in Antelope Valley, California, by water-supply sources, 1992–95 .....	100
Table A2.	Water-use information for self-supplied water users in Antelope Valley, California, by water-supply sources, 1992–95 .....	104
Table A3.	Deliveries of imported water to Antelope Valley from the California Aqueduct, 1992–95 .....	107
Table A4.	Use of reclaimed wastewater in Antelope Valley, California, 1992–95 .....	107

## CONVERSION FACTORS, VERTICAL DATUM, AND ABBREVIATIONS

### CONVERSION FACTORS

	<b>Multiply</b>	<b>By</b>	<b>To obtain</b>
	acre	0.4047	hectare
	acre-foot (acre-ft)	1,233	cubic meter
	acre-foot per year (acre-ft/yr)	1,233	cubic meter per year
	foot (ft)	0.3048	meter
	foot per day (ft/d)	0.3048	meter per day
	foot per year (ft/yr)	0.3048	meter per year
	square foot per day (ft <sup>2</sup> /d)	0.09290	square meter per day
	gallon per minute per foot [(gal/min)/ft]	0.2070	liter per second per meter
	inch (in.)	2.54	centimeter
	inch per year (in./yr)	25.4	millimeter per year
	mile (mi)	1.609	kilometer
	square mile (mi <sup>2</sup> )	259.0	hectare

Temperature in degrees Fahrenheit (°F) may be converted to degrees Celsius (°C) as follows:

$$^{\circ}\text{C} = (^{\circ}\text{F} - 32) / 1.8.$$

### Vertical Datum

**Sea level:** In this report, “sea level” refers to the National Geodetic Vertical Datum of 1929 (NGVD of 1929)—a geodetic datum derived from a general adjustment of the first-order level nets of both the United States and Canada, formerly called Sea Level Datum of 1929.

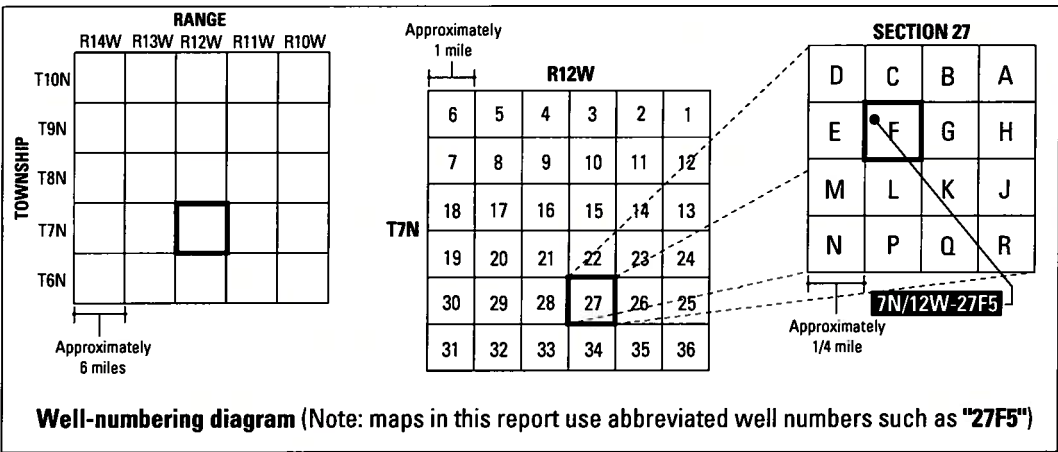
### Abbreviations

AVEK	Antelope Valley/East Kern Water Agency
AVWG	Antelope Valley Water Group
BCF	Block-Centered Flow Package
CDPW	California Department of Public Works
CDWR	California Department of Water Resources
CIMIS	California Irrigation Management Information System
HFB	Horizontal Flow Barrier Package
IBS1	Interbed Storage 1 Package
INSAR	interferometric synthetic aperture radar
MODFLOW	modular three-dimensional finite-difference ground-water flow model
SWP	state water project
SWRCB	State Water Resources Control Board (California)

UCCE	University of California Cooperative Extension
USGS	U.S. Geological Survey
d <sup>-1</sup>	per day
ft <sup>-1</sup>	per foot

# WELL-NUMBERING SYSTEM

Wells are identified and numbered according to their location in the rectangular system for the subdivision of public lands. Identification consists of the township number, north or south; the range number, east or west; and the section number. Each section is divided into sixteen 40-acre tracts lettered consecutively (except I and O), beginning with "A" in the northeast corner of the section and progressing in a sinusoidal manner to "R" in the southeast corner. Within the 40-acre tract, wells are sequentially numbered in the order they are inventoried. The final letter refers to the base line and meridian. In California, there are three base lines and meridians; Humboldt (H), Mount Diablo (M), and San Bernardino (S). All wells in the study area are referenced to the San Bernardino base line and meridian (S). Well numbers consist of 15 characters and follow the format 007N012W27F005S. In this report, well numbers are abbreviated and written 7N/12W-27F5. Wells in the same township and range are referred to only by their section designation, 27F5. The following diagram shows how the number for well 7N/12W-27F5 is derived.



# Simulation of Ground-Water Flow and Land Subsidence in the Antelope Valley Ground-Water Basin, California

By David A. Leighton *and* Steven P. Phillips

## ABSTRACT

Antelope Valley, California, is a topographically closed basin in the western part of the Mojave Desert, about 50 miles northeast of Los Angeles. The Antelope Valley ground-water basin is about 940 square miles and is separated from the northern part of Antelope Valley by faults and low-lying hills. Prior to 1972, ground water provided more than 90 percent of the total water supply in the valley; since 1972, it has provided between 50 and 90 percent. Most ground-water pumping in the valley occurs in the Antelope Valley ground-water basin, which includes the rapidly growing cities of Lancaster and Palmdale. Ground-water-level declines of more than 200 feet in some parts of the ground-water basin have resulted in an increase in pumping lifts, reduced well efficiency, and land subsidence of more than 6 feet in some areas. Future urban growth and limits on the supply of imported water may continue to increase reliance on ground water. To better understand the ground-water flow system and to develop a tool to aid in effectively managing the water resources, a numerical model of ground-water flow and land subsidence in the Antelope Valley ground-water basin was developed using old and new geohydrologic information.

The ground-water flow system consists of three aquifers: the upper, middle, and lower aquifers. The aquifers, which were identified on the basis of the hydrologic properties, age, and depth of the unconsolidated deposits, consist of gravel, sand, silt, and clay alluvial deposits and clay and silty clay lacustrine deposits. Prior to

ground-water development in the valley, recharge was primarily the infiltration of runoff from the surrounding mountains. Ground water flowed from the recharge areas to discharge areas around the playas where it discharged either from the aquifer system as evapotranspiration or from springs. Partial barriers to horizontal ground-water flow, such as faults, have been identified in the ground-water basin. Water-level declines owing to ground-water development have eliminated the natural sources of discharge, and pumping for agricultural and urban uses have become the primary source of discharge from the ground-water system. Infiltration of return flows from agricultural irrigation has become an important source of recharge to the aquifer system.

The ground-water flow model of the basin was discretized horizontally into a grid of 43 rows and 60 columns of square cells 1 mile on a side, and vertically into three layers representing the upper, middle, and lower aquifers. Faults that were thought to act as horizontal-flow barriers were simulated in the model. The model was calibrated to simulate steady-state conditions, represented by 1915 water levels and transient-state conditions during 1915–95 using water-level and subsidence data. Initial estimates of the aquifer-system properties and stresses were obtained from a previously published numerical model of the Antelope Valley ground-water basin; estimates also were obtained from recently collected hydrologic data and from results of simulations of ground-water flow and land subsidence models of the Edwards Air Force Base area. Some of these initial estimates were modified during model calibration. Ground-water pumpage for agriculture

was estimated on the basis of irrigated crop acreage and crop consumptive-use data. Pumpage for public supply, which is metered, was compiled and entered into a database used for this study. Estimated annual pumpage peaked at 395,000 acre-feet (acre-ft) in 1952 and then declined because of declining agricultural production. Recharge from irrigation-return flows was estimated to be 30 percent of agricultural pumpage; the irrigation-return flows were simulated as recharge to the regional water table 10 years following application at land surface. The annual quantity of natural recharge initially was based on estimates from previous studies. During model calibration, natural recharge was reduced from the initial estimate of 40,700 acre-ft per year (acre-ft/yr) to 30,300 acre-ft/yr.

Results of the model simulations indicate that ground-water storage declined more than 8.5 million acre-ft from 1915 to 1995. During the period of peak pumping (1949–53), pumpage averaged 363,000 acre-ft/yr, and 79 percent of the ground water withdrawn came from storage primarily from layer 1 (the upper aquifer). Water released from compaction of the aquitards accounted for about 21,600 acre-ft/yr of the ground water removed from storage. Downward leakage from layer 1 into layer 2 (the middle aquifer) accounted for most (86 percent) of the pumpage from layer 2. For the simulation period 1991–95 (a period representing current conditions when pumpage for public supply exceeded agricultural pumpage), pumpage averaged 81,700 acre-ft/yr, and most of the ground water withdrawn from layer 2 came from downward leakage from layer 1. During this period, ground water removed from storage accounted for 17 percent of the total pumpage and recharge from irrigation return accounted for about 39 percent of the total pumpage. Ground water removed from storage as a result of compaction of aquitards was reduced to about 3,800 acre-ft/yr.

The calibrated model was used to simulate the response of the aquifer to future pumping scenarios. Results of the simulation of scenario 1, for which total annual pumpage for 1996–2025

remained at the level specified for 1995, showed that water levels continued to rise (as much as 36 feet) in agricultural areas, continuing the long-term recovery from drawdown caused by historical agricultural pumpage. In the areas where pumping for public supply is concentrated, water levels continued to decline and subsidence continued in the central part of the ground-water basin. Water-level declines were largest (more than 100 feet) in the south-central part of the ground-water basin; most of the public-supply pumpage occurs in this area. As much as 1.9 feet of additional subsidence was simulated in the central part of the ground-water basin from 1996 to 2025. For scenario 2, public-supply pumpage was increased by 3.3 percent annually, and annual agricultural pumpage was increased by 75 percent more than that specified for 1995. Pumpage increases for scenario 2 resulted in significant water-level declines in the southern and northeastern part of the Lancaster subbasin; most pumping for public supply occurs in these areas. Results of this simulation showed that water levels declined more than 150 feet in the south-central part of the ground-water basin and that an additional 5 feet of subsidence was simulated in the central part of the basin.

## INTRODUCTION

Ground water is an important component of the water supply in Antelope Valley. Prior to 1972, ground water provided more than 90 percent of the total water supply in the valley. From the mid 1960s through the mid 1980s, ground-water pumpage declined owing to declines in agricultural production and, beginning in 1972, availability of imported water from the State Water Project (SWP). This steady decline in ground-water pumpage ceased in the mid 1980s due to increased urban growth and the associated demand for ground water. Since 1972, between 50 and 90 percent of the total water demand in the valley has been met using ground water (Templin and others, 1995). Ground-water-level declines have increased pumping lifts, reduced well efficiency, and caused aquifer-system compaction and more than 6 ft of land



subsidence in some areas (Ikehara and Phillips, 1994). Projected urban growth and limits on the available imported water may continue to increase the reliance on ground water and exacerbate aquifer-system compaction and land subsidence (Galloway and others, 1998).

Projections of water supply and demand indicate that the current supply may fall short of demand early in the 21st century (Kennedy/Jenks, 1995). Conjunctive use of surface and ground water, along with methods that can enhance or better use the ground-water resource, will likely become an important part of water-resource management in Antelope Valley. A thorough understanding of the ground-water system is needed to effectively manage the ground-water resource.

In the 1970s, the U.S. Geological Survey (USGS) developed a numerical ground-water flow model that was used by water managers to help make decisions regarding imported water from the SWP, reclaimed wastewater, and captured floodwater (Durbin, 1978). Since the development of this model, ground-water use in the valley has decreased substantially, and areas of ground-water withdrawals have changed from primarily agricultural areas to primarily urban areas. These changes in the state of the ground-water system emphasize the need for a better understanding of the system and the effects of water-management practices.

## **Purpose and Scope**

In 1992, the USGS began working with the Antelope Valley Water Group (AVWG) to provide information needed to manage the water resources in Antelope Valley. Results from two studies completed as part of that work are presented in reports by Templin and others (1995) and Ikehara and Phillips (1994). Templin and others (1995) describes land use, water supply and demand (1919–91), and water demand forecasts in the Antelope Valley. Ikehara and Phillips (1994) describes land subsidence and its relation to ground-water withdrawals. The results of these studies and improvements in modeling capabilities, combined with data collected since the development of the ground-water flow model of Antelope Valley in the 1970's (Durbin, 1978), have made it possible to

develop an updated numerical model of ground-water flow in Antelope Valley that includes the simulation of aquifer-system compaction and land subsidence. The model was developed to assist Antelope Valley water managers and planners.

The purpose of this report is to describe a conceptual model of the Antelope Valley ground-water basin, to describe the development and calibration of a numerical model of ground-water flow, aquifer-system compaction, and land subsidence, and to present results of simulated future pumping scenarios being considered by water managers. Available geohydrologic data and data collected during this study were used to develop the revised conceptual model of the flow system that forms the basis of the revised, updated numerical model of the Antelope Valley ground-water basin. The numerical model was calibrated and simulates ground-water flow, aquifer-system compaction, and land subsidence using water-level data for 1915–95 and land subsidence data for 1926–92. The model was used to provide insight into the geohydrology of the Antelope Valley ground-water basin, to test the sensitivity of the new model to aquifer-system parameters and hydrologic stresses, and to compare the potential effects of future pumping scenarios. Further, the results of this study can be used to guide future data-collection and aid in making informed water-management decisions.

## **Description of Study Area**

Antelope Valley, which is located in parts of Kern, Los Angeles, and San Bernardino Counties in the western part of the Mojave Desert, is about 50 mi northeast of Los Angeles ([fig. 1](#)). The valley is bounded on the south by the southeast-trending San Gabriel Mountains and on the northwest by the northeast-trending Tehachapi Mountains. The northern and eastern boundaries of the valley are formed by lower hills, ridges, and buttes. The valley is a topographically closed basin and the valley floor slopes gently toward several playas; surface-water runoff terminates in these playas. The altitudes of the valley floor, the interior hills, and the foothills range from 2,270 to 3,500 ft above sea level, and the surrounding mountains rise as high as 10,064 ft above sea level.



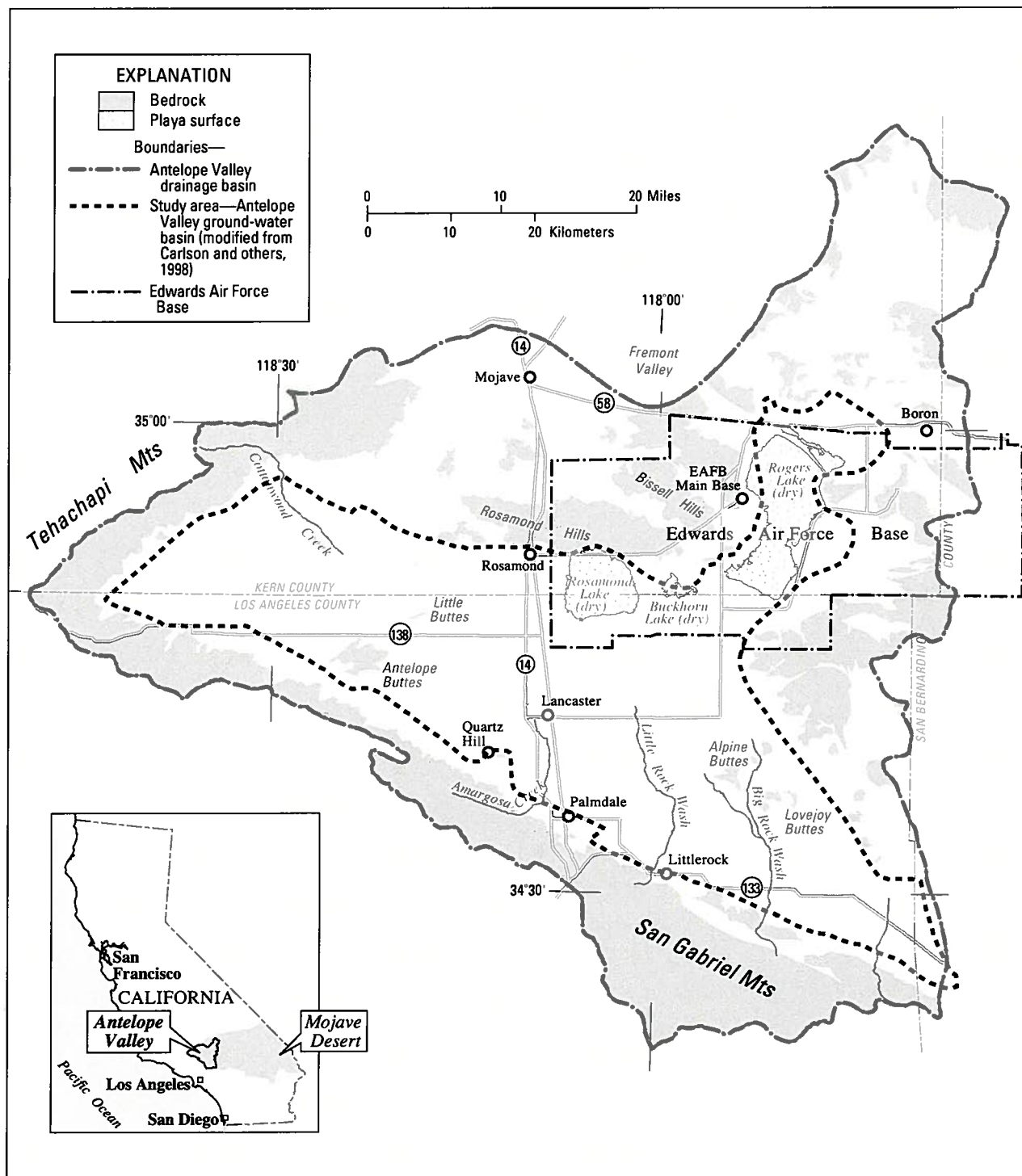


**Figure 1.** Location of study area, Antelope Valley, California.

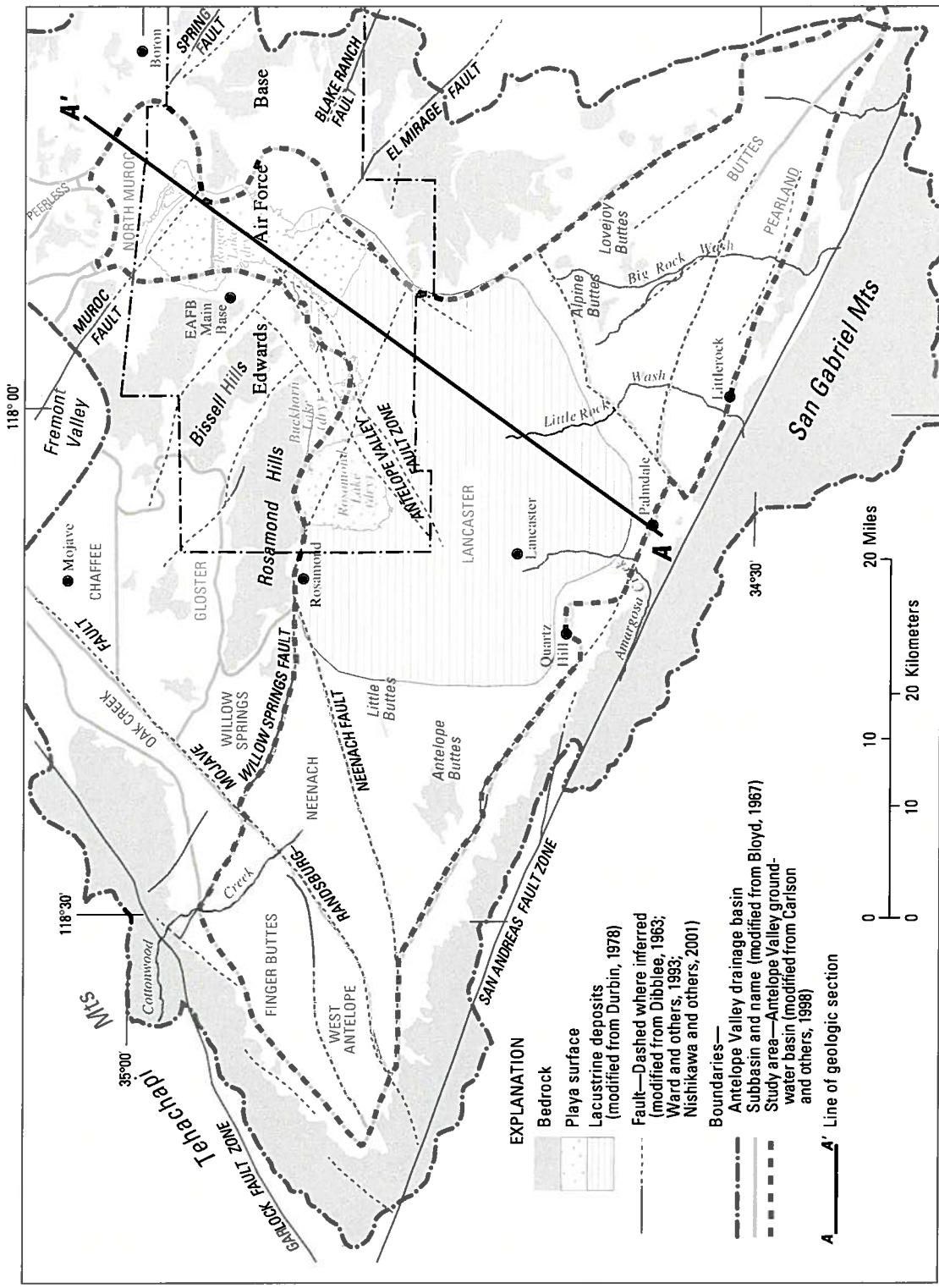


**Figure 2.** Location of faults, ground-water subbasins, line of geologic section, and approximate areal extent of lacustrine deposits in the Antelope Valley ground-water subbasin, California.

The climate in the study area is semiarid to arid. Average annual precipitation in the interior of the valley is less than 10 in. (Rantz, 1969), humidity is low, and temperatures range from below 32°F in the winter to more than 100°F in the summer. Most precipitation occurs between October and March. Land use in the valley is primarily urban, agricultural, industrial, and military. Lancaster and Palmdale are the largest cities in the valley; in 1988, they had a combined population of about 244,000 (California Department of Finance, 1998).

The Antelope Valley ground-water basin, which is the focus of this report, was defined by Carlson and others (1998) and is part of the Antelope Valley drainage basin (fig. 2). The Antelope Valley drainage basin has been divided into 12 ground-water subbasins (fig. 2) on the basis of faults, consolidated rocks, ground-water divides, and, in some cases, arbitrary boundaries (Thayer, 1946; Bloyd, 1967). The Antelope Valley ground-water basin covers about 920 mi<sup>2</sup>, and consists of seven of these subbasins; the Buttes, Finger Buttes, Lancaster, Neenach, North Muroc, Pearland, and West Antelope (fig. 2). The Lancaster subbasin is the largest and most developed of the subbasins. The Antelope Valley ground-water basin is separated from the northern part of Antelope Valley by faults and low-lying hills. Most of the urban and agricultural development and associated ground-water pumping in Antelope Valley occurs within the study area.

## Acknowledgments

The authors gratefully acknowledge the members of the Antelope Valley Water Group for their assistance during this study. They provided data, local knowledge, and advice that were important to the successful completion of the study. We also thank Loren Metzger of the USGS for his invaluable assistance in compiling the water-use data.

## GEOHYDROLOGY

The geohydrology of Antelope Valley is described in detail by previous investigators. The general geologic structure of Antelope Valley was inferred on the basis of a gravity survey by Mabey (1960). The surficial geology of the valley was mapped

and described by Dibblee (1952, 1957, 1958a, 1958b, 1959a, 1959b, 1959c, 1959d, 1960a, 1960b, 1963, 1967, 1981) and Noble (1953). Surveys by Johnson (1911) and Thompson (1929) provide information on ground-water conditions during the early ground-water development. Additional studies on the ground-water resources in Antelope Valley are documented in reports by Thayer (1946), the California Department of Water Resources (1947), the California Department of Public Works (1955), Snyder (1955), Dutcher and Worts (1963), Weir and others (1965), Bloyd (1967), Duell (1987), Londquist and others (1993), Rewis (1995), Carlson and others (1998), Carlson and Phillips (1998), and Nishikawa and others (2001). The geohydrology of Antelope Valley is summarized in the following sections, but the reader is referred to the aforementioned reports for a more detailed description.

## Geologic Setting

Underlying Antelope Valley are large sediment-filled structural depressions that are downfaulted between the Garlock and the San Andreas Fault zones. The bedrock complex in the valley forms the margins and the base of the ground-water basin and crops out in the highlands that surround the valley. This bedrock complex consists of pre-Cenozoic igneous rocks and consolidated Tertiary sedimentary rocks (Hewett, 1954; Dibblee, 1963).

In the Antelope Valley ground-water basin, a series of unconsolidated deposits of Quaternary age, some more than 5,000 ft thick (Benda and others, 1960; Mabey, 1960; R.C. Jachens, U.S. Geological Survey, written commun., 1991), overlies consolidated rocks and forms the basin fill. On the basis of the mode of deposition, Dutcher and Worts (1963) mapped these deposits as either alluvial or lacustrine. The alluvium consists of unconsolidated to moderately indurated, poorly sorted gravels, sands, silts, and clays. The older deep units within the alluvium typically are more compacted and indurated than the younger shallow units (Dutcher and Worts, 1963; Durbin, 1978). The fine-grained lacustrine deposits consist of sands, silts, and clays that accumulated in a large lake or marsh that at times covered large parts of the study area (Dibblee, 1967). These lacustrine deposits consist primarily of thick layers of blue-green silty clay, known locally as the blue clay member of the lacustrine deposits

(Dutcher and Worts, 1963), and a brown clay containing thin interbedded layers of sand and silt. Individual clay beds are as much as 100 ft thick and are interbedded with lenses of coarser material as much as 20 ft thick. The entire sequence of lacustrine deposits is as much as 300 ft thick in some areas (Dutcher and Worts, 1963). These deposits are overlain by as much as 800 ft of alluvium in the southern part of the Lancaster subbasin near Palmdale, become progressively shallower northward, and are exposed at the surface near the southern edge of Rogers Lake. Alluvial fans that were formed by the erosion of materials from the San Gabriel Mountains encroached upon an ancient lake where the lacustrine deposits were accumulating, forcing the the ancient lake, and associated lacustrine deposits, northward with time (Durbin, 1978). The areal extent of the lacustrine deposits is not well defined, but its approximate extent is shown in [figure 2](#).

Antelope Valley contains numerous faults ([fig. 2](#)), some of which act as partial barriers to ground-water flow. Most of these faults are described in reports by Mabey (1960), Dibblee (1960b, 1963), Dutcher and Worts (1963), and Ward and others (1993). More recent data and analysis have extended previously described faults and identified a previously unknown fault. Nishikawa and others (2001) suggest that the Muroc and the El Mirage Faults extend across Rogers Lake ([fig. 2](#)); the extensions of these faults were based on water-level data and results from sub-regional ground-water flow simulations. Nishikawa and others (2001) also identified a fault that trends from the northwest corner of Rosamond Lake southeast along the southern edge of Buckhorn Lake to the eastern edge of the study area ([fig. 2](#)). This fault, which may be an extension of the Willow Springs Fault, was inferred on the basis of water-level data; water levels are as much as 65 ft lower on the northeast side of the fault than on the southwest side. Large water-level differences between nearby wells in the Buttes subbasin suggest the existence of a previously unknown fault; this fault is thought to trend southeast of Lovejoy Buttes, parallel to the northeastern boundary of the Buttes subbasin ([fig. 2](#)).

## Aquifer System and Boundaries

The lateral boundaries of the Antelope Valley ground-water basin are formed, in most cases, by shallow or exposed bedrock. North of the Finger Buttes and the Neenach subbasins, the boundary of the ground-water basin is formed by the Willow Springs Fault ([fig. 2](#)). This fault is assumed to be an effective barrier to ground-water flow to and from subbasins to the north (Durbin, 1978). This assumption is supported by evidence that springs existed along the fault prior to ground-water development and, more recently, by large water-level differences over short distances across the fault (Carlson and others, 1998).

The historical conceptual model of the aquifer system in the Antelope Valley ground-water basin utilized a lithostratigraphic approach to divide the basin sediments into two major aquifers; an upper unconfined aquifer known locally as the “principal” aquifer and a “deep” aquifer overlain and confined by lacustrine deposits (Dutcher and Worts, 1963; Bloyd, 1967; Durbin, 1978). The principal aquifer was defined as the aluvial deposits that overlie the lacustrine deposits in the Antelope Valley ground-water basin south and west of Rogers Lake. The principal aquifer was assumed to be unconfined throughout its entire extent. The deep aquifer was defined as the alluvial deposits that underlie the lacustrine deposits throughout the Antelope Valley ground-water basin and the lacustrine and alluvial deposits in the Antelope Valley ground-water basin east and north of Rogers Lake. The deep aquifer was assumed confined in areas where it is overlain by the lacustrine deposits and unconfined to semiconfined in the Rogers Lake area where the principal aquifer and lacustrine deposits were assumed not to exist.

Paleomagnetic analyses of core samples collected during the drilling of monitoring site 7N/12W-27P5-8, south of Lancaster, indicate a change from normal polarity at 344 ft below land surface to reversed polarity at 450 ft below land surface (Fram and others, 2002). This reversal in polarity is interpreted as the transition from the Brunhes to the Matuyama polarity-chronostratigraphic units (John Hillhouse, U.S. Geological Survey, written commun., 1998), which occurred about 780,000 years ago (Cande and Kent, 1995). The lacustrine deposits were



encountered at a depth of about 740 ft below land surface at the monitoring site, indicating that these deposits are significantly older than 780,000 years. In contrast, the lacustrine deposits collected from less than 100 ft below land surface at Edwards Air Force Base interfinger with alluvial deposits less than 14,000 years old (Ponti, 1985). Therefore, the historical conceptual model groups alluvial deposits that are younger than 14,000 years with deposits that are older than 780,000 years in the same aquifer. In general, the alluvial deposits become more consolidated and indurated (hardened) with age, which decreases the ability of the aquifer material to transmit and store water. Because the hydraulic properties of the alluvial deposits change with time, the grouping of deposits of significantly different ages into the same aquifer is probably not reasonable.

Stratigraphic, hydrologic, and water-quality data collected since the early 1990s (Londquist and others, 1993; Rewis, 1993; Metzger and others, 2002) were used in this study to redefine the conceptual model of the Antelope Valley ground-water basin. The new conceptual model utilizes a chronostratigraphic approach instead of a lithostratigraphic approach to divide the ground-water basin into an upper, middle, and lower aquifer. Lithologic and geophysical logs of wells drilled in Lancaster (Metzger and others, 2002) and at Edwards Air Force Base south of Rogers Lake (Londquist and others, 1993; Rewis, 1993) indicate that the alluvial deposits become less permeable and more indurated at approximately 1,950 and 1,550 ft above sea level. These changes in properties were assumed to represent chronostratigraphic boundaries and were used to divide the ground-water basin into the three aquifers. The upper aquifer extends from the water table to an altitude of about 1,950 ft above sea level, the middle aquifer extends from 1,950 to 1,550 ft above sea level, and the lower aquifer extends from 1,550 ft above sea level to the altitude at which bedrock is encountered ([fig. 3](#)). Geophysical data are limited or nonexistent elsewhere in the basin and thus it was assumed that these changes in properties of the alluvium with depth were laterally extensive throughout the basin. The lacustrine deposits were assumed to be included in these aquifers.

The upper aquifer varies from unconfined to confined depending on the presence and vertical position of the thick lacustrine deposits within the aquifer. In the south part of the Lancaster subbasin,

from Palmdale to where Little Rock Wash crosses section A-A', the lacustrine deposits are below the upper aquifer, and the upper aquifer generally is unconfined. The upper aquifer may be locally confined in this area and in areas outside the extent of the lacustrine deposits owing to the presence of discontinuous interbedded aquitards. North of Little Rock Wash, the lacustrine deposits are present at shallower depths and are considered a part of the upper aquifer. In the northern part of the study area around Rogers Lake, the lacustrine deposits are exposed at land surface and form the upper part of the upper aquifer. In these areas where the lacustrine deposits are a part of the upper aquifer, the upper aquifer is confined below the lacustrine deposits.

In the southern part of the Lancaster subbasin, where the lacustrine deposits are deepest, the lacustrine deposits are part of the middle aquifer; but in the northern part of the subbasin, these deposits overlie the middle aquifer. Owing to the overlying lacustrine deposits and the discontinuous interbedded aquitards, the middle aquifer is assumed confined. If water levels were to decline below the confining aquitards, the middle aquifer could become unconfined in places.

The alluvium in the lower aquifer becomes increasingly consolidated and indurated with depth and, in the deepest parts of the basin, probably is able to transmit and store only small quantities of water. The lacustrine deposits overlie this aquifer except possibly in areas around Palmdale and Lancaster where the lacustrine may be partly contained within the lower aquifer. The lower aquifer is confined by the overlying lacustrine deposits and the discontinuous interbedded aquitards in the middle aquifer.

## Pre-Development Conditions

Prior to ground-water development in Antelope Valley, long-term ground-water conditions in the study area were in a state of dynamic equilibrium. That is, on a time scale of several years or decades, average annual natural recharge to the basin was balanced by average annual natural discharge, and ground-water levels generally fluctuated about long-term mean water levels that remained constant over time. Although the equilibrium of recharge and discharge was affected by dry and wet climatic cycles, the equilibrium was maintained over the long term.

## Recharge

The primary source of natural recharge to the basin is infiltration of precipitation runoff from the surrounding mountains (primarily from the San Gabriel Mountains south of the valley) in ephemeral stream channels. This recharge, defined as mountain-front recharge, generally occurs at the heads of the alluvial fans and along the stream channels near where the streams enter the valley ([fig. 4](#)). During periods of high runoff, these streams can flow onto the valley floor, which may result in some recharge along stream channels and washes. Other sources of natural recharge include direct infiltration of precipitation and lateral ground-water underflow from adjacent bedrock areas

and basins, both of which probably are small compared with mountain-front recharge. Precipitation over the valley floor generally is less than 10 in./yr (Rantz, 1969) and evapotranspiration rates [pan evaporation rate is about 114 in./yr (Bloyd, 1967)] and soil moisture requirements are high; therefore, recharge from direct infiltration of precipitation is negligible (Snyder, 1955; Durbin, 1978). Lateral ground-water flow from fractures in adjacent bedrock, from the Willow Springs subbasin south across the Willow Springs Fault, and from other areas adjacent to the study area also may recharge the basin, but the quantity of recharge from these sources is unknown and probably is negligible (Bloyd, 1967).

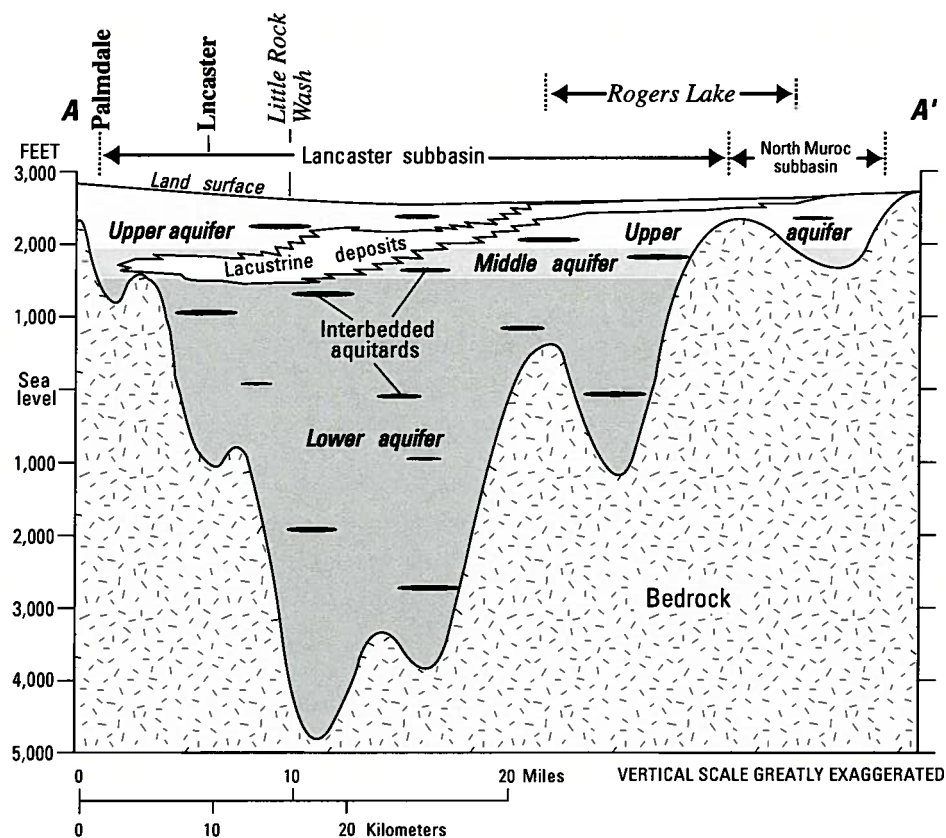


**Figure 3.** Generalized geologic section showing relation of lacustrine deposits to aquifers in the Lancaster and the North Muroc subbasins in the Antelope Valley ground-water basin, California (modified from Londquist and others, 1993). Line of section is shown on [figure 2](#).

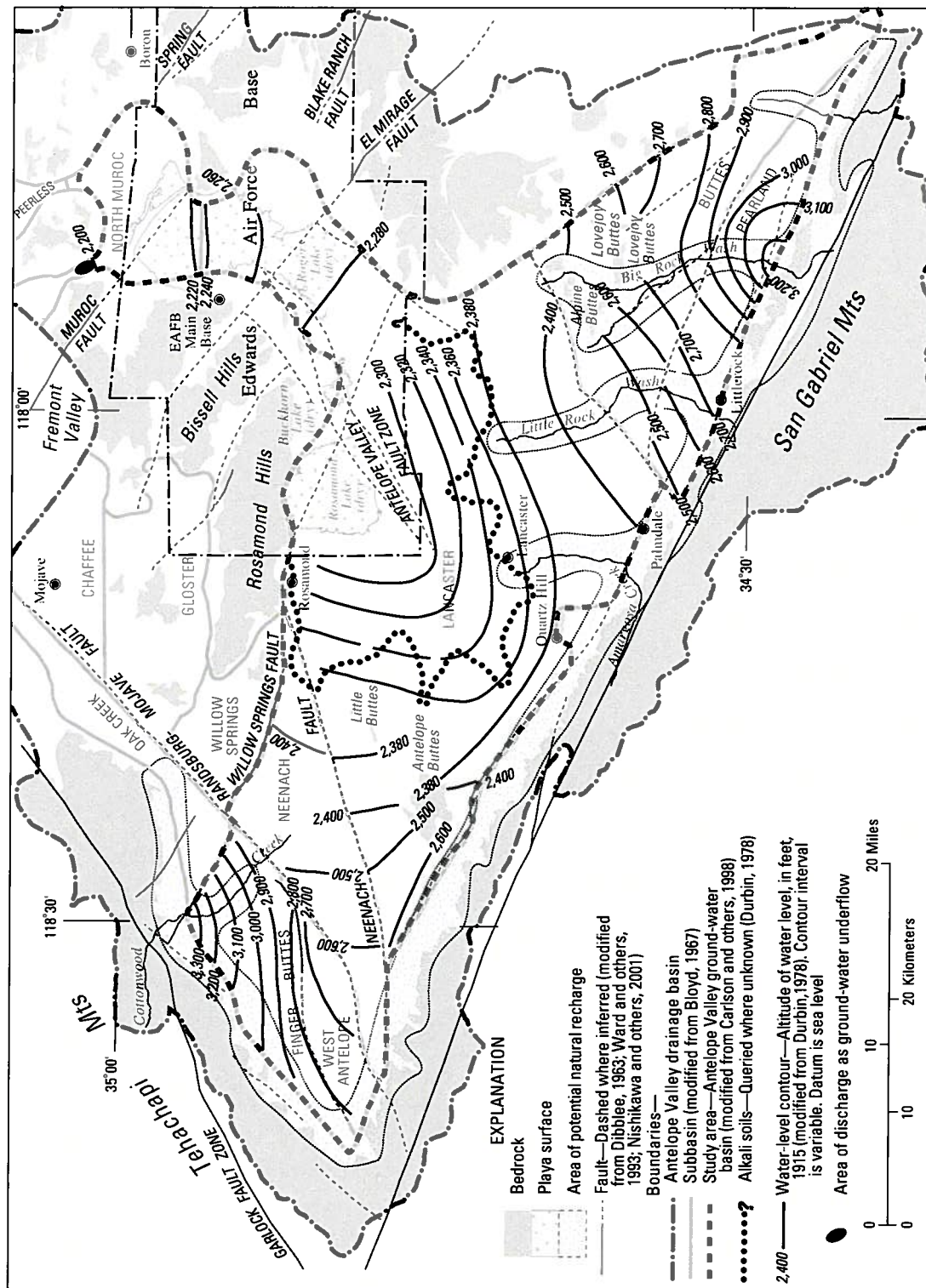


**Figure 4.** Ground-water levels in 1915 and location of areas of potential natural recharge, natural discharge as ground-water underflow, and alkali soils in the Antelope Valley ground-water basin, California.

The quantity of mountain-front recharge in Antelope Valley was estimated during previous investigations: all estimates were based on rainfall, runoff, and channel-geometry data. Londquist and others (1993) summarized these estimates and concluded that those by Bloyd (1967) and Durbin (1978) probably are the most representative of actual recharge in the valley because their estimates were based on long-term discharge and climatological data. Bloyd (1967) estimated that annual mountain-front recharge was about 58,000 acre-ft using a surface-water drainage area of the entire Antelope Valley (558 mi<sup>2</sup>). Durbin (1978) estimated that the annual mountain-front recharge was about 40,700 acre-ft, which is based on the surface-water drainage area of the Antelope Valley ground-water basin (385 mi<sup>2</sup>). Bloyd's (1967) and Durbin's (1978) estimates resulted in similar values for mountain-front recharge—104 and 106 acre-ft/mi<sup>2</sup> of surface-water drainage area, respectively. Applying Bloyd's (1967) estimate of recharge per square mile to the surface-water drainage area used by Durbin (1978) resulted in an estimated annual mountain-front recharge of about 40,040 acre-ft for the Antelope Valley ground-water basin, which is similar to Durbin's (1978) estimate of annual mountain-front recharge (40,700 acre-ft). Results from a study of the infiltration of surface runoff in the Mojave River Basin (Izbicki and others, 1995), which is immediately east of Antelope Valley, indicate that recharge from surface runoff in ephemeral streams is limited in this arid environment. Izbicki and others (1995) used water-quality analyses, ground-water age-dating techniques, and ground-water flow modeling to estimate recharge. The results from Izbicki and others (1995) suggest that natural recharge in the Antelope Valley ground-water basin may be less than that estimated by Bloyd (1967) and Durbin (1978).

#### Discharge

The primary source of discharge of water from the basin prior to ground-water development was from evapotranspiration in the lower parts of the valley where the water table was within 10 ft of land surface (Lee, 1912). The pan evaporation rate in Antelope Valley is about 114 in./yr (Bloyd, 1967) and represents the upper limit of bare-soil evaporation. A large area of alkali soils ([fig. 4](#)) (Durbin, 1978) and the existence of phreatophytes in the north central part of the ground-water basin, which require saturated soil within the root

zone, indicate that the water table was near land surface at one time and that evapotranspiration was significant (Thompson, 1929). Evapotranspiration by mesquite, a common phreatophyte in the study area, ranges between 0.1 and 1.4 ft/yr, depending on areal density (Lines and Bilhorn, 1996). Durbin (1978) estimated that prior to ground-water development, discharge from the basin owing to evapotranspiration was about 39,400 acre-ft/yr; he based this estimate on a mass balance. Other types of discharge from the basin included lateral ground-water underflow and springs. Bloyd (1967) and Durbin (1978) stated that ground-water underflow occurred through a gap in the bedrock in the northwest corner of the North Muroc subbasin into the Fremont Valley Basin. Bloyd (1967) estimated that 100 to 500 acre-ft/yr and Durbin (1978) estimated that about 1,000 acre-ft/yr flowed through this gap. Discharge by springs was thought to be less than 300 acre-ft/yr (Johnson, 1911; Thompson, 1929).

#### Post-Development Conditions

Development of the ground-water resource in Antelope Valley has caused significant changes in the amount, distribution, and type of recharge and discharge. New sources of recharge include irrigation return flow and infiltration of treated wastewater, and the primary source of discharge, evapotranspiration, has been replaced by ground-water pumping.

#### Recharge

Since the development of irrigated agriculture in the Antelope Valley ground-water basin, large amounts of irrigation water have been applied to crops; much of this water may have percolated below the root zone and contributed recharge to the ground-water basin. Snyder (1955) reported that agricultural recharge probably reached the water table by the early 1950s. Durbin (1978), however, assumed that this water had not reached the water table in 1961 based on water-quality data, which indicated that the dissolved-solids concentration in ground water had not changed. He reported that the existence of layers of fine-grained material above the water table may have prevented or delayed the downward migration of this water. Durbin (1978) also reported that the concentration of dissolved solids started to increase in the 1960s, which indicated that irrigation water may have begun to reach the water



table. Rising water levels and high nitrate concentrations in areas that historically have been used for agricultural production since the mid 1970s support the assumption that infiltration of irrigation water has contributed recharge to the ground-water basin.

Infiltration of treated wastewater may also contribute recharge to the ground-water basin. The largest producers of treated wastewater in the study area are the Palmdale Water Reclamation Plant and the Lancaster Water Reclamation Plant (Templin and others, 1995). Beginning in 1975, treated wastewater has been disposed of in ponds or on spreading grounds (areas where water is spread over the land surface to evaporate or infiltrate below land surface). A small amount of the treated wastewater is reclaimed and used primarily for agriculture (Templin and others, 1995). The quantity of disposed wastewater available for infiltration and potential recharge was estimated by subtracting estimated evaporation from the quantity of treated wastewater that is disposed of in ponds or on spreading grounds (David Lambert, County Sanitation

District of Los Angeles County, written commun., 1996). Treated wastewater from the Palmdale Water Reclamation Plant is spread on approximately 60 acres of land. At the Lancaster Water Reclamation Plant, treated wastewater is disposed of in ponds that encompass about 430 acres. On the basis of a pan evaporation rate of 114 in./yr (9.5 ft/yr) for Antelope Valley (Bloyd, 1967), about 570 acre-ft/yr of the treated wastewater from the Palmdale Water Reclamation Plant and about 4,085 acre-ft/yr of the treated wastewater from the Lancaster Reclamation Plant is lost to evaporation. The annual quantity of treated wastewater discharged to spreading ponds and the estimated potential annual infiltration of wastewater in the ponds are shown in [table 1](#). Results of studies at the Lancaster Water Reclamation Plant indicate that infiltration of the ponded water probably does not reach the regional water table owing to the high clay content of the sediments (David Lambert, County Sanitation District of Los Angeles County, written commun., 1996).

**Table 1.** Annual treated wastewater discharged to ponds and spreading grounds, and potential annual infiltration of the treated wastewater in the Antelope Valley ground-water basin, 1975–95

[Discharge data from David Lambert (County Sanitation Districts of Los Angeles County, written commun., 1996). acre-ft, acre-feet. —, no data]

Year	Lancaster Water Reclamation Plant		Palmdale Water Reclamation Plant	
	Wastewater discharge (acre-ft)	Potential infiltration of wastewater (acre-ft)	Wastewater discharge (acre-ft)	Potential infiltration of wastewater (acre-ft)
1975	840	0	—	—
1976	1,280	0	—	—
1977	1,700	0	—	—
1978	2,160	0	—	—
1979	1,980	0	—	—
1980	2,170	0	—	—
1981	2,320	0	—	—
1982	2,120	0	—	—
1983	2,770	0	—	—
1984	2,590	0	1,100	530
1985	3,090	0	2,000	1,430
1986	4,210	125	2,580	2,010
1987	5,140	1,055	3,510	2,940
1988	3,660	0	3,730	3,160
1989	2,100	0	3,960	3,390
1990	2,270	0	5,440	4,870
1991	2,410	0	5,110	4,540
1992	3,400	0	6,150	5,580
1993	5,150	1,065	7,080	6,510
1994	4,980	895	7,480	6,910
1995	7,000	2,915	8,070	7,500

Mountain-front recharge is affected by climatic conditions, which have not changed significantly during the years represented by this study. On the basis of the limited data available on mountain-front recharge, we assumed that the quantity of mountain-front recharge probably has remained fairly constant over time. However, the encroachment of land development into areas where mountain-front recharge occurs may affect this source of recharge. Lateral ground-water flow from adjacent areas is being affected by changes in the water-level gradient, but the quantity of lateral flow is small and the changes in this component of natural recharge have little effect on total natural recharge in the basin.

#### Discharge

The primary form of discharge from the ground-water basin is ground-water pumpage. The use of ground water for irrigation in the Antelope Valley began in the 1800s; but, until about 1915, the quantity of ground-water pumpage was small. Beginning in 1915, the number of wells drilled in Antelope Valley increased significantly resulting in increases in annual pumpage. Historical pumpage was estimated by Snyder (1955), Durbin (1978), California Department of Water Resources (1980, 1990, and 1991), and Templin and others (1995); their estimates are presented in [figure 5](#) along with estimates calculated for this current study. The large differences in the estimates of pumpage may be due to differences in the methods used to estimate pumpage and in the area represented by the estimate. In 1919, pumpage was estimated to be about 31,000 acre-ft (California Department of Water Resources, 1980). By the early to mid 1950s, pumpage had increased to its highest levels; estimates of peak annual pumpage ranged from about 260,000 acre-ft/yr (Templin and others, 1995) to about 480,000 acre-ft/yr (California Department of Water Resource, 1980). The pumpage database developed by Templin and others (1995) underestimates the pumpage in the ground-water basin, because it does not include agricultural pumpage

estimates for the Kern County part of the study area. Increased pumping costs owing to increased pumping lifts and rising electricity costs resulted in a decline in pumpage beginning in the mid 1950s. In 1972, imported water from northern California became available further reducing the demand for ground water.

Owing to the differences and uncertainties in the previous estimates of pumpage and the incomplete record for the model period (1915–95), annual pumpage was recalculated for this study ([fig. 5](#)). The revised estimates, which were calculated using the previous estimates and the new data collected during this study, indicate that pumpage reached a high of 395,000 acre-ft in 1951 and a modern (post 1915) low of 70,600 acre-ft in 1990. Pumpage for the period 1915–51 was based on the estimates of Snyder (1955). Snyder (1955) estimated pumpage for 1924–51 using both annual power-consumption data and crop consumptive-use data for intermittent years. The estimates of pumpage from these data were nearly equal ([fig. 5](#)), and were assumed valid for this study. The pumpage for 1952–95 was calculated for this study using irrigated crop acreage data, crop consumptive-use data, and data from the pumpage database created by Templin and others (1995).

Owing to the known limitations in the agricultural component of the pumpage data in the pumpage database created by Templin and others (1995), only the public-supply data from the pumpage database presented by Templin and others (1995) were used for 1952–95 estimates presented in this study. Pumpage for public supply is metered and therefore was assumed to be well documented in the pumpage database. Data compiled from public-supply agencies support this assumption. Pumping of small quantities of ground water for domestic use occurs in the study area, but, because it was not measured, it was not included in estimates of annual pumpage.

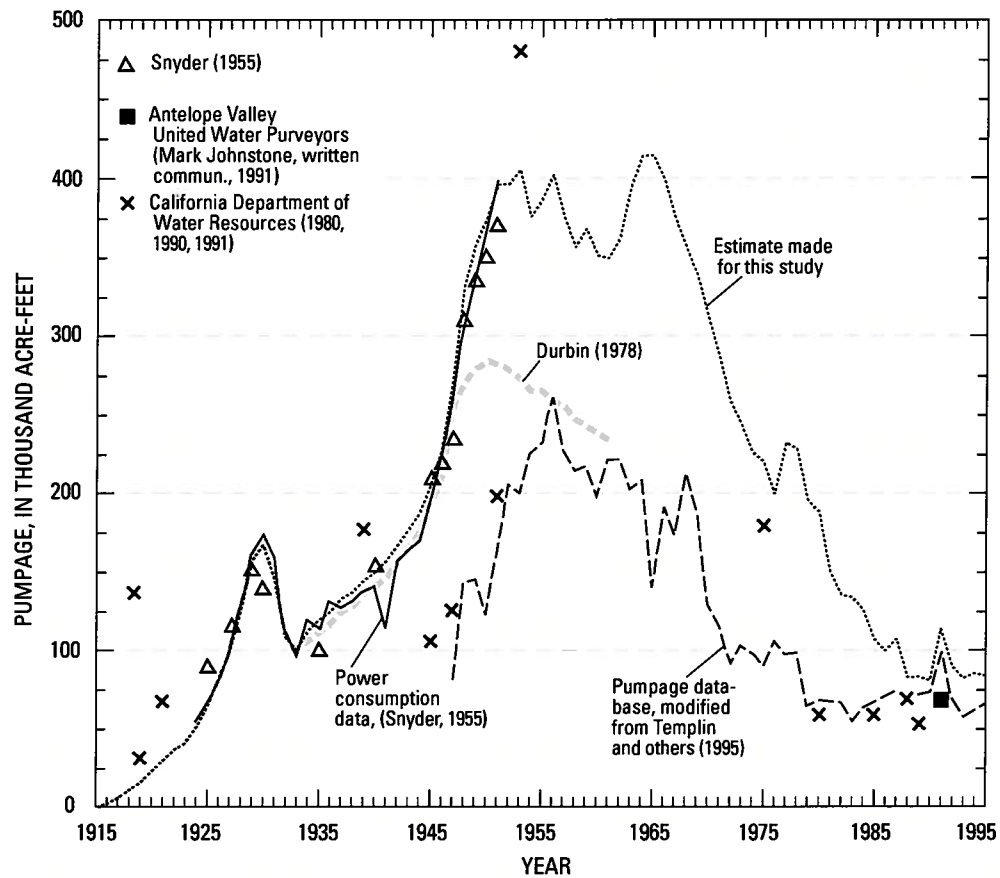


**Figure 5.** Estimated ground-water pumpage in Antelope Valley, California, 1915–95.

**Table 2.** Unit consumptive use of crops grown in Antelope Valley, California, 1952–95

[Unit consumptive use in acre-feet per acre; CDPW, California Department of Public Works; CIMIS, California Irrigation Management Information System; UCCE, University of California Cooperative Extension. —, no data]

Crop	Source			
	Snyder (1955)	CDPW (1955)	Templin and others (1995)	CIMIS/UCCE <sup>1</sup> (1994)
Alfalfa	3.37	3.6	4.3	4.8
Pasture	3.18	3.4	4.3	4.8
Orchard	2.6	2.8	2.6	—
Sugar beets	2.54	2.6	—	—
Field crops	2.1	2.1	2.2	—
Truck crops	1.92	2.0	1.5	—

<sup>1</sup> Reference evapotranspiration ( $ET_0$ )  $\times$  crop coefficient ( $K_c$ ) [ $ET_0$  from California Irrigation Management Information System (CIMIS) (2001) and  $K_c$  from University of California Cooperative Extension (1994)].

The agricultural component of annual pumpage for 1952–95 was estimated by calculating the total annual crop consumptive use from irrigated crop acreage data obtained from the Los Angeles County Agricultural Commissioner and unit consumptive-use data for the crops. Unit consumptive use is defined as the quantity of water, in acre-feet, used per acre of crop grown. Published estimates of the unit consumptive use of crops grown in Antelope Valley ([table 2](#)) are from the California Department of Public Works (1955), Snyder (1955), and Templin and others (1995). The estimates reported by Templin and others (1995) were from the California Department of Water Resources (CDWR). Estimates also were calculated for the unit consumptive use of alfalfa and pasture ([table 2](#)); these estimates were calculated using crop coefficients (University of California Cooperative Extension, 1994) and the reference evapotranspiration rate for Antelope Valley. The reference evapotranspiration rate data are from the California Irrigation Management Information System (CIMIS), a repository of climatological data used for irrigation management and operated by the CDWR.

CIMIS uses local climatological data to determine a reference evapotranspiration rate ( $ET_0$ ) for unstressed (well-watered) pasture. The unit consumptive use ( $ET_c$ ) for a given crop is calculated as the product of  $ET_0$  and the crop coefficient ( $K_c$ ) that relates the evapotranspiration rate of the given crop to a reference crop (pasture). The normal year  $ET_0$  for the ground-water basin was estimated by averaging the normal year  $ET_0$  data for Lancaster and Palmdale obtained from CIMIS. For this study, ground-water pumping for irrigation of alfalfa was assumed to occur only from March through October: the total  $ET_0$  for these months in a normal year is 4.8 ft. The University of California Cooperative Extension (1994) reports that the  $K_c$  for alfalfa ranges from 0.4 to 1.2, depending on the stage of growth, but that some researchers recommend using a  $K_c$  value of 1.0 for alfalfa. A  $K_c$  value of 1.0 was used for this study, which resulted in a unit consumptive use of 4.8 ft, which was the same as that for pasture.

The  $ET_c$  values for orchard, sugar beets, and field crops are consistent among the sources shown in [table 2](#). The  $ET_c$  values estimated by Snyder (1955) for these crops were used to calculate the annual consumptive use of these crops for 1952–95 so that the

values were consistent with those used by Snyder (1955) to estimate agricultural pumpage for 1915–51. Because the estimates of  $ET_c$  for alfalfa and pasture are not consistent among the sources shown in [table 2](#), the annual consumptive use for alfalfa and pasture for 1952–95 was calculated using the  $ET_c$  values estimated from  $K_c$  and  $ET_0$  data. The  $ET_c$  for alfalfa and pasture (4.8 acre-ft/acre) was used to calculate annual consumptive use for 1952–95 because these values were based on the most current crop consumptive-use studies. However, annual consumptive-use estimates for alfalfa and pasture were not recalculated for 1915–51 using the current unit consumptive-use values of 4.8 acre-ft/acre because annual crop acreage data were not available for this period.

Annual crop acreage data for 1952–95 are shown in [table 3](#). Onions were assumed to be a field crop and, therefore, the  $ET_c$  for field crops reported by Snyder (1955) ([table 2](#)) was used to calculate the total annual consumptive use of onions. The total annual crop consumptive use in the study area for 1952–95 ([table 3](#)) was calculated using the following equation:

$$CU_T = (A_{alf} \times CU_{alf}) + \quad (1)$$

$$(A_{past} \times CU_{past}) + (A_{orch} \times CU_{orch}) +$$

$$(A_{beets} \times CU_{beets}) + (A_{onions} \times CU_{onions})$$

where

---

$CU_T$  is the total annual crop consumptive use [ $L^3$ ],

$A_{alf}$  is the area of irrigated alfalfa [ $L^2$ ],

$CU_{alf}$  is the unit consumptive use for alfalfa [ $L$ ],

$A_{past}$  is the area of irrigated pasture [ $L^2$ ],

$CU_{past}$  is the unit consumptive use for pasture [ $L$ ],

$A_{orch}$  is the area of irrigated orchards [ $L^2$ ],

$CU_{orch}$  is the unit consumptive use for orchards [ $L$ ],

$A_{beets}$  is the area of irrigated sugar beets [ $L^2$ ],

$CU_{beets}$  is the unit consumptive use for beets [ $L$ ],

$A_{onions}$  is the area of irrigated onions [ $L^2$ ], and

$CU_{onions}$  is the unit consumptive use for onions [ $L$ ].

---

**Table 3.** Crop area acreage, annual crop consumptive use, and total applied water used for irrigation in the Los Angeles County part of Antelope Valley, California, 1952–95

[Crop area data from Los Angeles County Agricultural Commissioner (1952–95), written commun.]

Year	Crop area, in acres					Total annual crop consumptive use, in thousand acre-feet	Total applied water, in thousand acre-feet
	Alfalfa	Orchard	Pasture	Onions	Beets		
1952	36,000	3,408	4,108	0	0	199.8	285.5
1953	36,400	3,530	4,300	0	0	202.8	289.8
1954	33,200	3,616	4,400	0	0	188.2	268.8
1955	34,800	3,830	4,060	0	0	196.0	280.0
1956	35,900	3,740	4,000	70	0	200.8	286.9
1957	34,000	2,645	3,700	140	0	185.8	265.4
1958	31,800	2,644	3,800	415	0	176.1	251.5
1959	32,600	2,716	3,800	640	0	180.7	258.2
1960	32,500	2,772	1,900	670	0	175.7	250.9
1961	32,000	2,396	1,800	50	435	171.0	244.3
1962	32,000	2,432	1,600	50	2,125	174.9	249.9
1963	36,500	2,470	1,400	90	2,150	196.3	280.5
1964	38,000	2,420	1,700	100	2,660	205.4	293.4
1965	38,000	2,384	2,000	160	1,466	203.1	290.1
1966	36,000	2,385	2,000	170	1,470	193.5	276.5
1967	34,000	2,088	2,000	0	1,660	182.6	260.9
1968	32,000	2,097	1,800	80	1,584	172.5	246.5
1969	30,000	1,838	1,500	0	1,520	160.6	229.4
1970	27,700	1,855	1,500	60	1,500	149.7	213.9
1971	25,400	1,867	1,000	0	1,500	137.3	196.1
1972	22,400	1,591	1,000	80	1,500	121.7	173.9
1973	21,400	1,590	400	240	1,220	115.0	164.3
1974	19,800	1,540	400	250	1,070	106.7	152.4
1975	19,000	1,393	400	700	1,200	103.4	147.8
1976	20,000	1,162	375	1,200	1,868	109.8	156.9
1977	23,000	1,162	375	2,500	3,700	131.6	188.0
1978	23,000	1,180	400	1,700	3,200	128.8	184.0
1979	22,800	1,219	0	1,715	2,200	124.5	177.8
1980	22,500	1,349	100	425	3,860	125.4	179.2
1981	20,000	1,015	100	977	2,775	110.2	157.5
1982	16,200	1,046	100	1,433	340	86.9	124.2
1983	13,757	1,104	200	1,810	317	76.5	109.2
1984	12,176	820	0	1,477	260	66.1	94.5
1985	10,671	852	0	1,580	0	58.6	83.8
1986	8,413	704	0	1,481	0	46.9	67.0
1987	8,895	700	0	1,497	0	49.2	70.3
1988	7,620	700	0	1,702	0	43.5	62.2
1989	6,300	800	0	1,675	0	37.6	53.7
1990	6,211	815	0	1,550	0	37.0	52.8
1991	5,768	705	0	1,690	0	34.6	49.5
1992	5,222	728	0	1,665	0	32.1	45.8
1993	5,532	738	0	1,564	0	33.4	47.7
1994	5,565	830	0	1,346	0	33.5	47.9
1995	5,480	842	0	1,669	0	33.9	48.4



The total water applied for agriculture in the Los Angeles county section of the ground-water basin (table 3) was calculated by dividing total annual crop consumptive use by irrigation efficiency. Irrigation efficiency was assumed to be 70 percent on the basis of previous studies (California Department of Public Works, 1955; Snyder, 1955), a comparison of water application rates (Orloff and others, 1989), and crop consumptive-use rates for alfalfa (University of California Cooperative Extension, 1994). The actual irrigation efficiency likely is spatially and temporally variable and controlled by several factors including irrigation practices and soil characteristics; this variability was not represented in this study. The agricultural component of annual pumpage for 1952–95 was estimated by subtracting imported water, local surface-water diversions, and reclaimed wastewater used for agriculture from the total annual water applied for agriculture.

Records of annual irrigated crop acreage and agricultural pumpage are not available for Kern County and, therefore, estimated agricultural pumpage for that part of the study area was based on the relation between land use and ground-water use for 1961 and 1987. Land-use maps and agricultural pumpage data for Los Angeles County were used to estimate the quantity of ground-water pumpage per acre of agricultural land in 1961 and 1987. This ratio of pumpage per acre of agricultural land was then applied to agricultural land-use data for Kern County to estimate agricultural pumpage for the Kern County part of the study area for those years. In both 1961 and 1987, agricultural pumpage in the Kern County part of the study area was about 18 percent of the annual agricultural pumpage in the Los Angeles County part of the study area. This relation was assumed constant for the period 1952–95.

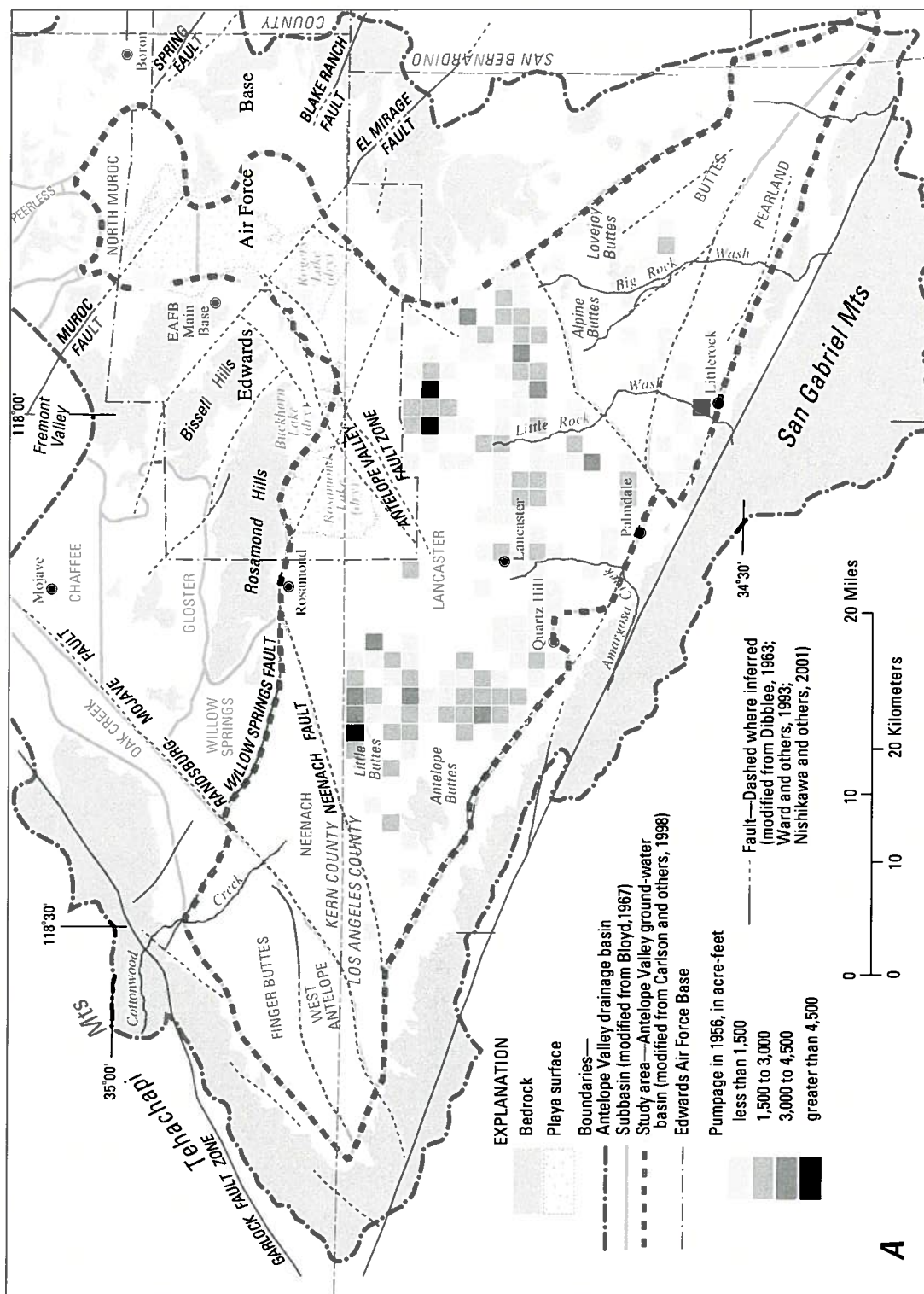
The spatial distribution of pumpage in the study area changed as agriculture declined in the late 1960s and 1970s and as urban areas grew in the 1980s. Data from the pumpage database were used to show changes in the spatial distribution of pumpage in the ground-water basin. Although the agricultural component of the pumpage database is known to be incomplete, it was assumed that the spatial distribution of pumpage in the database is representative of the spatial distribution

of actual pumpage in the basin. Prior to the 1980s, ground water was pumped primarily for agricultural use and mainly in the western and eastern parts of the Lancaster subbasin ([fig. 6A](#)). Since the 1980s, much of the pumpage has been for urban use, and the pumping centers have shifted from agricultural areas to urban areas near Rosamond, Edwards Air Force Base, Lancaster, and Palmdale ([fig. 6B](#)).

Natural discharge from evapotranspiration is greatly affected by changes in water levels caused by ground-water pumping. The water table has declined to a depth at which natural discharge from evapotranspiration is minimal. As with natural recharge, natural discharge as ground-water underflow is affected by changes in water-level gradients, but ground-water underflow is only a small component of the overall water budget for the basin.

## Ground-Water Levels and Movement

Prior to ground-water development, the depth to water in the Lancaster subbasin was less than or equal to 50 ft below land surface in most of the subbasin, and, in the areas around the playas, artesian conditions existed. In the western part of the Lancaster subbasin and in the southern part near Palmdale, the depth to water was about 200 ft below land surface. Data on the depth to water in the Buttes, Finger Buttes, Neenach, Pearland, and West Antelope subbasins are limited, especially for the upslope parts of these subbasins. Available data indicate that the depth to water in these subbasins ranged from about 50 ft below land surface in the lower part of the Neenach subbasin to about 200 ft below land surface in the higher parts of the Buttes, Pearland, and Finger Buttes subbasins. In the North Muroc subbasin, depths to water ranged from 50 to 100 ft below land surface. Water-level altitudes were highest in the Finger Buttes (3,300 ft above sea level) and Pearland (3,200 ft above sea level) subbasins ([fig. 4](#)) and lowest around the playas in the northeast part of the Lancaster subbasin (2,300 ft above sea level) and in the North Muroc subbasin (2,200 ft above sea level) ([fig. 4](#)). Around the playas, water levels were near land surface, and ground water was discharged in these areas largely by evapotranspiration and springs.



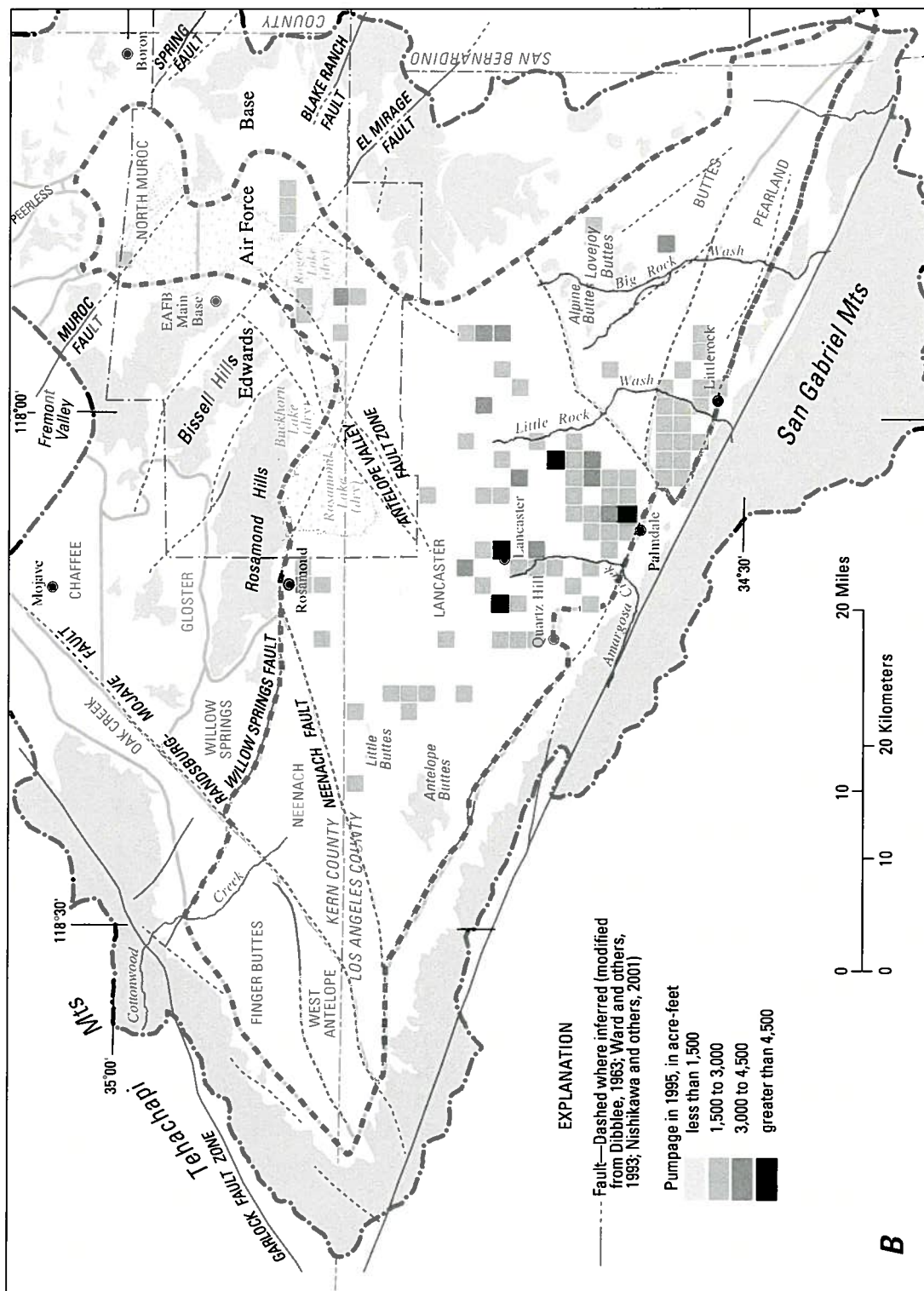


Figure 6.—Continued.



Ground water moves from areas of high water-level altitudes to areas of low water-level altitudes; therefore, the general direction of ground-water flow can be inferred from contours of water level. Ground water flowed from areas of recharge along the mountain fronts and stream channels toward areas of discharge around Rosamond, Buckhorn, and Rogers Lakes (dry) ([fig. 4](#)). In the Finger Buttes and West Antelope subbasins, ground water generally moved from northwest to southeast. In the Neenach subbasin, ground water generally moved from west to east. In the Buttes and Pearland subbasins, ground water generally moved from southeast to northwest. In the Lancaster subbasin, ground water moved from the upslope areas in the southwestern, southern, and southeastern parts of the subbasin to the discharge areas in the northern and northeastern part of the subbasin. In the North Muroc subbasin, there was a small water-level gradient toward the north where some ground water flowed into the Fremont Valley Basin.

Since the 1920s, ground-water use has exceeded estimated natural recharge. This overdraft has caused water levels to decline by more than 200 ft in some areas and by at least 100 ft in most of the study area. In agricultural areas, declining water levels began to level off in the late 1970s and, in some areas, water levels began to rise. Since 1983, water levels have risen by as much as 45 ft in areas where land use is predominately agriculture (Carlson and others, 1998). In urban areas, water levels have continued to decline.

Water-level data collected in spring 1996 (Carlson and others, 1998) represent regional water levels after more than 75 years of ground-water development in the basin ([fig. 7](#)). In the Lancaster subbasin, depth to water is more than 100 ft below land surface throughout most of the subbasin and the water table has declined to a level that has eliminated the discharge of ground water by evapotranspiration. In the eastern and western parts of the subbasin where most of the agricultural pumping has occurred, depth to water is more than 200 ft below land surface; in some areas, depth to water is more than 300 ft below land surface. In the area around Palmdale, where most of the pumping for public supply has occurred, depth to water is more than 500 ft below land surface. In the Finger

Buttes, Neenach, and West Antelope subbasins, depth to water ranges from about 150 ft to more than 350 ft below land surface. In the Buttes and Pearland subbasins, depth to water ranges from about 50 ft to about 250 ft below land surface, and in the North Muroc subbasin, depth to water ranges from about 100 ft to near 200 ft below land surface. Water-level altitudes are highest in the Neenach (2,800 ft above sea level) Pearland (2,800 ft above sea level) and Finger Buttes subbasins (data from a single data point in the Finger Buttes subbasin suggest that the water-level altitudes in this subbasin may be about 3,200 ft above sea level) (Carlson and others, 1998). The lowest water-level altitude is in the Lancaster subbasin in the area around Palmdale (2,050 ft above sea level) ([fig. 7](#)).

In the Neenach subbasin, ground water now moves to the northeast and flows into the Lancaster subbasin. In the Buttes and Pearland subbasins, ground water generally continues to move southeast to northwest. In the Lancaster subbasin, ground water flows from areas of natural recharge toward areas of low water-level altitude in the south-central part of this subbasin ([fig. 7](#)). Although not evident from the contours shown on [figure 7](#), there also is an area of low water-level altitude centered near the primary production wells at Edwards Air Force Base, near the south end of Rogers Lake (Carlson and others, 1998); ground water flows from the boundary between the Lancaster and North Muroc subbasin toward this ground-water low (Rewis, 1995). An area of high water-level altitude exists in the central part of the Lancaster subbasin southwest of Rosamond Lake ([fig. 7](#)); the high water levels may be the result of limited agricultural pumping and low-permeability alluvial material in this area. Because pumping for agriculture has been limited, little drawdown has occurred over time. Recharge from the infiltration of wastewater from the Lancaster Water Reclamation Plant discharged to ponds in the area also may be contributing to the high water-level altitudes. In the North Muroc subbasin, the water-level gradient is fairly flat, but a small amount of water may continue to flow toward the Fremont Valley Basin from the North Muroc subbasin.

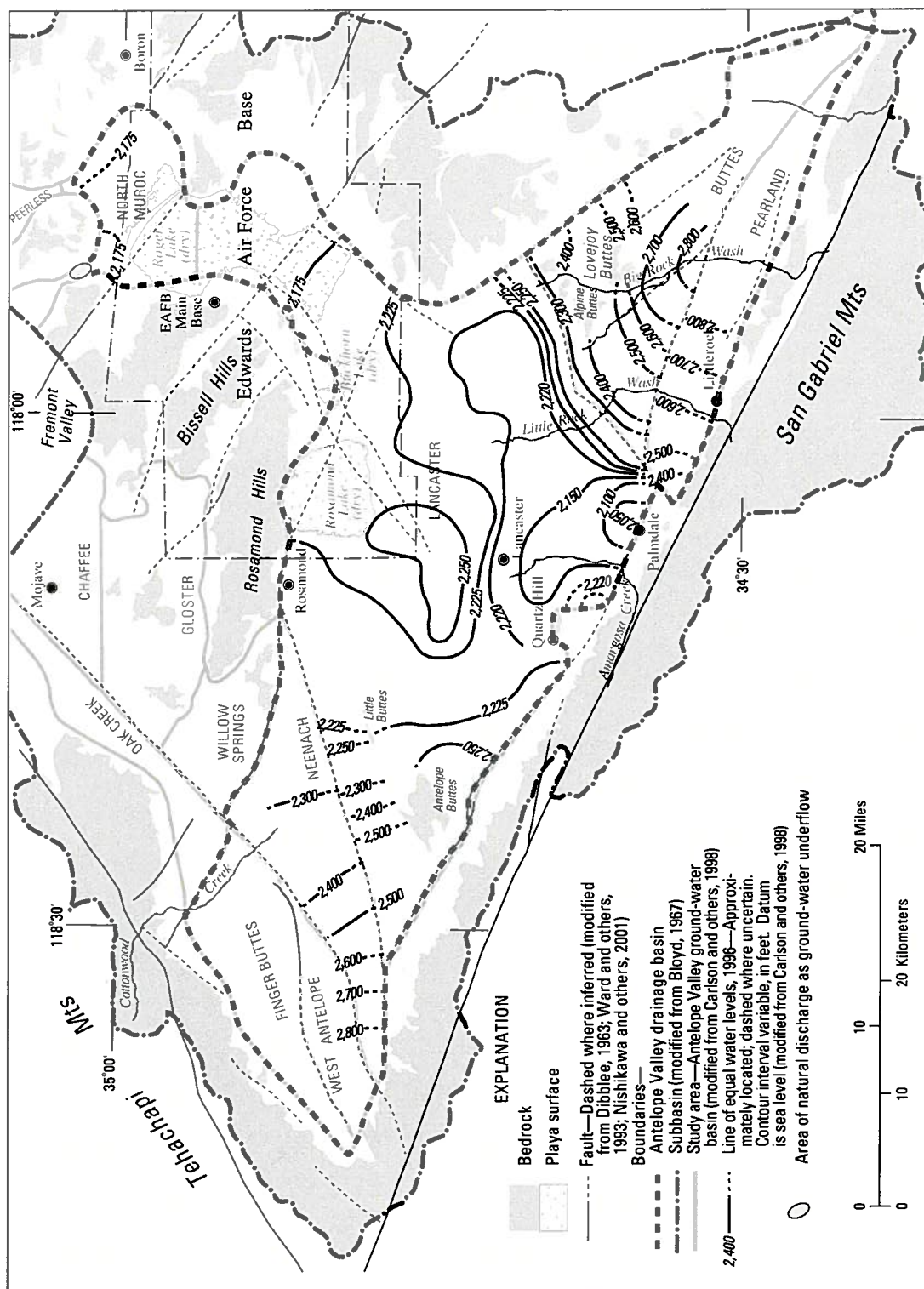


**Figure 7.** Ground-water levels in spring 1996 and location of area of natural discharge as ground-water underflow in the Antelope Valley ground-water basin, California.

## LAND SUBSIDENCE AND AQUIFER-SYSTEM COMPACTION

Land subsidence is the gradual settling or sudden sinking of the Earth's surface owing to subsurface movement of earth materials. One of the principal causes of land subsidence is the gradual compaction of susceptible aquifer systems that can accompany ground-water level declines caused by ground-water pumping (Galloway and others, 1999). Results of Global Positioning System and spirit leveling surveys indicate that as much as 6.6 ft of subsidence occurred in the valley between 1930 and 1992 (fig. 8) (Ikehara and Phillips, 1994). The spatial variability in the amount of land subsidence in Antelope Valley is affected by the magnitude of water-level declines and the distribution of compressible sediments. The large amount of subsidence measured around bench marks BM 474 and BM 1171A and between Little Buttes and Rosamond (fig. 8) is the result of water-level declines coupled with a significant thickness of compressible sediments in the aquifer system. No measurable land subsidence was detected near Palmdale, although it is an area of large water-level declines (Carlson and others, 1998). The lack of subsidence in this area indicates that compressible sediments may not exist or water levels may not have declined to the level at which inelastic (permanent) compaction of the sediments would occur. The results of a more recent study, which used satellite-based interferometric synthetic aperture radar (InSAR) to measure land subsidence during the period October 20, 1993, to December 22, 1995, indicated that locally, more than 0.16 ft of subsidence occurred and likely is still occurring in the valley (Galloway and others, 1998). Detrimental effects of land subsidence include the loss of aquifer storage, increased flooding, cracks and fissures at land surface, damage to man-made structures, and intangible economic costs.

Compaction of the aquifer system occurs when the hydraulic head or fluid pressure in compressible, fine-grained sediments declines, releasing porewater in the compressible sediments from storage (Fluid pressure has units of stress and is equal to hydraulic head times the specific weight of water). For a constant total stress on the aquifer system the associated decrease in fluid pressure is accompanied by an equivalent increase in the effective or intergranular stress on the granular matrix or skeleton of the aquifer system, resulting in aquifer-system compaction. The magnitude of the compaction is governed by the compressibility of the sediments which varies by an order of magnitude or more depending on whether the intergranular stress changes are in the elastic or inelastic range of stress for the compacting sediments. Elastic compaction is compaction that occurs when the skeletal structure of the sediments is not permanently rearranged: it can be reversed by an associated rise in hydraulic head. Inelastic compaction is compaction that occurs when there is a permanent rearrangement of the skeletal structure of the sedimentary matrix; it cannot be reversed by a rise in hydraulic head, and, therefore, results in a permanent lowering of land surface and a loss of ground-water storage capacity. The point to which hydraulic heads must decline to cause inelastic compaction in the compressible sediments is termed the preconsolidation head. When hydraulic head in the compressible sediments declines below the existing preconsolidation head, permanent compaction can occur and a new lower preconsolidation head is established. When heads fluctuate above the preconsolidation head, generally small magnitude elastic (reversible) compaction occurs. Detailed discussions of the mechanics of compaction and its relation to land subsidence are given in reports by Leake and Prudic (1991), Ikehara and Phillips (1994), Galloway and others (1998), and Galloway and others (1999).

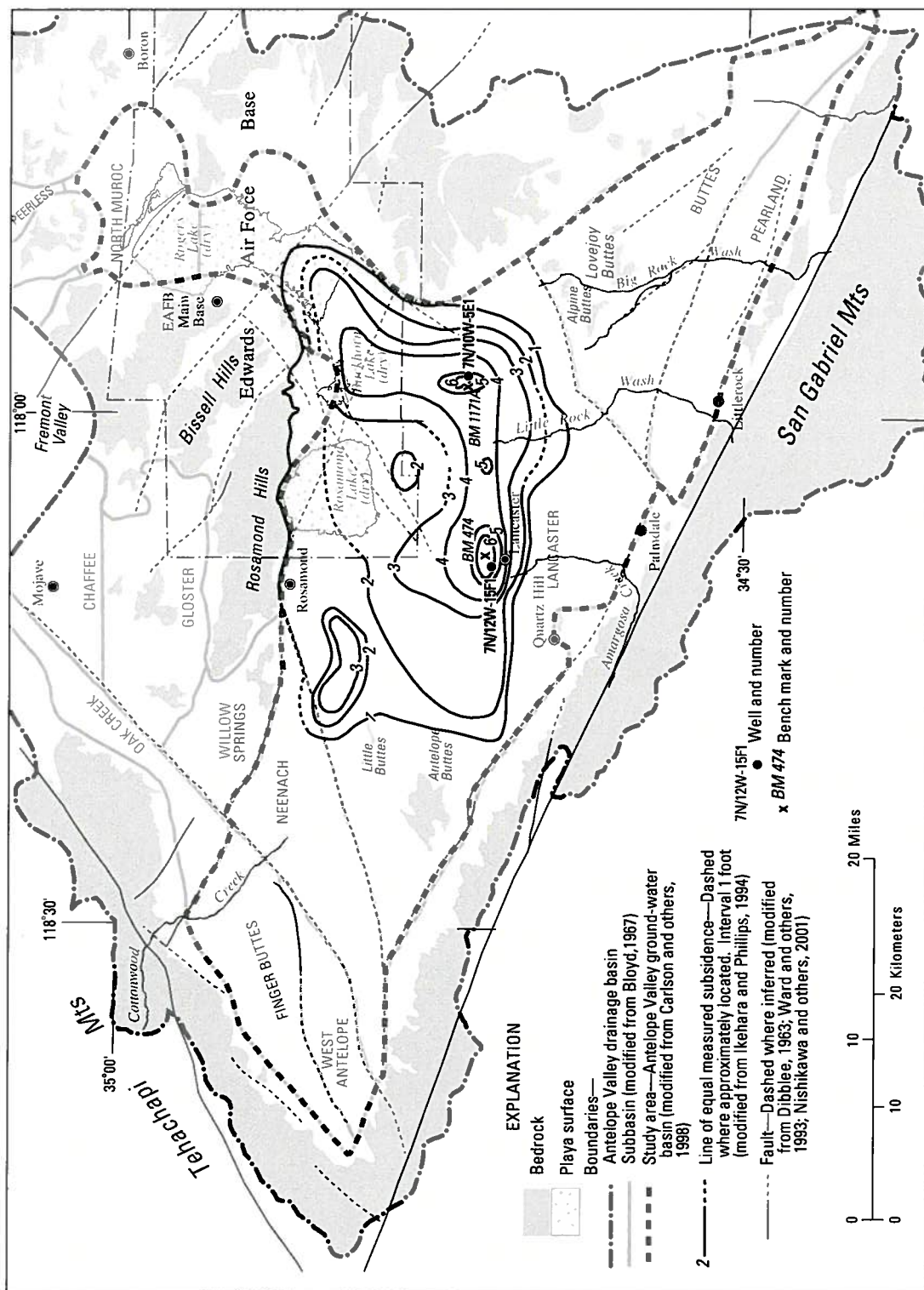


**Figure 8.** Measured subsidence in the Antelope Valley ground-water basin, California, 1930–92.



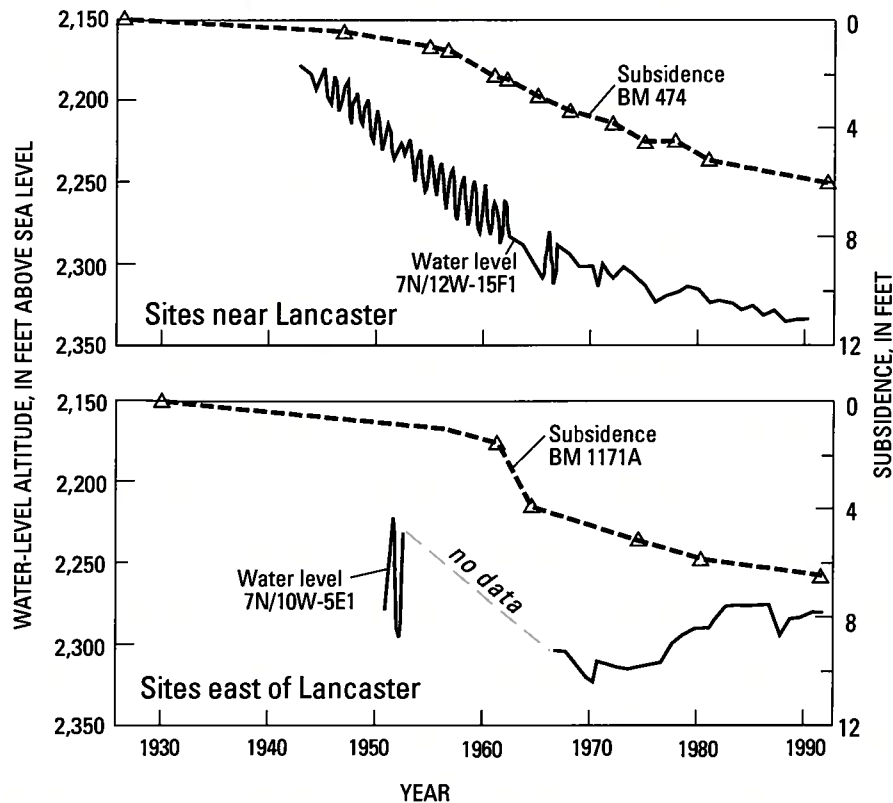


**Figure 9.** Paired water-level and land-subsidence data for sites near and east of Lancaster, Antelope Valley, California (modified from Ikehara and Phillips, 1994). Location of bench marks and wells are shown on figure 8.

As noted earlier, the ground-water system in Antelope Valley is made up of alluvial and lacustrine sedimentary deposits. The alluvial deposits consist of sand and gravel interbedded with thin, fine-grained silt and clay layers. The lacustrine deposits consist of thick clay layers interbedded with thin coarse-grained material. Compaction can occur in both the thin and the thick fine-grained silt and clay layers that form confining beds, or aquitards; little compaction, however, can occur in the sand and gravel deposits. As described by Freeze and Cherry (1979), "... the term aquitard has been coined to describe the less-permeable beds in a stratigraphic sequence. These beds may be permeable enough to transmit water in quantities that are significant in the study of regional ground-water flow, but their permeability is not sufficient to allow the completion of production wells within them." The thickness of the aquitards affects the rate and the duration of aquifer-system compaction. The thickness of the aquitard affects the rate at which the fluid pressure of the aquitard equilibrates with the fluid

pressure of the surrounding coarse-grained material; thin aquitards equilibrate faster than thick aquitards. Hydraulic heads in aquifer material surrounding the thick aquitards may recover to levels higher than preconsolidation head, but compaction can continue to occur until the hydraulic heads in the thick aquitards equilibrate with hydraulic heads in the surrounding coarse-grained deposits. This equilibration can take years to complete and is termed residual compaction. The fluid-pressure equilibration between thick or thin aquitards and the surrounding aquifer results in release from or uptake to storage in the aquitards and involves fluid-flow between the aquitards and aquifer. This flow is primarily vertical as the lateral extent of aquitards is generally much greater than their thickness.

The relation between hydraulic head, which is measured as water levels in wells, and compaction, which is typically measured as land subsidence at land surface, can be seen in [figure 9](#). The measured land subsidence at BM 474 near Lancaster is directly related to the continuous water-level decline measured in

nearby well 7N/12W-15F1. The measured land subsidence at BM 1171A east of Lancaster is related to the water-level decline measured in nearby well 7N/10W-5E1 from about 1950–70, however the continued measured land subsidence from 1970s to the early 1990s does not correspond to the measured water-level recovery in the nearby well during this same time period. The subsidence that occurred at BM 1171A from the 1970s to the early 1990s may be the result of residual compaction.

## **SIMULATION OF GROUND-WATER FLOW**

The objective of constructing a numerical ground-water flow model of the Antelope Valley ground-water basin was to gain a better understanding of the aquifer system and to develop a tool for evaluating and predicting aquifer responses to various water-management alternatives. Because land subsidence has been occurring in the Antelope Valley since the 1930s (Ikehara and Phillips, 1994; Galloway and others, 1998), a significant amount of the water being pumped in the valley may come from the compacting sediments. It is important, therefore, that a model of the valley have the capability to simulate compaction. Results of aquifer-system compaction simulations can be used to evaluate the potential for future compaction and land subsidence due to water-level declines in the valley.

The numerical model used for this study is the USGS modular three-dimensional finite-difference ground-water flow model (MODFLOW) (McDonald and Harbaugh, 1988). The basic MODFLOW code was used with the Interbed Storage 1 (IBS1) Package (Leake and Prudic, 1991) to simulate aquifer-system compaction and land subsidence and the Horizontal Flow Barrier (HFB) Package (Hsieh and Freckleton, 1993) to simulate the effect of horizontal barriers, such as faults, to ground-water flow. Ground-water levels were calculated at discrete points by solving simultaneous equations that approximate the partial differential equation for ground-water flow. The discrete points are the result of discretization of the model area into a series of layered rectangular model cells with the points (or nodes) located at the center of model cells. Land subsidence is computed at a model cell by summing the compaction simulated in each of the model layers, and is reported for the model cell in the uppermost layer.

The model can simulate ground-water levels and fluxes and aquifer-system compaction on the basis of the ability of the aquifer system to transmit water (transmissivity), its capacity to store and release water (storage coefficient), and the applied hydrologic stresses (recharge and discharge). The model, however, is only an approximation of the aquifer system being simulated and, therefore, cannot exactly duplicate or represent the actual system. Because model development requires the use of data, assumptions, and simplifications to approximate the system, the model is only as accurate as the assumptions and data used to develop the model.

### **Model Discretization and Boundaries**

The model grid consists of 43 rows and 60 columns with a total of 2,580 square cells (fig. 10). Each cell represents 1 mi<sup>2</sup> with a distance of 5,280 ft (1 mi) on a side. The aquifer system was discretized vertically into three layers. Layer 1 represents the upper aquifer and is unconfined throughout most of the ground-water basin. Around the southern part of Rogers Lake and west to Rosamond Lake, where surface clays act as a confining unit for the aquifer, layer 1 was simulated as confined or unconfined, depending on the water level. Where layer 1 is unconfined, the upper boundary of the layer is the water table. Where layer 1 is confined, the upper boundary of the layer is the bottom of the confining clay, which is 61 to 285 ft below land surface. The lower boundary of layer 1 is at an altitude of 1,950 ft above sea level. Layer 2 is confined and represents the middle aquifer, which extends from 1,950 to 1,550 ft above sea level. Layer 3 is confined and represents the lower aquifer, which extends from 1,550 to 1,000 ft above sea level. Layers 1, 2, and 3 have 921, 626, and 536 active model cells, respectively. The lacustrine deposits in each aquifer are included in the layers representing the aquifers. Alluvial material at depths below 1,000 ft above sea level was assumed to be well-indurated, impermeable, and not a significant part of the regional flow system. Where the altitude of bedrock is above the defined layer bottom, the layer bottom is equal to the altitude of bedrock. The model grid and the lateral boundaries of the model layers are shown in [figure 10](#).

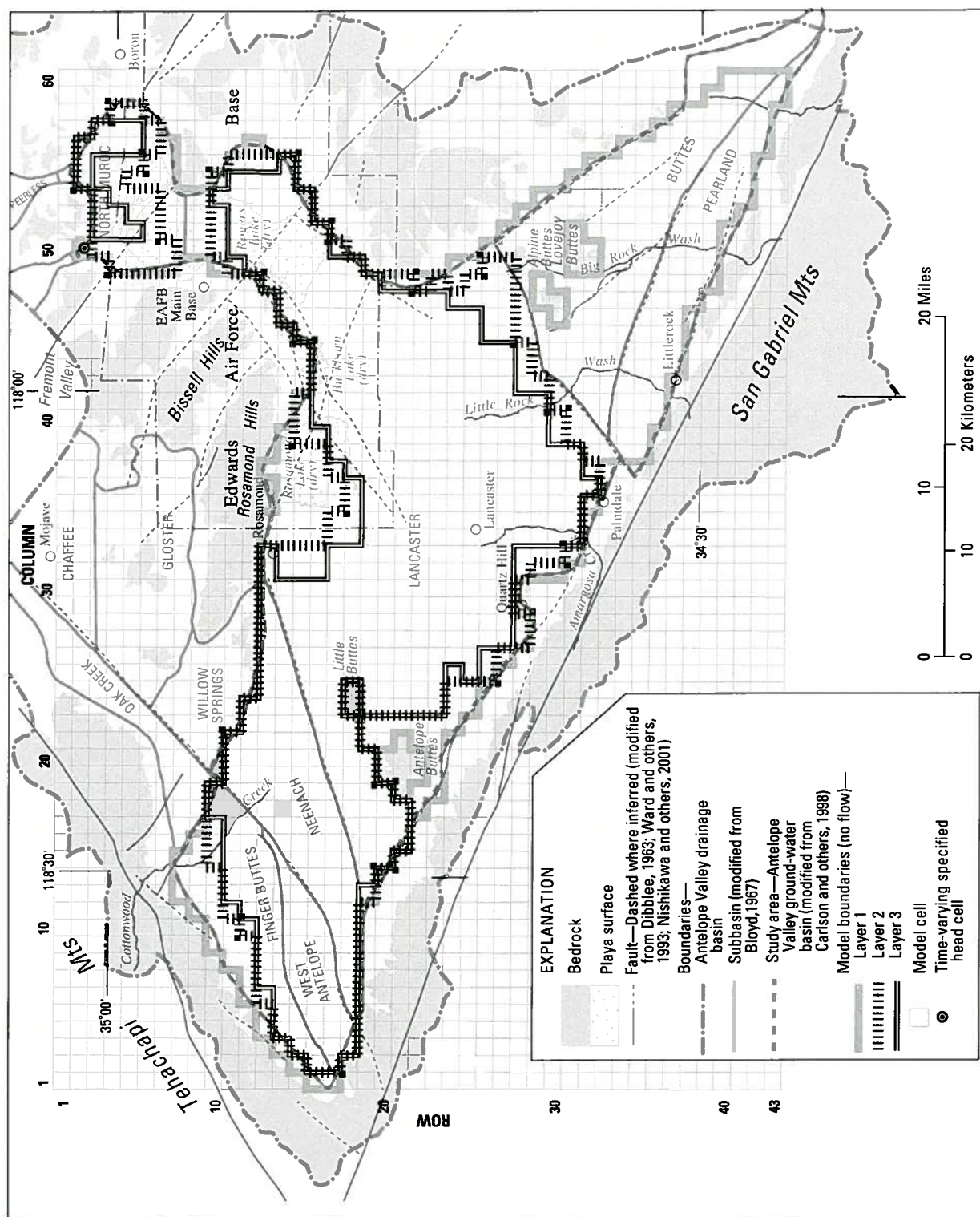


**Figure 10.** Model grid and boundaries of model layers in the ground-water flow model of the Antelope Valley ground-water basin, California.

Temporally, the model was discretized into 81 stress periods, each 1 year in length, in which specified stresses were held constant. These 1-year periods were selected to correspond to the intervals when ground-water pumpage was reported and water levels in wells in the monitoring network were measured. Water levels and aquifer-system compaction in each active model cell were output from the model at the end of each stress period.

Except for the area around Rogers Lake where layer 1 may be confined by clay, the upper boundary of the model is the water table. It was simulated as a free-surface boundary that was allowed to move vertically in response to imbalances in the inflows and outflows to the model. The lateral boundaries of the model are all no-flow boundaries, except one boundary cell representing the area north of Rogers Lake where ground water discharges into the Fremont Valley. No water enters or leaves the system at the no-flow boundaries. These lateral boundaries are located at the contact between the aquifer and bedrock or barrier faults. To simulate discharge into Fremont Valley, the model cell for layer 1 for this location was designated as a time-varying specified-head boundary ([fig. 10](#)) where water can enter or leave the system as determined by the water-level gradient between this cell and adjacent active cells. The specified head in this cell was varied for each stress period on the basis of water-level data from nearby wells (Nishikawa and others, 2001). The lower boundary of the model also is a no-flow boundary. This no-flow boundary is located where the aquifer comes into contact with bedrock or at an altitude of 1,000 ft above sea level, below which the deposits were assumed to be non-water-bearing.

## Model Parameters

Simulation of ground-water flow and fluxes and aquifer-system compaction requires specifying aquifer-system properties and stresses. Aquifer-system properties can vary considerably both horizontally and

vertically and thus cannot be precisely represented in a numerical model. The aquifer-system properties specified for each active cell in the model are estimates of the average conditions in the area represented by the cell. Similarly, stresses applied to the system (recharge and discharge) are estimates for the area represented by each cell. The initial aquifer-system properties, with the exception of the storage coefficients for confined aquifers specified for layers 1 and 2, were obtained from the Durbin (1978) model. Recharge and pumpage were estimated as described in earlier sections of this report. Selected properties and stresses were modified within reasonable limits during model calibration: the modifications were made on the basis of recently collected hydrologic data and parameters used in the ground-water flow models of the Edwards Air Force Base area (Sneed and Galloway, 2000; Nishikawa and others, 2001).

### Hydraulic Conductivity and Transmissivity

Ground-water flow within the model layers was assumed to be horizontal. Hydraulic conductivity and transmissivity are properties that, in conjunction with the horizontal hydraulic gradient, control horizontal flow of ground water. Hydraulic conductivity is a measure of the water transmitting properties of aquifer material; coarse and (or) well-sorted material have a higher hydraulic conductivity than fine and (or) poorly sorted material. Transmissivity is the product of hydraulic conductivity and saturated thickness and represents the water-transmitting properties of the saturated section of the aquifer. Hydraulic conductivity was specified for layer 1 and transmissivity was specified for layers 2 and 3, because layer 1 is unconfined throughout most of the basin and layers 2 and 3 are confined. Hydraulic conductivity was specified for layer 1 to allow the model to compute changes in the transmissivity as the saturated thickness changes in the aquifer.



Total aquifer-system transmissivity (the combined transmissivities represented by model layers 1–3, in feet squared per day) was estimated from specific-capacity data by multiplying the specific capacity (in gallons per minute per foot of drawdown) by a conversion factor of 230 (Thomasson and others, 1960). The specific-capacity data used to calculate transmissivity for this current study were from Bloyd (1967) and from more recent data from wells owned by the Los Angeles County Department of Public Works (James Hong, Los Angeles County Department of Public Works, Waterworks and Sewer Maintenance Division, written commun., 1997). The current estimates of transmissivity were consistent with those used in the Durbin (1978) model, which were obtained using data from Bloyd (1967). Transmissivities estimated from specific-capacity data probably are only approximations of the total transmissivity of the aquifer system because the wells from which the specific-capacity data were obtained were not perforated over the entire thickness of the aquifer system.

The initial transmissivity of layer 2 was calculated as the product of the saturated thickness (400 ft, except where bedrock is higher than 1,550 ft above sea level) and a hydraulic conductivity of 10 ft/d. The initial transmissivity of layer 3 was calculated as the product of the saturated thickness (550 ft, except where bedrock is higher than 1,000 ft above sea level) and a hydraulic conductivity of 2 ft/d. The hydraulic-conductivity values used for layers 2 and 3 were based on values from the Edwards Air Force Base model (Nishikawa and others, 2001) and on the preliminary results of modeling of the southern part of the Lancaster subbasin (Phillips and others, in press). The initial transmissivity of layer 1 was calculated by subtracting the sum of the initial transmissivities for layers 2 and 3 from the total transmissivity calculated from the specific-capacity data. The initial hydraulic conductivity for layer 1 was then calculated by dividing the initial layer 1 transmissivity by the pre-development saturated thickness of layer 1, which was estimated using water-level estimates from Durbin (1978) (fig. 4). To avoid unreasonably low values of hydraulic conductivity in layer 1, a minimum hydraulic-conductivity value of 2 ft/d was specified for the cells in that layer. The transmissivity of layers 2 and 3 remained constant throughout the entire simulation

period because the water table never declined below the top of layer 2. Initial hydraulic-conductivity and transmissivity values for the area around Rogers Lake were modified to generally agree with the values used in a three-dimensional model developed by for the Edwards Air Force Base area (Nishikawa and others, 2001).

#### Vertical Leakance

Ground-water flow between model layers was assumed to be vertical and to occur when there is a difference in hydraulic head between layers. The vertical conductance between layers, which represents the ability of the aquifer to transmit water vertically, is calculated by the model using a specified vertical leakance value and the cell dimensions. The vertical leakance between model cells, which is a function of cell thickness and vertical hydraulic conductivity, was calculated outside the model using the following equation from McDonald and Harbaugh (1988):

$$\lambda_{k+1/2} = \frac{1}{\frac{\Delta z_k / 2}{Kz_k} + \frac{\Delta z_{k+1} / 2}{Kz_{k+1}}}, \quad (2)$$

where

---

$\lambda_{k+1/2}$  is the vertical leakance between layers  $k$  and  $k+1$  [ $t^{-1}$ ],

$\Delta z_k$  is the thickness of layer  $k$  [L],

$\Delta z_{k+1}$  is the thickness of layer  $k+1$  [L],

$Kz_k$  is the vertical hydraulic conductivity of layer  $k$  [ $Lt^{-1}$ ], and

$Kz_{k+1}$  is the vertical hydraulic conductivity of layer  $k+1$  [ $Lt^{-1}$ ].

---

Equation 2 strongly weights the smaller of the two vertical hydraulic conductivity values. For example, if one layer contains thick lacustrine deposits of silt and clay and the other layer contains mostly alluvial deposits of sand and gravel, the vertical leakance between the layers is dependant mostly on the vertical hydraulic conductivity of the lacustrine deposits. The vertical hydraulic conductivities of layers 1, 2, and 3 were assumed to be one-hundredth of the horizontal hydraulic conductivities in areas where the lacustrine deposits are not present between the centers of adjacent layers. Where lacustrine deposits are

present in a layer, the vertical hydraulic conductivity of the lacustrine deposits was used for that layer. An estimate of  $1.0 \times 10^{-2}$  ft/d was used for the vertical hydraulic conductivity of the lacustrine deposits, which is consistent with the value used by Durbin (1978) and three orders of magnitude higher than the value used by Nishikawa and others (2001).

#### Storage Coefficient

The storage (specific yield or storage coefficient) of water-bearing material is the quantity of water released from storage per unit area per unit decline in hydraulic head. The water released from storage is derived from the compression of the granular matrix (skeleton) of the aquifer system and the expansion of fluid. In confined and unconfined aquifer systems the release of water from storage in low-permeability, unconsolidated fine-grained sediments is accompanied by some degree of compression of the fine-grained sediments. The relation between changes in head, expressed as an equivalent change in pore-fluid pressure, and compression of the aquifer system is based on the principle of effective stress first proposed by Terzaghi (1925) for one-dimensional vertical consolidation of saturated sediment,

$$\sigma_e = \sigma_T - p, \quad (3)$$

where effective or intergranular stress ( $\sigma_e$ ) is the difference between the total stress ( $\sigma_T$ ) and the pore-fluid pressure ( $p$ ). Under this principle, when the total stress remains constant, a change in pore-fluid pressure causes an equivalent change in effective stress within the aquifer system, which causes the aquifer system to expand or compress under the new load. In aquifer systems, conditions that cause changes in the total stress include the erosion or aggradation of sediment at land surface, or more commonly a change in the position of the water table overlying confined aquifers. For purposes of this discussion, the total stress is assumed constant.

When the effective stress is decreased by an increase in pore-fluid pressure, the aquifer system expands elastically. When the effective stress is increased by a reduction in pore-fluid pressure and the effective stress does not exceed the maximum past effective stress, the aquifer system compresses elastically. When a reduction in pore-fluid pressure

causes an increase in effective stress that exceeds the previous maximum effective stress, the pore structure of the fine-grained sediments (aquitards) in the aquifer system undergoes significant rearrangement, resulting in permanent (inelastic) rearrangement of the granular structure, a reduction in pore volume and permanent compaction of the aquitards.

The elastic and inelastic skeletal compressibilities,  $\alpha'_k$ , of the aquitards are expressed in terms of the skeletal specific storages,  $S'_{sk}$ ,

$$S'_{sk} = S'_{ske} = \alpha'_{ke} p g, \quad \sigma_e \leq \sigma_e(\max), \quad (4)$$

$$S'_{sk} = S'_{skv} = \alpha'_{kv} p g, \quad \sigma_e > \sigma_e(\max),$$

where the primes denote aquitard properties, the subscript  $k$  refers to the skeletal component of specific storage, or compressibility, subscripts  $e$  and  $v$  refer to the elastic and virgin (inelastic) properties,  $p$ , is fluid density, and  $g$  is gravitational acceleration. For a change in effective stress, the aquitard deforms elastically when the effective stress is less than the previous maximum effective stress,  $\sigma_e(\max)$ ; when the effective stress is greater than  $\sigma_e(\max)$ , the aquitard deforms inelastically. The previous maximum stress is termed the preconsolidation stress or, expressed as an equivalent hydraulic head is termed the preconsolidation head.

In typical aquifer systems composed of unconsolidated to semi-consolidated Cenozoic sediments,  $S'_{skv}$  is generally 30 to several hundred times larger than  $S'_{ske}$  (Ireland and others, 1984). The product of the elastic or inelastic skeletal specific storage and the aggregate thickness of the aquitards,  $\sum b'$ , is the aquitard skeletal storage coefficient  $S'_k$ :

$$S'_k = S'_{ke} = S'_{ske} (\sum b'), \quad \sigma_e \leq \sigma_e(\max), \quad (5)$$

$$S'_k = S'_{kv} = S'_{skv} (\sum b'), \quad \sigma_e > \sigma_e(\max),$$

for the elastic ( $S'_{ke}$ ) and inelastic ( $S'_{kv}$ ) range of skeletal compressibility, respectively. A similar set of equations, one for the coarse-grained aquifers and one for pore water, relates the compressibility of the aquifer skeleton ( $\alpha_k$ ) to the aquifer skeletal storage coefficient ( $S_k$ ) and the compressibility of water ( $\beta_w$ ) to the component of aquifer-system storage attributed to the pore water ( $S_w$ ):

$$S_k = S_{sk} (\sum b) = \alpha_k p g (\sum b), \quad (6)$$

$$S_w = \beta_w p g [n (\sum b) + n' (\sum b')], \quad (7)$$

where  $\sum b$  is the aggregate thickness of the aquifers and  $n$  and  $n'$  are the porosities of the aquifers and aquitards, respectively. For coarse-grained aquifers interbedded with compressible aquitards, the difference between the elastic and inelastic compressibilities of the aquifer skeleton is considered relatively insignificant, and  $\alpha_k \equiv \alpha_{ke}$ .

The aquifer-system storage coefficient  $S$  is defined as the sum of the skeletal storage coefficients of the aquitards and aquifers (equations 5–6) plus the storage attributed to water compressibility (equation 7). Thus,

$$S = S'_k + S_k + S_w. \quad (8)$$

For compacting aquifer systems,  $S'_{skv} \gg S_{sw}$  (specific storage of water), and the inelastic storage coefficient of the aquifer system is approximately equal to the inelastic aquitard skeletal storage coefficient,  $S_v \equiv S'_{kv}$ . In confined aquifer systems subject to large-scale overdraft, the volume of water derived from permanent aquitard compaction can typically range from 10 to 30 percent of the total volume of water pumped and represents a one-time mining of stored ground water and a small permanent reduction in the storage capacity of the aquifer system.

In unconfined aquifer systems the skeletal storage coefficients described above also govern the compressibility of the fine-grained sediments below the water table and contribute to the volume of water released from storage when heads decline, and is defined by the specific yield,  $S_y$ , of the aquifer system. Water derived from storage in unconfined aquifer systems primarily results from the gravity drainage of pore water from the sediments and its value is typically in the range of 0.1–0.3, somewhat less than the porosity, and somewhat greater than the specific retention of the sediments. Typically,  $S_y \gg S$  by two to three orders of magnitude.

For confined and unconfined aquifers, the IBS1 Package requires that storage coefficient terms be specified for the elastic skeletal storage coefficient ( $S_{ke}$ ), and inelastic aquitard skeletal storage coefficient ( $S'_{kv}$ ) (Leake and Prudic, 1991). For confined aquifers, in order to account for the component of storage related

to the compressibility of water,  $S_w$  was entered as the storage coefficient in the BCF package of MODFLOW. Within MODFLOW these three storage components ( $S_{ke}$ ,  $S'_{kv}$ , and  $S_w$ ) are summed and the storage coefficient of the aquifer system,  $S$ , is implemented for each model layer. For unconfined aquifers, IBS1 requires the two components of the skeletal storage coefficient. In contrast with the procedure used to implement the aquifer-system storage coefficient for confined aquifers, the specific yield ( $S_y$ ) was entered as the storage term in the input file for the BCF package for layer 1, and this value was used by the model where and when unconfined aquifer conditions occurred in that model layer. Note that the specific yield of an unconfined aquifer is many orders of magnitude greater than storage coefficient associated with the compressibility of water. Therefore, the water released from storage owing to the expansion of water is negligible with respect to the amount released by the gravity drainage of pore water. In this model, it was assumed that compaction occurs only in layers 1 and 2. Because little pumping occurs in layer 3 and because sediments in layer 3 have been subjected to fairly large overburden stress, it was assumed that there is little potential for compaction of this layer.

The initial storage coefficients for the model were calculated using specific-storage values obtained from one-dimensional (Sneed and Galloway, 2000) and three-dimensional (Nishikawa and others, 2001) models of ground-water flow and aquifer-system compaction at Edwards Air Force Base. The specific storage values range from  $4.2 \times 10^{-7} \text{ ft}^{-1}$  for the compressibility of water ( $S_{sw}$ ) to  $3.5 \times 10^{-4} \text{ ft}^{-1}$  for the inelastic skeletal specific storage ( $S'_{skv}$ ) of thick (greater than 18 ft) aquitards (table 4). The initial storage coefficients for the compressibility of water ( $S_w$ ) and elastic skeletal storage ( $S_k$ ) for layers 1 and 2 were calculated as the product of the respective specific-storage value and the saturated thickness of the layer. The initial inelastic aquitard skeletal storage coefficients ( $S'_{kv}$ ) were calculated as the product of the inelastic specific storage of thick aquitards and the estimated total thickness of aquitards within the aquifer.

**Table 4.** Specific storage values used in calculating storage coefficients for layers 1 and 2 in the ground-water flow model of the Antelope Valley ground-water basin, California

[Data from Sneed and Calloway, 2000; Nishikawa and others, 2001.  
ft<sup>-1</sup>, per foot]

	Specific storage (ft <sup>-1</sup> )
Compressibility of water.....	4.2×10 <sup>-7</sup>
Elastic skeletal specific storage..	1.7×10 <sup>-6</sup>
Inelastic skeletal specific storage for thin aquitards (less than or equal to 18 feet thick)	4.0×10 <sup>-5</sup>
Inelastic skeletal specific storage for thick aquitards (greater than 18 feet thick)	3.5×10 <sup>-4</sup>

The total thickness of the aquitards in layers 1 and 2 was estimated from the percentage of the fine-grained sediments in these layers that was determined from descriptions of the aquifer material noted in selected well drillers' logs. The percentage of fine-grained sediments ranged from 13 to 50 percent of the thickness of each layer. The inelastic aquitard skeletal storage coefficient was specified only for those areas of layers 1 and 2 where subsidence of more than 1 ft had been measured in the study area (fig. 8). Compaction was not simulated for layer 3; therefore, the storage coefficient for layer 3 was estimated by multiplying the specific storage of the aquifer by the thickness of the layer (550 ft). A specific storage of  $2.0 \times 10^{-6}$  ft<sup>-1</sup> was assumed representative of the aquifer materials in layer 3, resulting in a storage coefficient of  $1.0 \times 10^{-3}$ . This value was used throughout layer 3, regardless of the thickness of the layer, except for the model area near Rogers Lake, north of the Willow Springs Fault. The storage coefficient calibrated by Nishikawa and others (2001) during the simulation of ground-water flow and land subsidence at Edwards Air Force Base ( $5.71 \times 10^{-4}$ ) was used in the model area north of Willow Springs Fault.

Specific-yield values used in the Durbin (1978) model for the unconfined aquifer ranged from 0.05 to 0.20; these values were used as initial values for the upper aquifer. Microgravity measurements collected

from 1996–98 as part of an injection, storage, and recovery test at Lancaster were used to estimate a specific yield of about 0.13 (Howle and others, 2003).

#### Preconsolidation Head

As noted earlier, inelastic compaction of compressible sediments occurs when water levels decline below the preconsolidation head. Accurate estimates of preconsolidation head values are critical for the simulation of subsidence (Sneed and Galloway, 2000); the initial values of preconsolidation head for the model were based on results from the one-dimensional model of ground-water flow at Edwards Air Force Base (Sneed and Galloway, 2000). Initial preconsolidation head values were specified from 0 to 50 ft below pre-development water levels only for those areas that have 1 ft of measurable subsidence (fig. 8). If future water levels decline below preconsolidation heads outside the areas of subsidence shown in figure 8, then subsidence may occur in those areas. The magnitude and distribution of preconsolidation heads for the areas that have no measurable subsidence are not known and, therefore, calibration of preconsolidation heads for these areas is not possible. Subsidence was not simulated for those areas because there is no constraint for the range of preconsolidation heads.



## Horizontal-Flow Barriers

Nine faults that transect the ground-water basin were simulated as partial barriers to ground-water flow ([fig. 11](#), [table 5](#)). The Horizontal-Flow Barrier (HFB) package (Hsieh and Freckleton, 1993) was used to simulate these faults as horizontal-flow barriers. The HFB package allows for the simulation of thin, vertical, low-permeability geologic features, such as vertical faults and fine-grained material, that act as partial barriers to horizontal ground-water flow. The function of each simulated barrier is to lower the horizontal conductances between two adjacent model cells. The barriers are defined by a hydraulic characteristic, which for unconfined aquifers is the hydraulic conductivity of the fault divided by the width of the fault and for confined aquifers is the transmissivity of the fault divided by the width of the fault. Each barrier may be subdivided into segments and each segment may have a different hydraulic characteristic. All the barriers simulated in the model were assumed to extend through all three model layers. The hydraulic characteristic value for each segment ([table 5](#)) was determined by model calibration.

The simulated barriers include an unnamed fault between Finger Buttes and West Antelope subbasins (barrier 1), the Randsburg–Mojave Fault (barrier 2), the Neenach Fault (barrier 3), and an unnamed fault between the Buttes and Pearland subbasins (barrier 4) ([fig. 11](#), [table 5](#)). These four barriers were simulated as partial barriers to ground-water flow in the Durbin (1978) model. The fault separating the Buttes and Pearland subbasins from the Lancaster subbasin ([fig. 11](#)) was not simulated as a barrier to flow in the Durbin (1978) model. This fault also was not simulated as a barrier to flow in this model. Five of the faults simulated as partial barriers to flow were not simulated as barriers in the Durbin (1978) model. These faults include the extensions of the Muroc Fault (barrier 5) and the El Mirage Fault (barrier 6) across Rogers Lake and an extension of the Willow Springs fault from the northwest corner of Rosamond Lake southeast along the southern edge of Buckhorn Lake to the eastern edge of the study area (barrier 7). These faults were simulated as partial barriers to flow in the Edwards Air Force Base model (Nishikawa and others, 2001). Two

additional partial barriers to flow were inferred from water-level data and model calibration; one barrier southeast of Lovejoy Buttes, parallel to the northeast boundary of the Buttes subbasin (barrier 8), and one barrier south of Rosamond Lake, trending northwest-southeast from the Neenach Fault to the eastern edge of the study area (barrier 9). These barriers are believed to be related to faults that are not exposed at land surface.

## Model Stresses

Hydraulic heads in the ground-water flow system respond to stresses on the system, which correspond to recharge and discharge. As noted earlier, recharge to the ground-water system includes natural recharge from mountain-front runoff and stream infiltration in the upper reaches of ephemeral streams and artificial recharge of irrigation-return flow and treated wastewater. Discharge from the ground-water systems includes evapotranspiration, ground-water outflow, and ground-water pumpage.

### Natural Recharge

Natural recharge from mountain-front runoff and stream infiltration was simulated as areal recharge to layer 1, the location of the recharge cells are shown in [figure 12](#). The initial value of total annual natural recharge was assumed to be 40,700 acre-ft, the value simulated in the Durbin (1978) model. The distribution of natural recharge was based on the location and size of the intermittent streams used to estimate natural recharge (Durbin, 1978). The initial annual recharge specified for these cells ranged from 65 to 3,800 acre-ft for each cell. Natural recharge did not vary from year to year because data were limited, which precluded simulating seasonal or annual variations in natural recharge. Results from a study by Bouwer (1982) indicate that seasonal and annual fluctuations in infiltration are attenuated as a function of sediment particle size in the unsaturated zone and vertical distance to the water table. Natural recharge was not specified for the entire reach of streams in the basin because the streams are intermittent and flow does not always occur over the entire length of the stream.

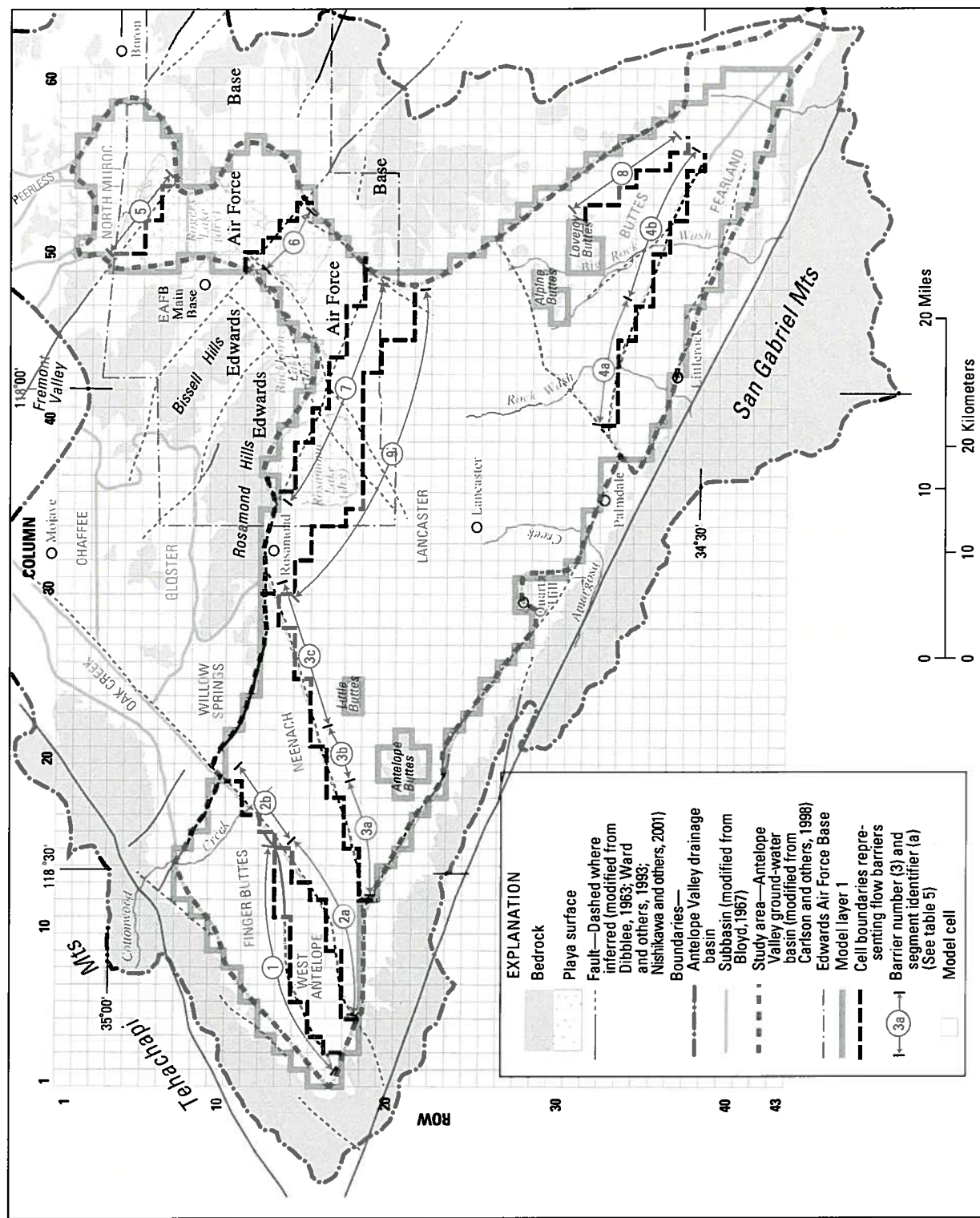


**Figure 11.** Location of barriers to horizontal ground-water flow simulated in the ground-water flow model of the Antelope Valley ground-water basin, California.



**Table 5.** Hydraulic characteristics of the horizontal-flow barriers simulated in the ground-water flow model of the Antelope Valley ground-water basin, California

[d<sup>-1</sup>, per day; ft/d, foot per day. —, no barrier simulated in this layer]

Barrier No.	Segment	Barrier name	Hydraulic characteristic		
			Layer 1 (d <sup>-1</sup> )	Layer 2 (ft/d)	Layer 3 (ft/d)
1		( <sup>1</sup> )	0.00008	0.0008	0.0008
2	a	Randsburg–Mojave Fault	.00007	.0007	.0007
	b		.00002	.0002	.0002
3	a	Neenach Fault	.0008	.008	.008
	b		.002	.02	.02
	c		.004	.04	.04
4	a	( <sup>1</sup> )	.0004	—	—
	b		.0003	—	—
5		Muroc Fault	.001	.01	.01
6		El Mirage Fault	.001	.01	.01
7		Willow Springs Fault	.0001	.001	.001
8		( <sup>1</sup> )	.00001	—	—
9		( <sup>1</sup> )	.00001	.0001	—

<sup>1</sup> Unnamed

### Artificial Recharge

Artificial recharge in the ground-water basin, as noted earlier, includes the infiltration of irrigation-return flows of pumped ground water and imported water used for agriculture and treated wastewater discharged to spreading ponds.

### Irrigation-Return Flow

Irrigation-return flow is that portion of the water applied to crops that is not consumptively used by the crops. Irrigation efficiency, which is defined as the percentage of applied water used by the crops, was assumed to be 70 percent, leaving as much as 30 percent of the applied irrigation water available to return to the water table as irrigation-return flow. In Antelope Valley, most of the applied water is for the production of alfalfa. The irrigation efficiency was estimated on the basis of the quantity of irrigation water applied to alfalfa [approximately 6.6 ft/yr (Orloff and others, 1989)] and the quantity of water consumed by alfalfa [approximately 4.8 ft/yr (table 2)]. Estimates of irrigation efficiency by Snyder (1955) and by the California Department of Public Works (1955) were about 50 percent; however,

consumptive-use estimates at the time of these two studies (3.4–3.6 ft/yr) were lower than current estimates (4.8 ft/yr). The current consumptive-use estimates were considered more accurate than the consumptive-use estimates used by researchers in the 1950s; therefore, an irrigation efficiency of 70 percent was assumed valid for the entire simulation period.

Because pumpage has caused ground-water levels to decline more than 100 ft throughout most of the ground-water basin and owing to the existence of thin aquitards within the aquifers, recharge from water applied for agriculture probably did not reach (recharge) the water table until about 10 years after application. The actual delay in irrigation-return flow reaching the water table probably is variable depending on the depth to water and the existence of fine-grained layers in the unsaturated zone. Irrigation-return flows were simulated as wells that had positive flow rates (i.e., flow recharging the ground-water flow system) at the cells where agricultural pumpage was simulated (fig. 5). The areas that had irrigation-return flows remained constant during 1915–51 but varied annually during 1952–95. Annual agricultural recharge varied from 0 to 111,000 acre-ft.

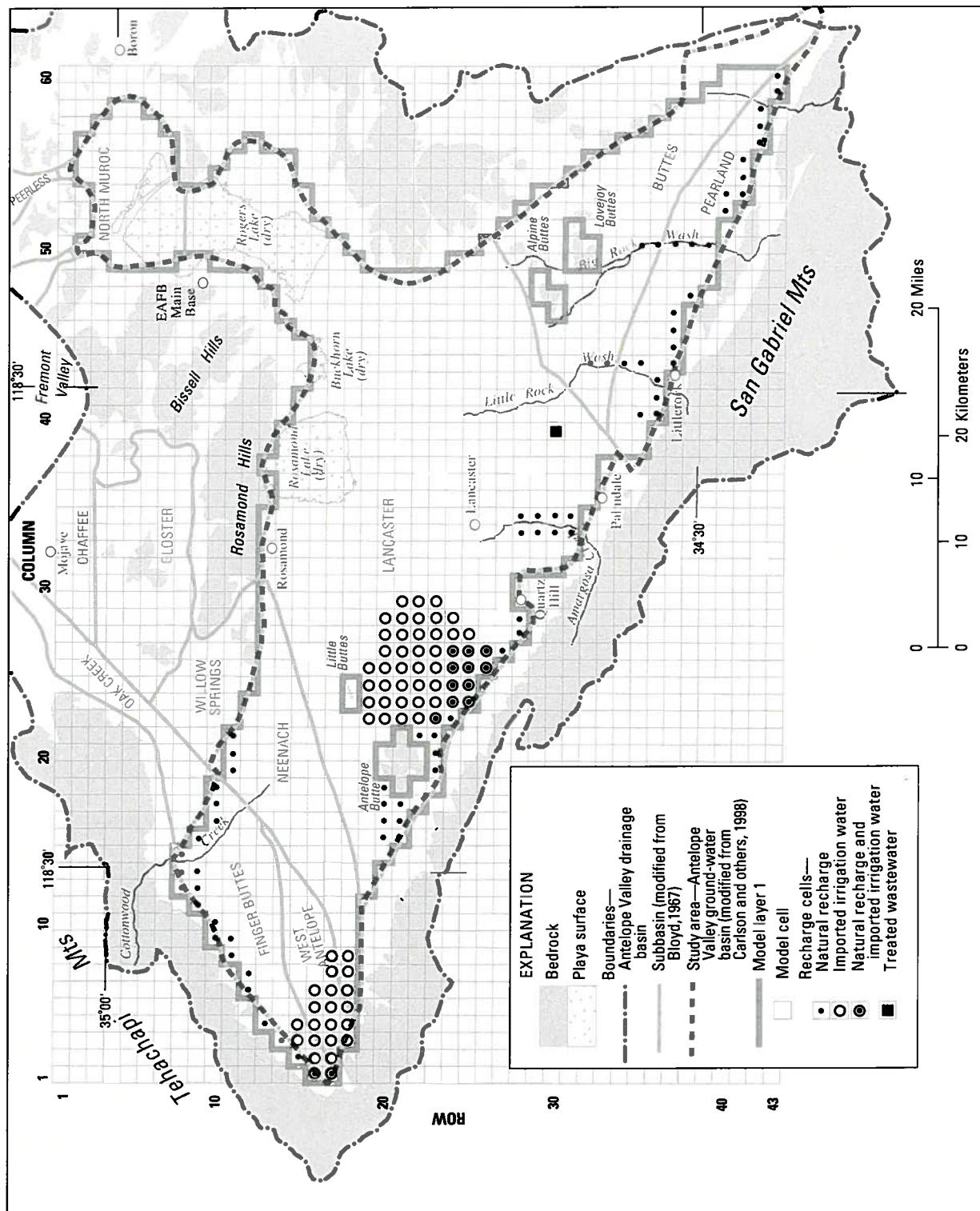


**Figure 12.** Location of model cells used to simulate natural recharge, recharge of imported water used for irrigation, and recharge of treated wastewater in the ground-water flow model of the Antelope Valley ground-water basin, California.

Beginning in 1972, water was imported from northern California to Antelope Valley by way of the California aqueduct. Records of deliveries of imported water from the Antelope Valley–East Kern Water Agency (AVEK) show that growers began using large quantities of imported surface water in 1976. The records also indicate that most of the imported water was delivered to two areas of the valley; (1) the western part of the Lancaster subbasin, east of Antelope Buttes, and (2) the far western part of the study area, in the Finger Buttes, Neenach, and West Antelope subbasins ([fig. 12](#)). Thirty percent of the annual imported water delivered to these areas was specified as irrigation-return flow and was simulated as wells that had positive flow rates into layer 1 of the model 10 years after the water was applied at land surface.

#### *Treated Wastewater*

The estimated annual quantity of treated wastewater that could infiltrate into the unsaturated zone is shown in [table 1](#). The treated wastewater is from urbanized parts of the study area that are served by the water reclamation plants. Recharge from septic systems in the rural parts of the study area was assumed to be negligible. Recharge from treated wastewater was assumed to reach the water table in the year that it was applied at land surface because this source of water is essentially constant and the rate of infiltration per acre is much greater than that for agriculture. Recharge from the Palmdale Water Reclamation Plant was applied to only one cell ([fig. 12](#)) for 1984–95, the years in which recharge from the treated wastewater was estimated to occur ([table 1](#)). On the basis of results of infiltration studies at the Lancaster Water Reclamation Plant, the assumption was made that recharge of treated wastewater from the plant does not reach the regional water table, and, therefore, it was not simulated for this site.

#### *Natural Discharge*

Evaporation from bare-soil and transpiration by phreatophytes in areas where the water table was near land surface were simulated using the Evapotranspiration Package developed by McDonald and Harbaugh (1988). These areas were identified using maps that show the area of flowing wells in 1908

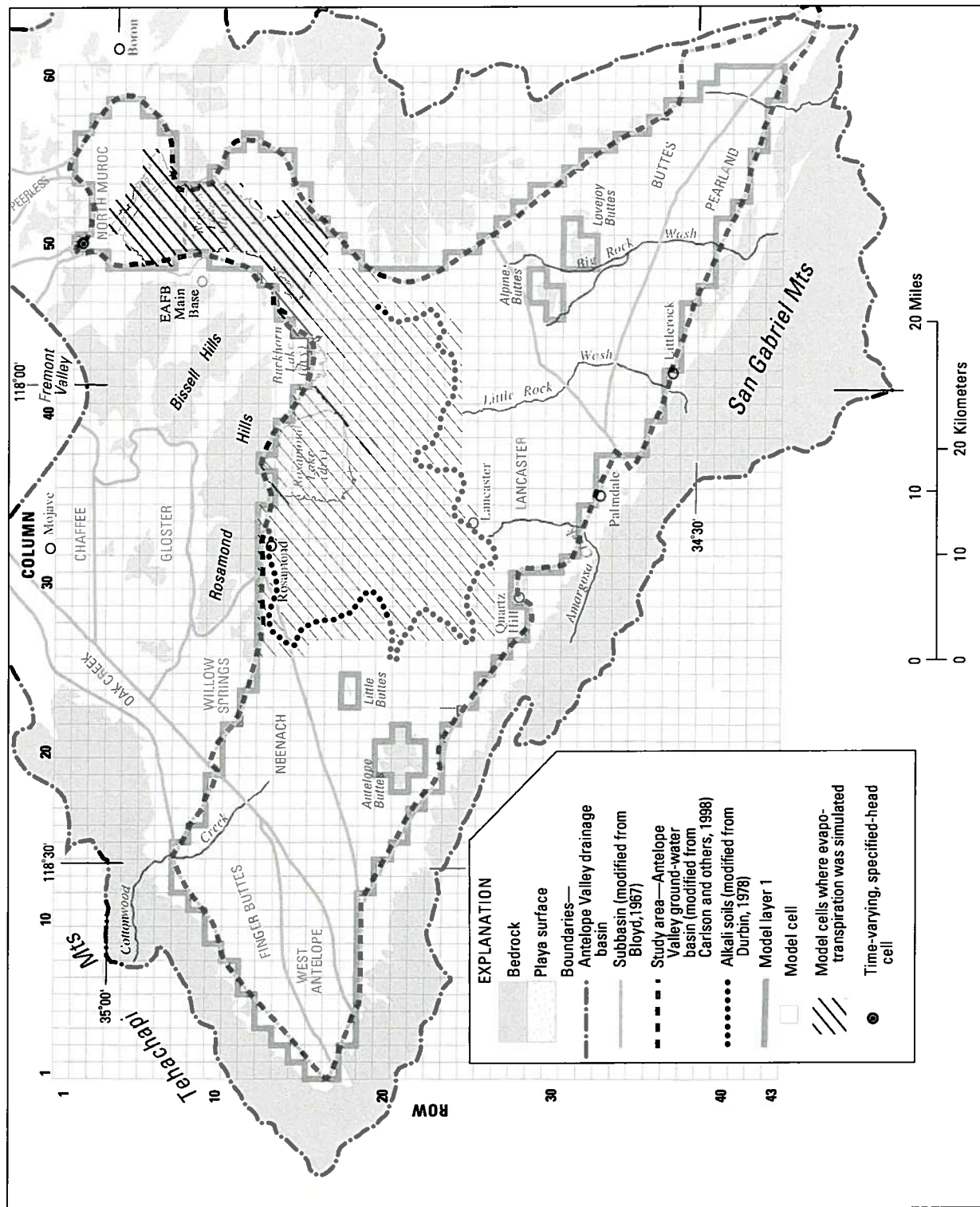
(Johnson, 1911) and alkali soils (Durbin, 1978) ([fig. 13](#)). Estimates of evapotranspiration rates in Antelope Valley were based on results reported by Lines and Bilhorn (1996) in the nearby Mojave River Basin. An annual maximum evapotranspiration rate of 0.6 ft/yr was specified when the water table was at land surface and was decreased linearly to zero when the water table reached a depth of 10 ft below land surface.

Durbin (1978) estimated that 1,000 acre-ft/yr of ground water is discharged as ground-water underflow north of Rogers Lake into Fremont Valley: this estimate was based on the water-level gradient and the cross-sectional area of the aquifer. Water-level data from nearby wells indicate that the gradient at that location has not been constant over time, which suggests that subsurface ground-water flow has not been constant (Nishikawa and others, 2001). Variable subsurface ground-water flow was specified in the transient-state simulation using a time-varying specified-head cell ([fig. 13](#)). The water level at the specified-head cell ([fig. 14](#)) was based on water-level data from nearby wells (Nishikawa and others, 2001), and flow out of the study area into Fremont Valley was calculated by the model using the gradient between the specified-head cell and adjacent active cells.

#### *Pumpage*

Total annual pumpage specified in the model is shown in [figure 5](#). The spatial distribution of pumpage for 1915–51 was based on the Durbin (1978) model. The spatial distribution of pumpage for 1915–51 was concentrated primarily in agricultural areas and did not vary over time. The spatial distribution of pumpage for 1952–95 was based on the spatial distribution of pumpage in the database created by Templin and others (1995) and updated for this study ([see Appendix: Water Use 1992–95](#)). The pumpage database contains annual pumpage data for individual wells and information on the location of these wells. Well location data allowed the spatial distribution of pumpage in the model to vary for 1952–95, years when the primary pumping centers moved from agricultural areas to urban areas. The pumpage database, however, does not contain data for all agricultural pumpage in the study area; therefore, land-use data were used in conjunction with the database to simulate the distribution of agricultural pumpage.





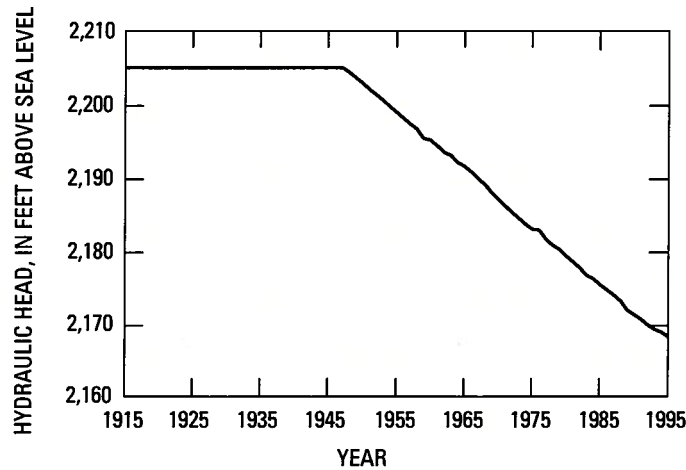


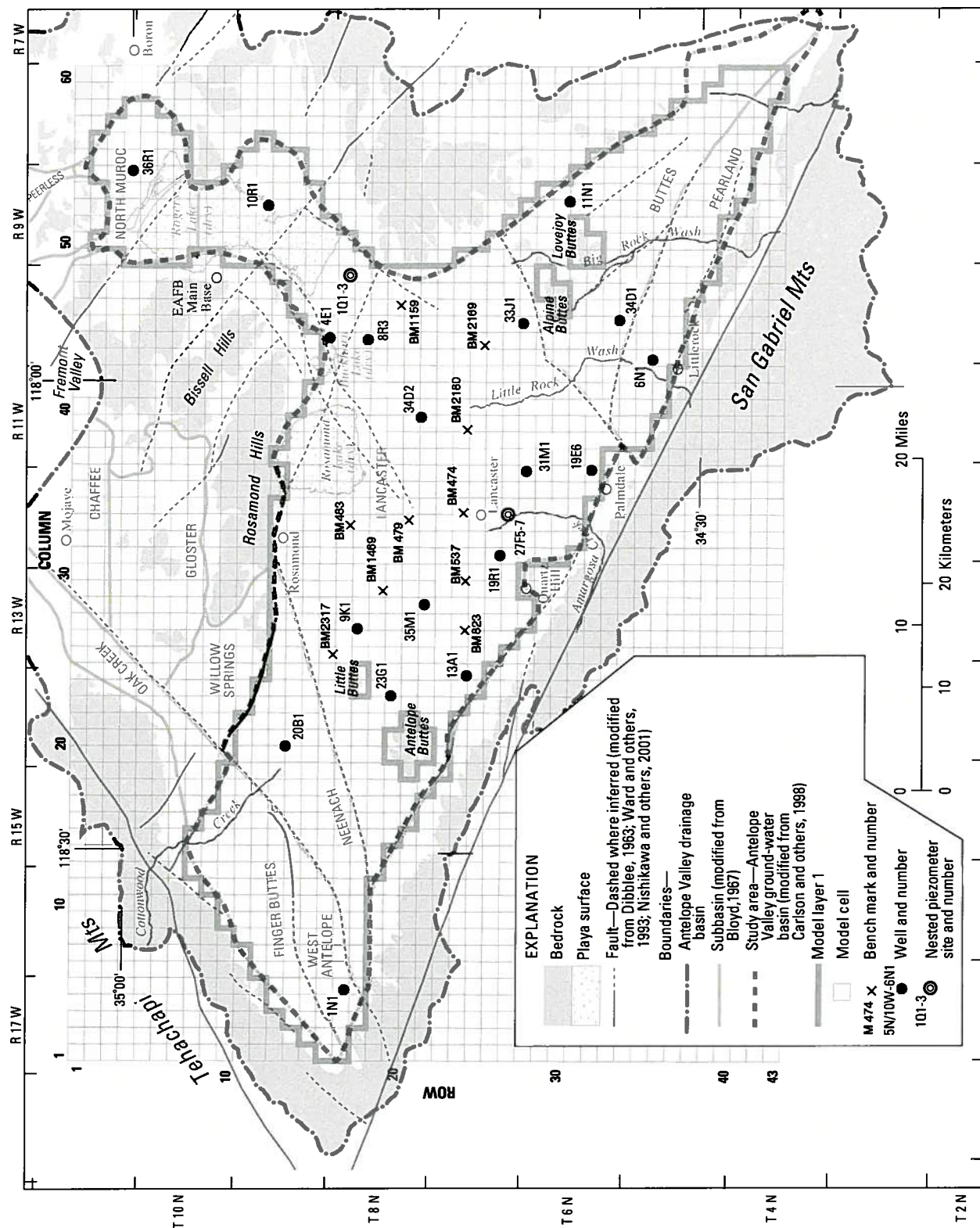
**Figure 14.** Time-varying specified hydraulic head used for the north boundary of the ground-water flow model of the Antelope Valley ground-water basin, California (modified from Nishikawa and others, 2001).

A comparison of the spatial distribution of pumpage in the database and land-use data for 1961 and 1987 indicated that the database does not have pumpage data for areas of agricultural land use in the West Antelope and the western Neenach subbasins. The land-use data showed that about 6.8 percent of the total agricultural land in the study area was in these areas; therefore, the annual agricultural pumpage for these areas was assumed to be 6.8 percent of the total annual agricultural pumpage. Agricultural pumpage in the West Antelope and the western Neenach subbasins was distributed to model cells corresponding to the location of the agricultural land use. Pumpage in these areas was assumed to have occurred between 1934 and 1986: this assumption was based on a comparison of simulated water levels and measured water levels for well 8N/17W-1N1 (well location shown in [fig. 15](#)) in the West Antelope subbasin.

The spatial distribution and quantity of pumpage for public supply for 1919–91 was determined from the pumpage database compiled by Templin and others (1995) and for 1992–95 from water-use information compiled for this study ([Table A1](#) in the [Appendix](#)). The location and quantity of pumpage from public supply wells is well documented, and was not changed during the calibration process.

Because there was limited well-construction data available, all wells were assumed to be fully perforated in both layers 1 and 2. The proportion of pumpage from a layer was determined by dividing the transmissivity of that layer by the sum of the transmissivity of layers 1 and 2. The transmissivity of layer 1 was calculated as the product of hydraulic conductivity and initial (1915) saturated thickness. The vertical distribution of pumpage from layers 1 and 2 varied spatially but did not vary with time; therefore, a limitation of this approach is that the vertical distribution of pumpage does not change as the water table declines. In the aquifer system, changes in the saturated thickness of the upper aquifer changes the transmissivity of the upper aquifer, which affects the flow of water to wells. It was assumed that there was no pumpage from layer 3 because few wells in Antelope Valley are deep enough to penetrate the lower aquifer and because the transmissivity of this layer is low. This assumption is valid particularly for the earlier part of the simulation period when rates for total annual pumpage were highest. During the latter part of the simulation period, wells were drilled in the lower aquifer (layer 3) and thus some pumping occurred from this aquifer. The limited pumping that occurred only from the lower aquifer was simulated as pumpage from layers 1 and 2.





## Model Calibration

Model calibration is the process of making adjustments, within justifiable ranges, to initial estimates of selected model parameters and stresses to obtain reasonable agreement between simulated and measured values (for this model, water levels and land subsidence). Modifications were made to the initial estimates of the hydraulic conductivity of layer 1, the transmissivity of layer 2, specific yield, natural recharge, aquitard thickness, hydraulic characteristics of horizontal flow barriers, and preconsolidation head using a trial-and-error approach. Vertical leakance was recalculated after changes were made to any of the values used to calculate vertical leakance; hydraulic conductivity, transmissivity, or saturated thickness. The values of transmissivity and storage coefficient of layer 3 were not changed from the initial values during the model calibration process because reasonable changes in these values had negligible affect on model results.

Prior to 1915, there was little ground-water development in Antelope Valley and the ground-water flow system was in a time-averaged state of equilibrium. Inflows from recharge were balanced by outflows as evapotranspiration and ground-water underflow, and water levels were essentially unchanging. This state of equilibrium was simulated by the steady-state model that represents conditions in 1915. The addition of stress to the ground-water flow system owing to pumping resulted in an imbalance between inflows and outflows, which disturbed the state of equilibrium and resulted in time-varying or transient-state conditions. Ground-water conditions during the period 1915–95 were simulated with a transient-state model. During the calibration process both steady-state and transient-state simulations were used: the steady-state simulation was used to provide initial conditions for the transient-state simulation. Any changes made to the transient-state simulation were incorporated into the steady-state simulation and the steady-state simulation was rerun to ensure that the changes made during the transient-state simulation produced reasonable results for steady-state conditions. This process was repeated until a satisfactory match between measured and simulated results was obtained.

## Steady-State Simulation

The steady-state simulation of 1915 conditions was made to provide initial conditions for the transient-state simulation. The steady-state simulation requires initial estimates of hydraulic conductivity, transmissivity, vertical leakance, hydraulic characteristics of horizontal flow barriers, natural recharge, and evapotranspiration (maximum evapotranspiration rate and extinction depth). Storage coefficients are not required for a steady-state simulation.

For this study, only estimates of natural recharge and evapotranspiration were modified during the initial steady-state calibration. Initial estimates of hydraulic conductivity, transmissivity, vertical leakance, and hydraulic characteristics were modified during the transient-state calibration. A subsequent steady-state simulation was then run to verify that the changes made during the transient-state simulation to these parameters resulted in a reasonable steady-state simulation of 1915 conditions. Ground-water level measurements, made around 1915, from 21 wells were used to determine if the steady-state simulation provided reasonable initial conditions for the transient-state simulation ([fig. 16, table 6](#)).

The final calibrated distribution of natural recharge is shown in [figure 17](#); recharge ranged from 65 to 3,250 acre-ft/yr per cell. Total natural recharge in the calibrated steady-state simulation was 30,300 acre-ft/yr, 10,400 acre-ft/yr less than the natural recharge simulated in the Durbin (1978) model (40,700 acre-ft/yr). Most of the reduction in simulated natural recharge occurred in the Pearland and Buttes subbasins; natural recharge was decreased from an initial estimate of 26,500 acre-ft/yr (Durbin, 1978) to 16,200 acre-ft/yr. Simulated water levels were higher than the measured water levels in these subbasins when the initial value of natural recharge was simulated. No reasonable combination of hydraulic conductivity, transmissivity, and values of hydraulic characteristic of flow barriers resulted in acceptable simulated water levels for these subbasins when the initial value of natural recharge was used in the steady-state simulation.

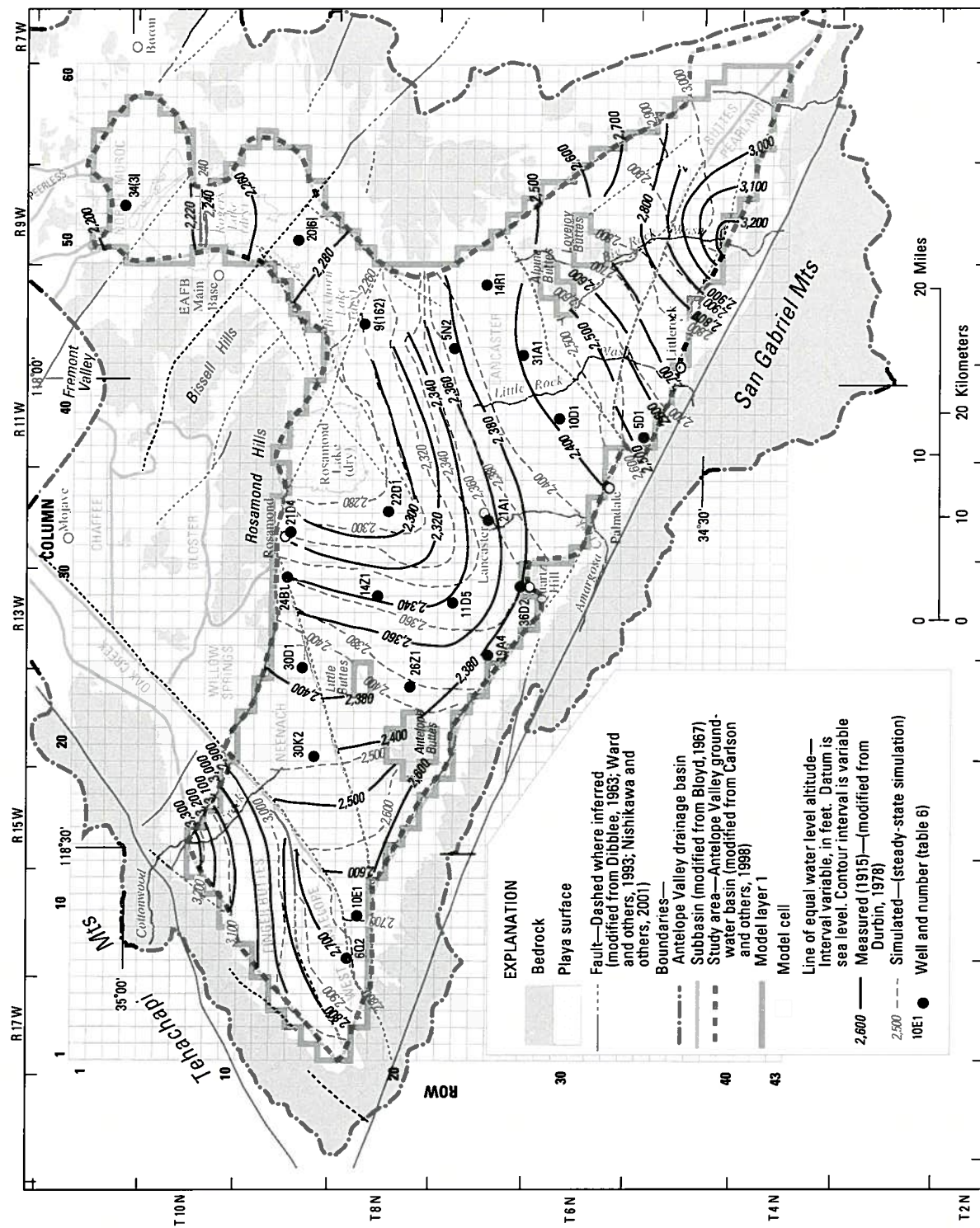


**Figure 16.** Location of wells used to calibrate the steady-state simulation and measured and simulated steady-state water levels from the ground-water flow model of the Antelope Valley groundwater basin, California.



**Table 6.** Measured and simulated (layer 1) water levels for wells used to calibrate the steady-state simulation of the ground-water flow model of the Antelope Valley ground-water basin, California

[State well No.: see well-numbering diagram; see figure 17 for location of wells; well depth in feet below land surface; water levels in feet above sea level; —, no data]

State well No.	Subbasin	Well depth	Year of measurement	Water levels		Difference, feet
				Measured	Simulated	
5N/11W-5D1	Pearland	403	1917	2,600	2,630	30
6N/11W-10D1	Lancaster	445	1915	2,430	2,434	4
7N/10W-5N2	Lancaster	404	1921	2,380	2,381	1
7N/10W-14R1	Lancaster	—	1921	2,403	2,414	11
7N/10W-31A1	Lancaster	300	1921	2,421	2,424	3
7N/12W-21A1	Lancaster	301	1915	2,354	2,346	-8
7N/13W-11D5	Lancaster	351	1917	2,341	2,351	10
7N/13W-19A4	Lancaster	75	1908	2,368	2,367	-1
7N/13W-36D2	Lancaster	466	1914	2,368	2,356	-12
8N/10W-9 (162) <sup>1</sup>	Lancaster	25±	1921	2,303	2,308	5
8N/12W-22D1	Lancaster	371	1910	2,278	2,283	5
8N/13W-14Z1	Lancaster	200	1907	2,348	2,357	9
8N/14W-26Z1	Lancaster	—	1909	2,376	2,382	6
8N/16W-6Q2	West Antelope	302	1909	2,824	2,847	23
8N/16W-10E1	Neenach	—	1909	2,682	2,701	19
9N/9W-20 (6) <sup>1</sup>	Lancaster	—	1917	2,275 <sup>3</sup>	2,253	-22
9N/12W-21D4	Lancaster	89	1909	2,316	2,318	2
9N/13W-24B1	Lancaster	63	1908	2,359	2,353	-6
9N/13W-30D1	Neenach	62	1908	2,400	2,439	39
9N/14W-30K2	Neenach	255	1908	2,445	2,494	49
11N/9W-34 (3) <sup>1</sup>	North Muroc	260	— <sup>2</sup>	2,196	2,224	28

<sup>1</sup>Number in parenthesis is the map number of the well as recorded by Thompson (1929, p. 348)

<sup>2</sup>Measured after 1915; Thompson (1929, p. 364)

<sup>3</sup>Flowing

The initial maximum simulated evapotranspiration rate of 0.6 ft/yr and extinction depth of 10 ft below land surface were unchanged. Specifying a higher maximum rate had little effect on model results, and specifying a lower maximum evapotranspiration rate resulted in simulated water levels that were significantly higher than the measured water levels.

The simulated steady-state water levels for layer 1 ranged from 22 ft lower to 49 ft higher than the measured water levels (table 6). The simulated water levels for wells in the Lancaster subbasin were within 12 ft of the measured water levels except for well 9N/9W-20(6) for which the simulated water levels

were 22 ft lower than the measured water levels. The simulated water levels ranged from 19 to 49 ft higher than the measured water levels in wells in the Neenach and West Antelope subbasins. The simulated water level for the single calibration well in the Pearland subbasin was 30 ft higher than the measured water level. The differences between the simulated and measured water levels in the Neenach, West Antelope, and Pearland subbasins were large because hydrologic data for these subbasins were limited. For wells in the Buttes and Finger Buttes subbasins, there were no water-level measurements available to calibrate the steady-state model.

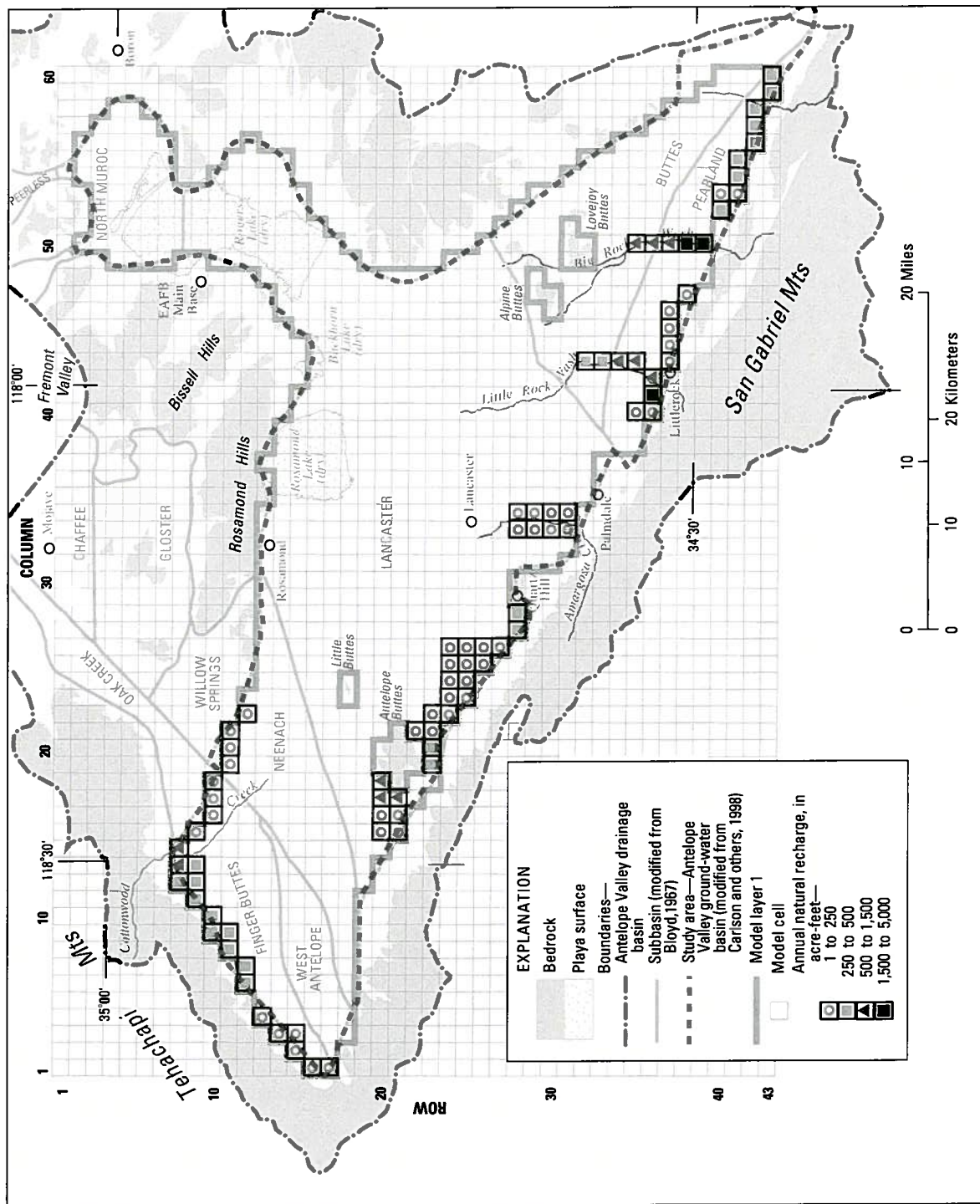


**Figure 17.** Areal distribution of natural recharge specified in the ground-water flow model of the Antelope Valley ground-water basin, California.



Contours of measured and simulated layer 1 water levels for 1915 are plotted together for comparison purposes on [figure 16](#). Ground-water flow direction inferred from the contours of simulated water levels is similar to flow direction inferred from the 1915 measured water-level contours. Ground-water flow is from recharge areas along the valley margins to discharge areas around the playas and the north boundary of the model. In the north Lancaster and North Muroc subbasins, the simulated water-level gradient to the north is less than the measured gradient. The largest differences between the measured and simulated water-level contours are in the Finger Buttes and Pearland subbasins: in these subbasins, the simulated water-level gradient is less than the measured gradient. The accuracy of the measured 1915 water-level contours for these two subbasins, however, is uncertain owing to the lack of available water-level data.

#### Transient-State Simulation

Calibration of the transient-state model involved trial-and-error adjustments of horizontal hydraulic conductivity, transmissivity, vertical leakance, storage coefficient, hydraulic characteristic of barriers, preconsolidation head, and artificial recharge of irrigation-return flows. New values of vertical leakance were calculated during the calibration process to incorporate changes in the hydraulic conductivity and saturated thickness of layer 1 and the transmissivity of layers 2 and 3. Model parameters for the area north of Willow Springs Fault (barrier 7 on [figure 11](#)) were modified from values used in the Edwards Air Force Base ground-water flow and land subsidence model (Nishikawa and others, 2001).

The transient-state model was calibrated using available water-level data from 24 wells for the period 1915–95 and subsidence data from 10 bench marks for the period 1926–92 ([fig. 15](#)). Data from 19 of the 24 wells were used to compare measured and simulated water levels over time; the wells were selected on the

basis of the length of water-level records and the spatial distribution of the wells. Data from two nested piezometer sites (wells 7N/12W-27F5–27F7 near Lancaster and wells 8N/10W-1Q1–1Q3 south of Rogers Lake) were used to compare the simulated and measured vertical hydraulic-head gradient between layers. The selection of the bench marks was based on the length of subsidence record and spatial distribution of the bench marks. The transient-state model was assumed to be calibrated when the simulated water levels matched the general magnitude and trend of the measured water levels, the general flow directions inferred from contours of the simulated water levels matched flow directions inferred from the contours of measured water levels, the onset and magnitude of land subsidence matched measured land subsidence, and the model parameters were within reasonable limits supported by the available geohydrologic data.

The calibrated values of the horizontal hydraulic conductivities used for layer 1 ranged from 2 to 30 ft/d ([fig. 18](#)). Modifications were made to the initial values of horizontal hydraulic conductivity primarily for the areas southwest, south, and east of Rosamond Lake and for the Buttes subbasin. For these areas, few, if any, aquifer-test data were available to estimate the transmissive properties of the aquifer. In the area around Rosamond Lake, water levels that were simulated using the initial values of horizontal hydraulic conductivity were too low; therefore, the initial values were decreased to increase the simulated water levels. Lacustrine deposits are present in the upper aquifer in this part of the basin ([fig. 3](#)), which may explain the low simulated hydraulic conductivity values. In the southeast part of Buttes subbasin, the horizontal hydraulic conductivity was decreased from an initial value of 10 ft/d to a value of 2 ft/d. In the northwest part of the subbasin, horizontal hydraulic conductivity was increased from an initial value of 25 to 30 ft/d in order to lower simulated water levels in the northwestern parts of the Buttes and Pearland subbasins.

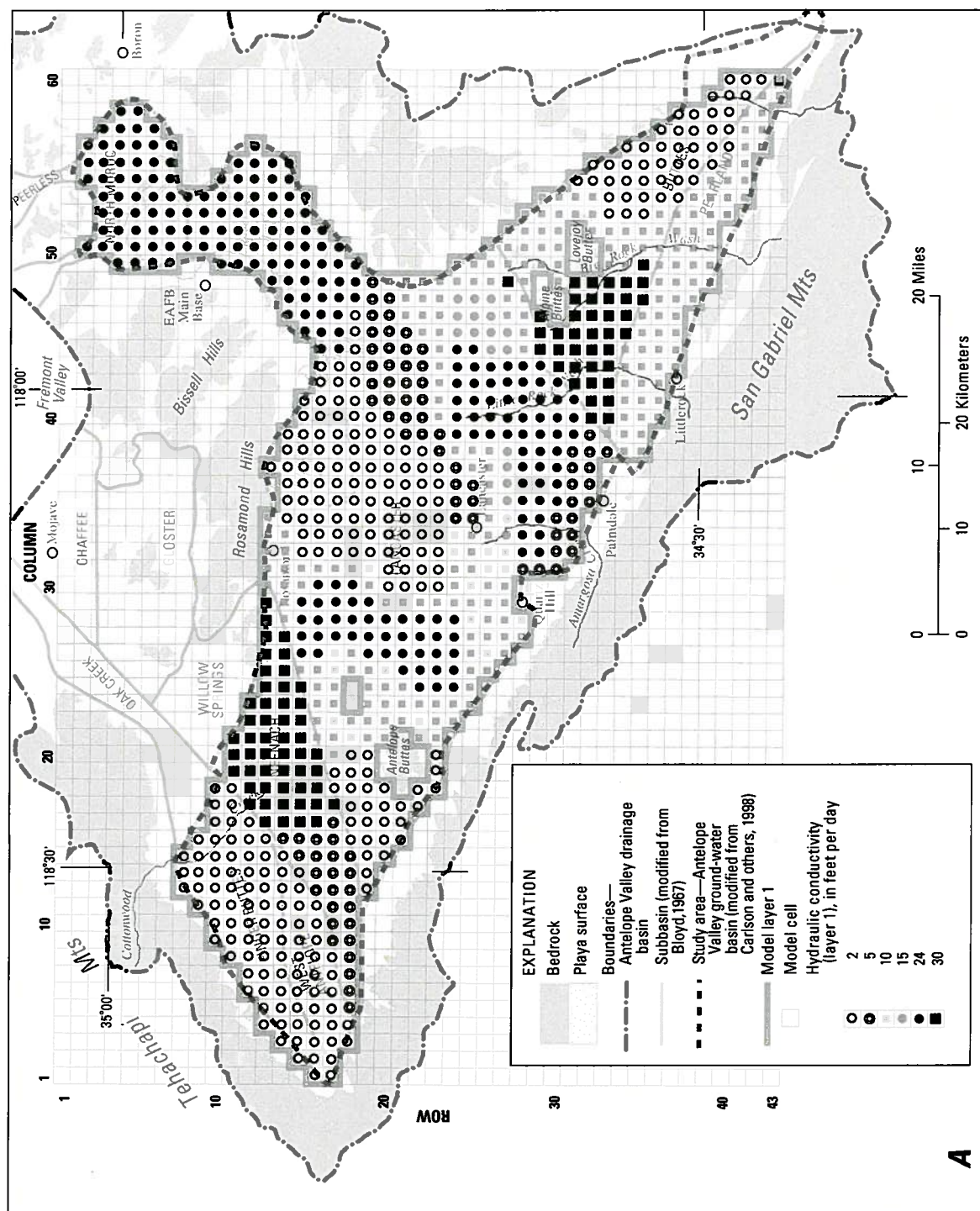


**Figure 18.** Areal distribution of (A) hydraulic conductivity for layer 1 and transmissivity for (B) layer 2 and (C) layer 3 in the ground-water flow model of the Antelope Valley ground-water basin, California.

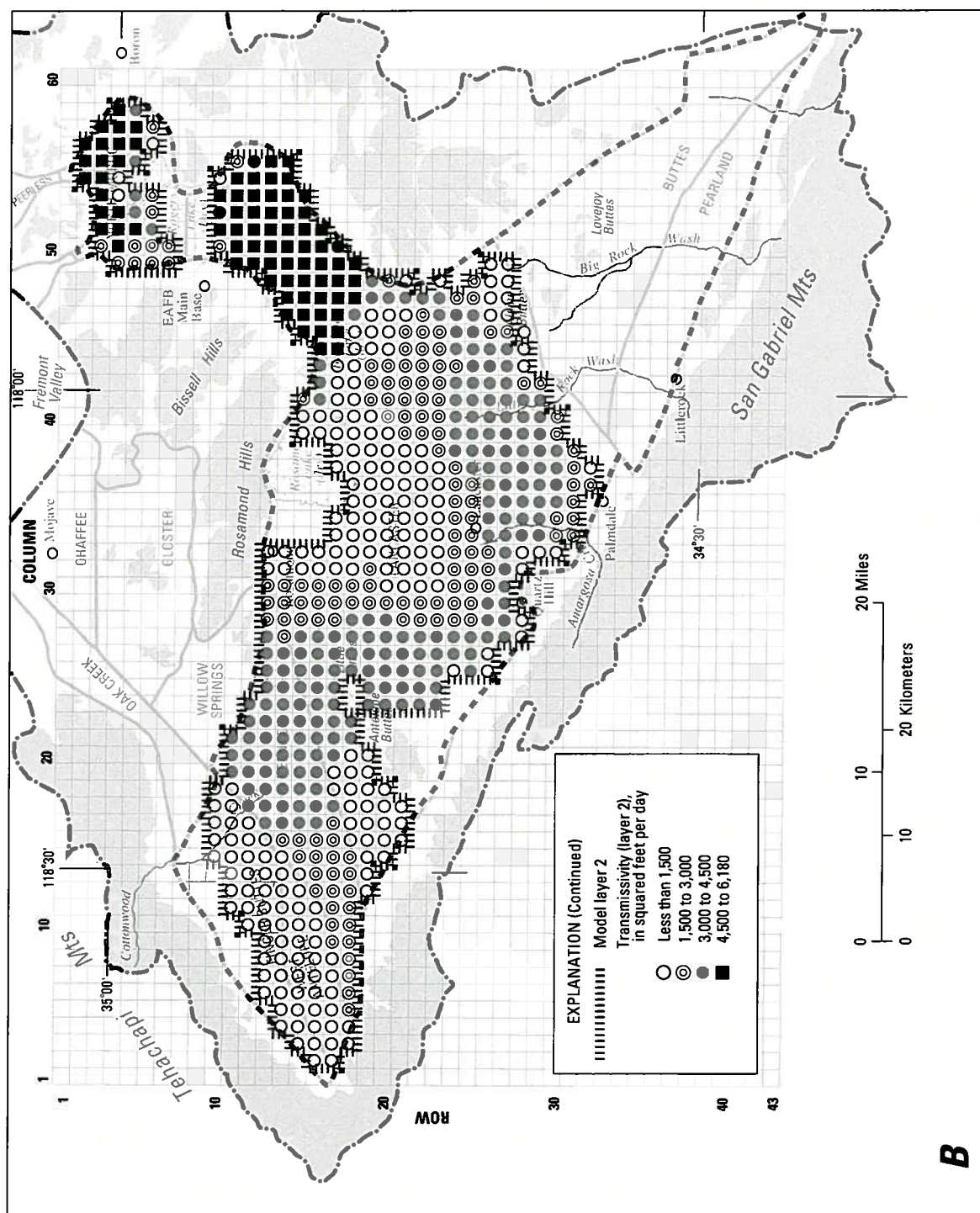


**Figure 18.**—Continued.



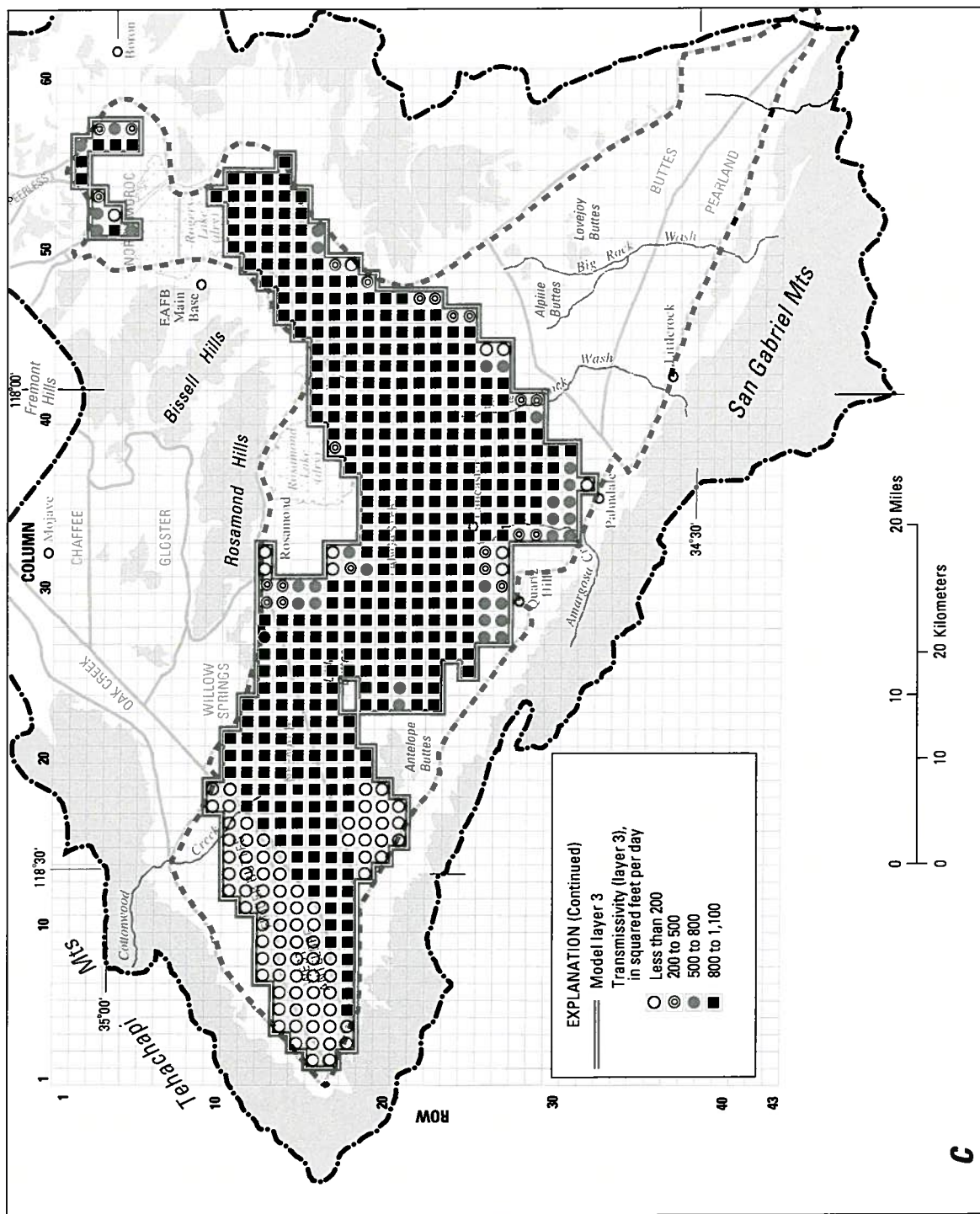


Figure 18.—Continued.

Transmissivity was specified for layers 2 and 3 in the model. Transmissivity was calculated outside the model using horizontal hydraulic conductivity and layer thickness. The horizontal hydraulic conductivity used to calculate the initial values of transmissivity for layer 2 was 10 ft/d. The thickness of layer 2 is 400 ft, except where the altitude of bedrock is higher than the 1,550 ft above sea level. During the calibration process, the horizontal hydraulic conductivity of layer 2 was adjusted in some areas to represent a distribution of sediments, which, in most cases, are coarse near the mountain fronts and fine near the valley center. For the area surrounding Rosamond Lake and south nearly to the city of Lancaster, the horizontal hydraulic conductivity used to calculate transmissivity for layer 2 was decreased to 2 ft/d. A transition zone having a horizontal hydraulic conductivity of 5 ft/d was specified between this area and the area to the south, which has a hydraulic conductivity of 10 ft/d. As required in layer 1, the horizontal hydraulic conductivity of layer 2 was decreased from 10 ft/d to 2 ft/d for the Finger Buttes and West Antelope subbasins and the western part of the Neenach subbasin. The horizontal hydraulic conductivity around the city of Palmdale was decreased from 10 ft/d to 5 ft/d to simulate the measured water-level declines in this area. Transmissivity for the area around Edwards Air Force Base was calculated using a horizontal hydraulic conductivity of 15 ft/d (Nishikawa and others, 2001). The calibrated transmissivities of layer 2 ([fig. 18B](#)) ranged from 11 to 6,000 ft<sup>2</sup>/d.

The transmissivity of layer 3 was calculated using a hydraulic conductivity of 2 ft/d. The thickness of layer 3 is 550 ft, except where the altitude of bedrock is greater than 1,000 ft above sea level. The transmissivities of layer 3 ([fig. 18C](#)) ranged from 24 to 1,100 ft<sup>2</sup>/d and were not adjusted during the calibration process.

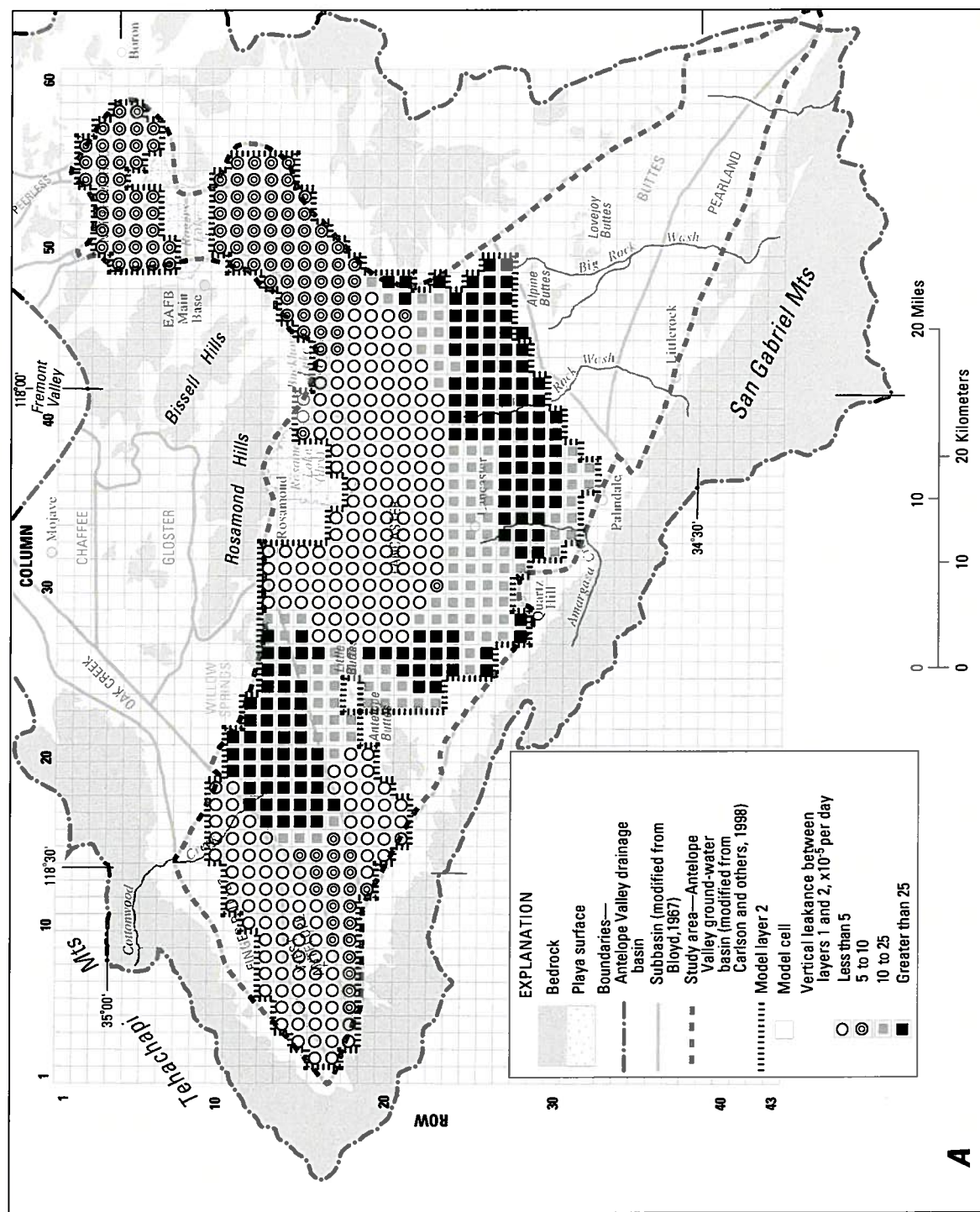
The vertical leakance between layers was calculated outside of the model using equation 2. The vertical hydraulic conductivity of a layer that contains lacustrine deposits was assumed equal to  $1.0 \times 10^{-2}$  ft/d. The vertical hydraulic conductivity of a layer that does not contain lacustrine deposits was assumed equal to one-hundredth of the horizontal hydraulic conductivity of that layer. Vertical-leakance values were recalculated to reflect changes in horizontal hydraulic conductivity, transmissivity, and saturated thickness. The final calibrated values for vertical leakance ranged from  $5.1 \times 10^{-8}$  to  $8.1 \times 10^{-4}$  ft/d between layers 1 and 2 and

from  $7.1 \times 10^{-6}$  to  $1.04 \times 10^{-4}$  ft/d between layers 2 and 3 ([fig. 19](#)). Calibration of vertical leakance in the model was difficult because the vertical hydraulic-head gradient has been measured at only a few sites.

Barriers to horizontal ground-water flow, such as faults, simulated in the model are shown in [figure 11](#) and the final calibrated hydraulic characteristic values are presented in [table 5](#). The hydraulic characteristic value of most of the faults simulated in this model initially were based on results from previous ground-water flow models [barriers 1–4 (Durbin, 1978) and barriers 5–7 (Nishikawa and others, 2001)]. The initial hydraulic-characteristic values of the barriers were modified during the calibration process to obtain acceptable water-level differences across the barriers. The northwest-southeast trending barrier (8), southeast of Lovejoy Buttes, was added to the model because the simulated water levels for well 6N/9W-11N1 ([fig. 15](#)) were consistently too high in the absence of a partial barrier to flow. Additional data are needed to verify the existence, location, and extent of this barrier. Barrier 9 ([fig. 11](#)) was added to the model to simulate the change in horizontal-flow characteristics where lacustrine deposits rise towards land surface and transect the upper and middle aquifers south of Rogers Lake (dry) ([fig. 3](#)). At this location, the lacustrine deposits may restrict the horizontal flow of ground water to areas of pumping to the south (Rewis, 1995, [fig. 4](#)). The delay and attenuated response, to pumpage, of water levels in well 8N/10W-8R3, located north of where the lacustrine deposits transect the upper and middle aquifers, compared to water levels in well 8N/11W-34D2, located south of the lacustrine deposits, could not be simulated without simulating a partial barrier (barrier 9, [fig. 11](#)) to ground-water flow at this location.

Initial values of specific yield in layer 1 were adjusted for several parts of the study area during the calibration process. The specific-yield values specified for the Neenach subbasin (0.12), for some parts of the Lancaster subbasin (0.12), and for areas east and north of Rogers Lake (0.10) were decreased from initial values (0.15 to 0.20). The calibrated specific-yield value for the part of the Lancaster subbasin near Lancaster (0.12) is consistent with values estimated using coupled microgravity and water-level data (0.13) (Jim Howle, U.S. Geological Survey, written commun., 2002). The specific-yield value specified for the area around Rosamond Lake (0.10) was increased from the initial value (0.05). The final distribution of specific yield (layer 1) is shown in [figure 20](#).





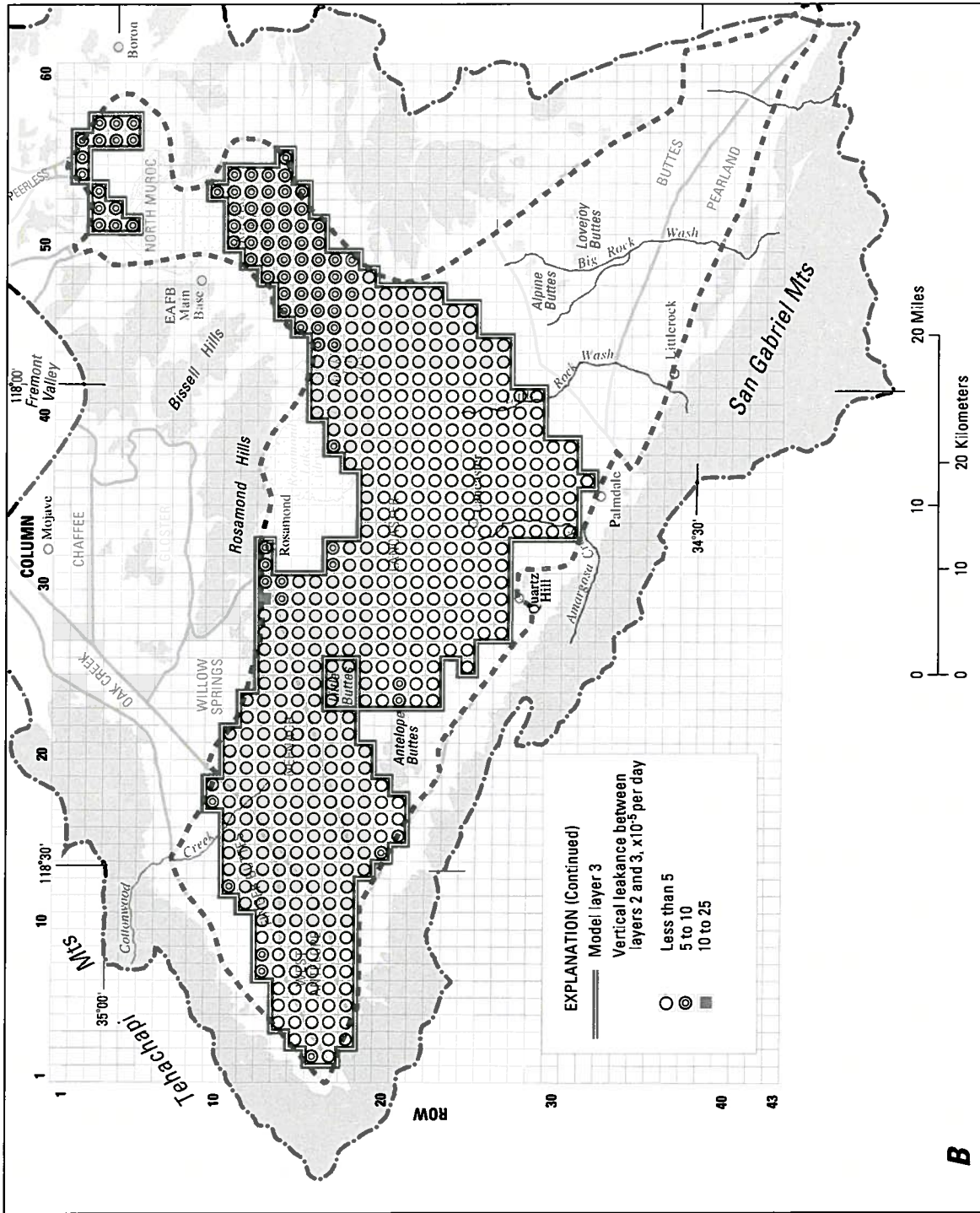
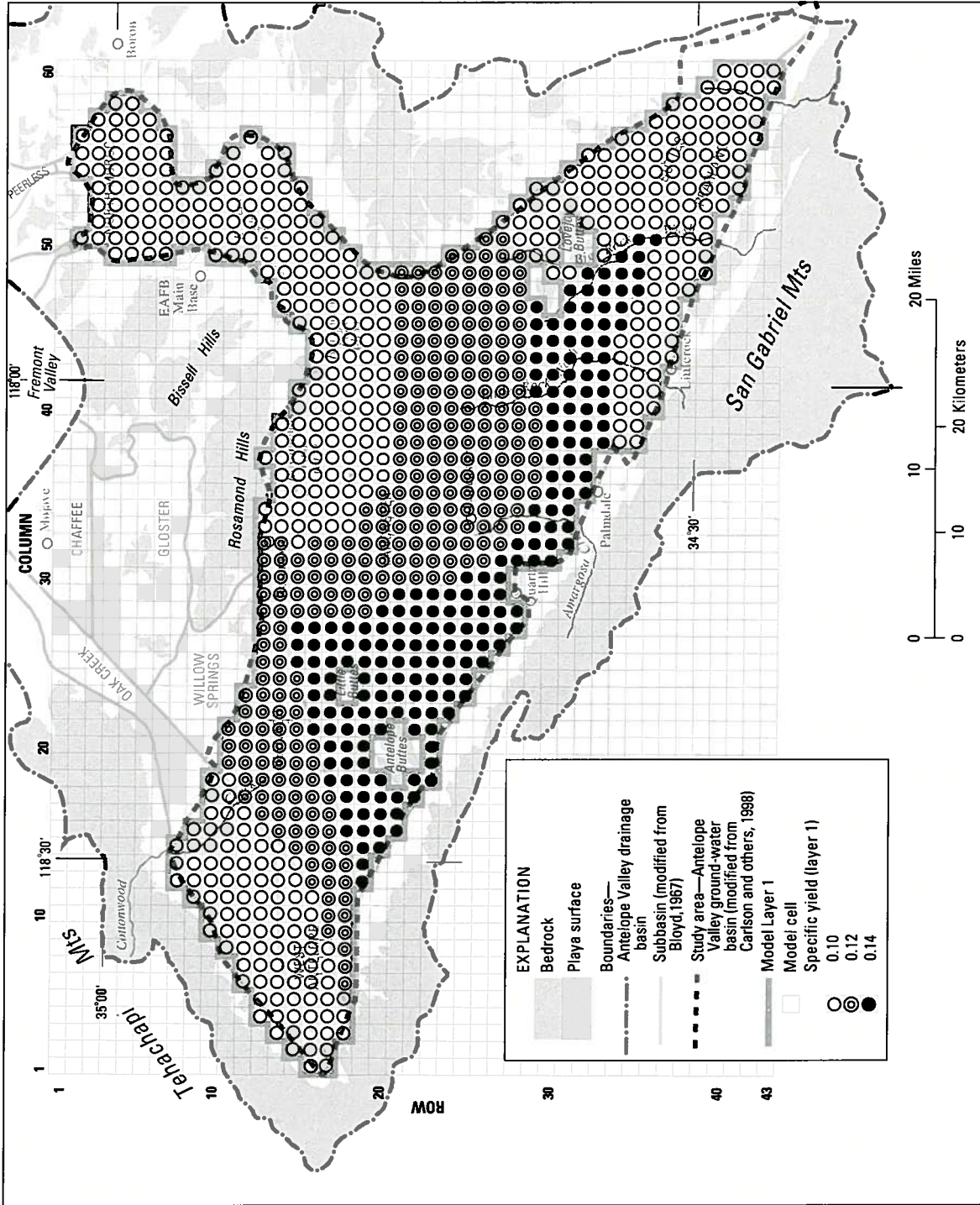


Figure 19—Continued.



**Figure 20.** Areal distribution of specific yield in layer 1 of the ground-water flow model in the Antelope Valley ground-water basin, California.



The initial storage coefficients representing the compressibility of water and elastic skeletal storage were not changed during the calibration process. The storage coefficient representing the compressibility of water ranged from  $0.3 \times 10^{-4}$  to  $5.1 \times 10^{-4}$  in layer 1 (fig. 21A) and from  $0.1 \times 10^{-4}$  to  $1.7 \times 10^{-4}$  in layer 2 (fig. 21B), depending upon the thickness of saturated sediments in these layers. The elastic skeletal storage coefficient ranged from  $1.0 \times 10^{-4}$  to  $2.07 \times 10^{-3}$  in layer 1 (fig. 22A) and from  $1.2 \times 10^{-5}$  to  $6.8 \times 10^{-4}$  in layer 2 (fig. 22B). The final inelastic storage coefficient was calculated using an inelastic skeletal specific storage of  $1.6 \times 10^{-4} \text{ ft}^{-1}$ , which is between the inelastic skeletal specific storage values for thick aquitards ( $3.5 \times 10^{-4} \text{ ft}^{-1}$ ) and thin aquitards ( $4.0 \times 10^{-5} \text{ ft}^{-1}$ ) reported by Sneed and Galloway (2000). The inelastic skeletal storage coefficient ranged from  $2.9 \times 10^{-3}$  to  $3.11 \times 10^{-2}$  in layer 1 (fig. 23A) and from  $3.2 \times 10^{-5}$  to  $2.88 \times 10^{-2}$  in layer 2 (fig. 23B). An inelastic skeletal storage coefficient was not specified for areas where subsidence has not been measured historically.

Calibrated preconsolidation head ranged from 0 to 160 ft below steady-state water levels in the area where subsidence was simulated (fig. 24). The preconsolidation head was adjusted until the timing of the onset of simulated subsidence matched measured subsidence. The variability in the calibrated preconsolidation head can be attributed to overconsolidation of the alluvium. Overconsolidation of an alluvial basin can be caused by removal of overburden by erosion, prehistoric ground-water level declines, desiccation, and diagenesis (Holzer, 1981).

Irrigation-return flows were simulated as 30 percent of the annual quantity of water applied for agricultural irrigation. During the transient-state calibration process it was determined that irrigation-return flows recharged the underlying aquifer 10 years after the water was applied for irrigation. The calibrated delay between the application of irrigation water and the recharge of the irrigation-return flows

was supported by the results of a simple unsaturated-zone model completed for this study using representative soil properties and depth to water measurements (Alan Flint, U.S. Geological Survey, written commun., 1999). Irrigation-return flows were applied directly to the model cells where agricultural pumping was simulated. In addition, irrigation-return flows were applied to the model cells where imported water was used for irrigation (fig. 12).

## Model Results

### Water Levels

Water-level hydrographs for 19 wells were used to compare simulated and measured water levels over time (fig. 25) (well locations shown on figure 15). The measured water levels for two wells (8N/10W-1Q3 and 8N/10W-4E1) were combined into one hydrograph to form a more complete period of record. The simulated water levels generally matched the trends of the measured water levels but did not always match the magnitude.

Twelve of the hydrographs compared simulated and measured water levels in the Lancaster subbasin. In general, the simulated water levels matched the measured water declines of more than 300 ft, which began in the 1920s, soon after pumpage exceeded estimates of natural recharge. In the southern part of the Lancaster subbasin (wells 6N/11W-19E6 and 7N/11W-31M1), the simulated water levels were more than 20 ft higher than the measured water levels after about 1970. In the western part of the Lancaster subbasin, east of Antelope Buttes (wells 7N/14W-13A1, 8N/13W-35M1, and 8N/14W-23G1), the simulated water levels generally were about 30 ft lower than the measured water levels. In the northeastern part of the Lancaster subbasin, the simulated water level in layer 3 at well 8N/10W-8R3 was about 20 ft lower than the measured water level after the late-1950s.

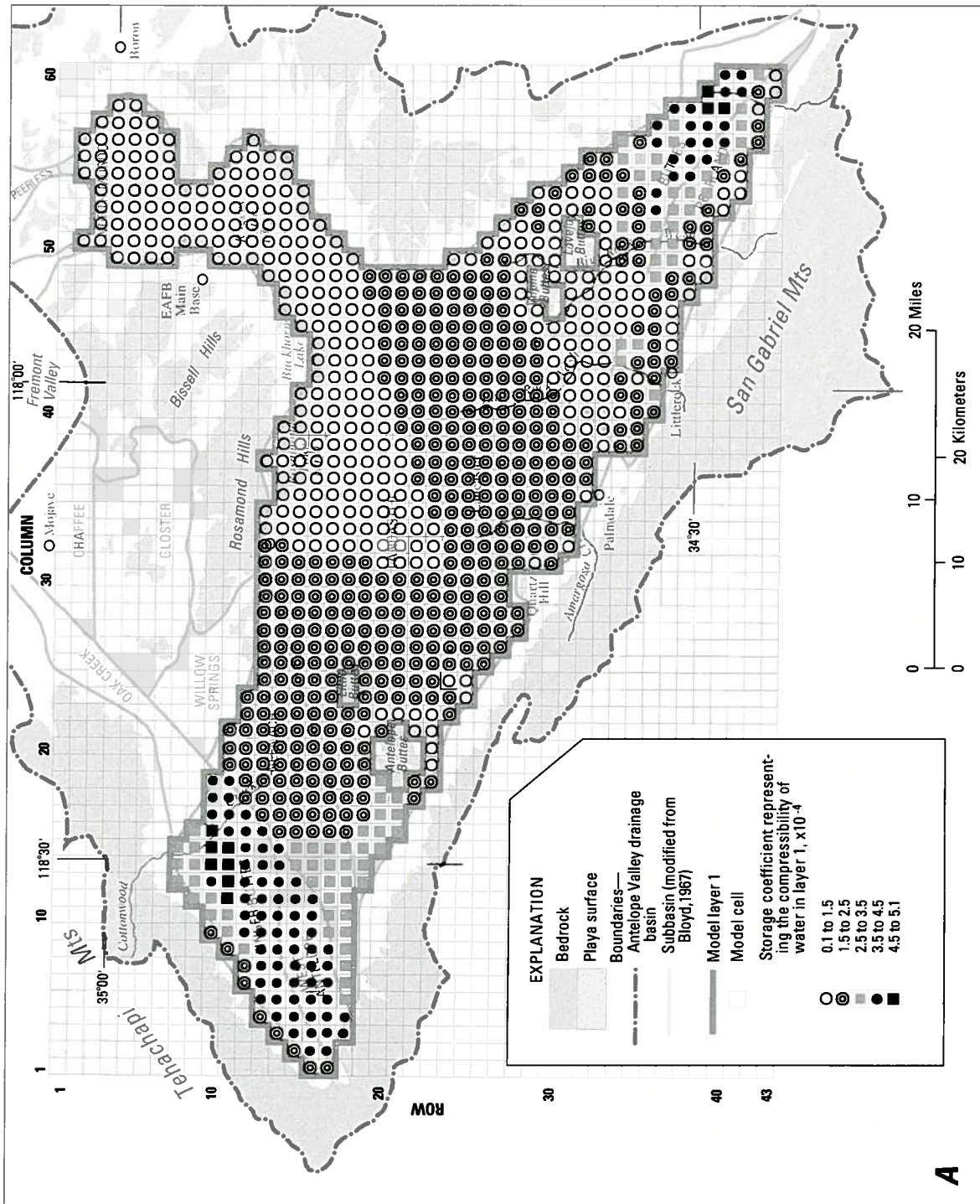


**Figure 21.** Areal distribution of the storage coefficient representing the compressibility of water for (A) layer 1 and (B) layer 2 in the ground-water flow model of the Antelope Valley ground-water basin, California.



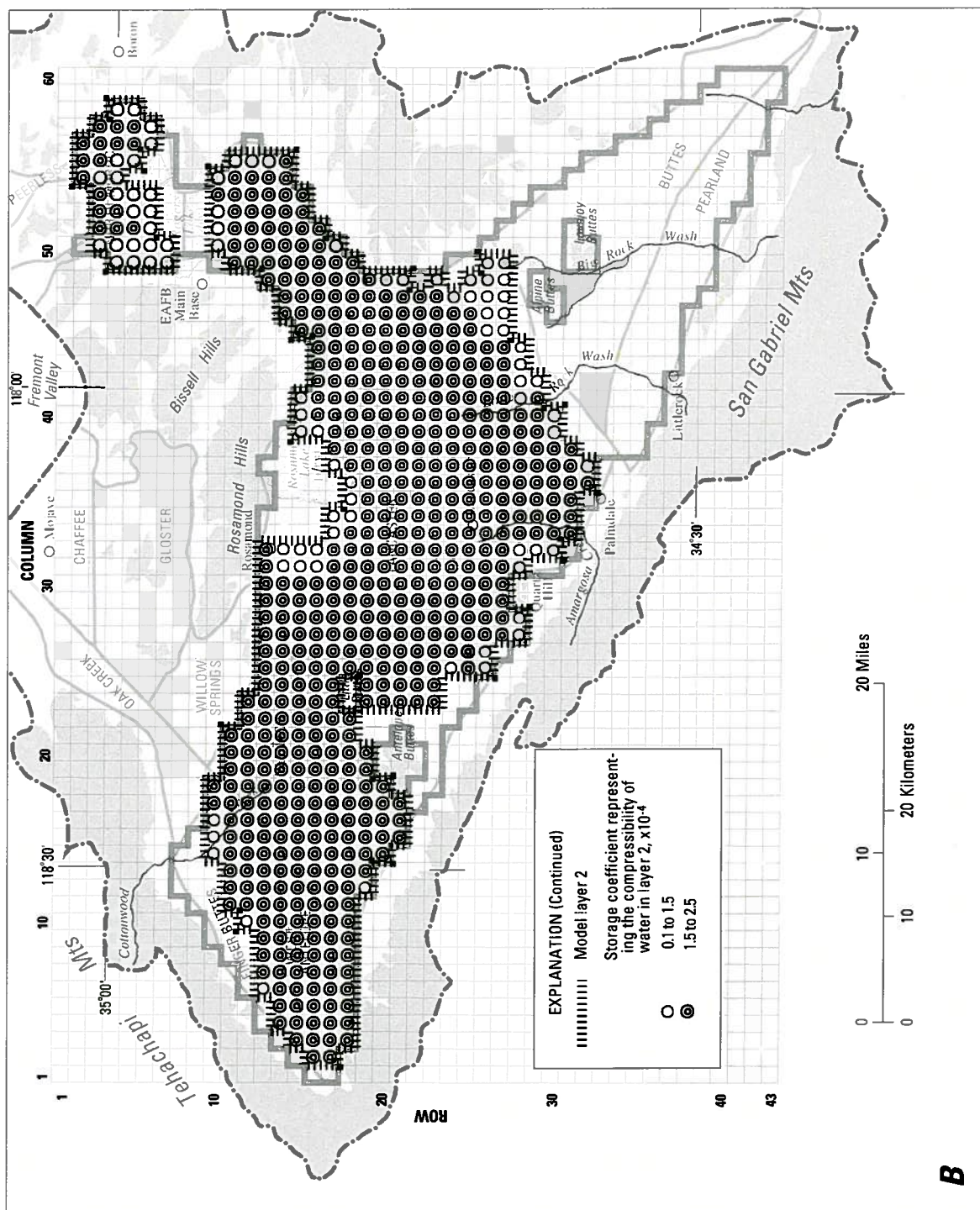
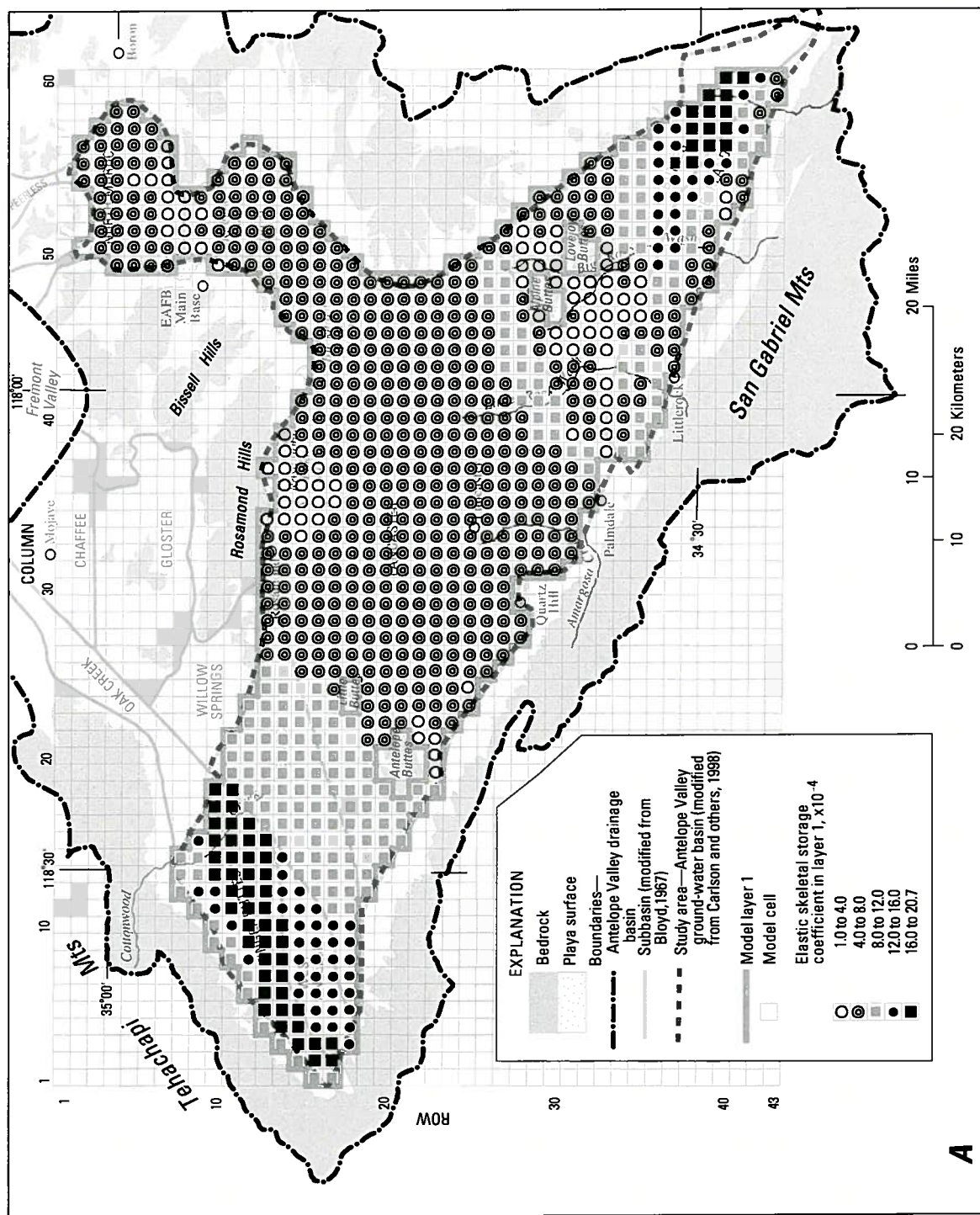


Figure 21.—Continued.



**Figure 22.** Areal distribution of the elastic skeletal storage coefficient for (A) layer 1 and (B) layer 2 in the ground-water flow model of the Antelope Valley ground-water basin, California.





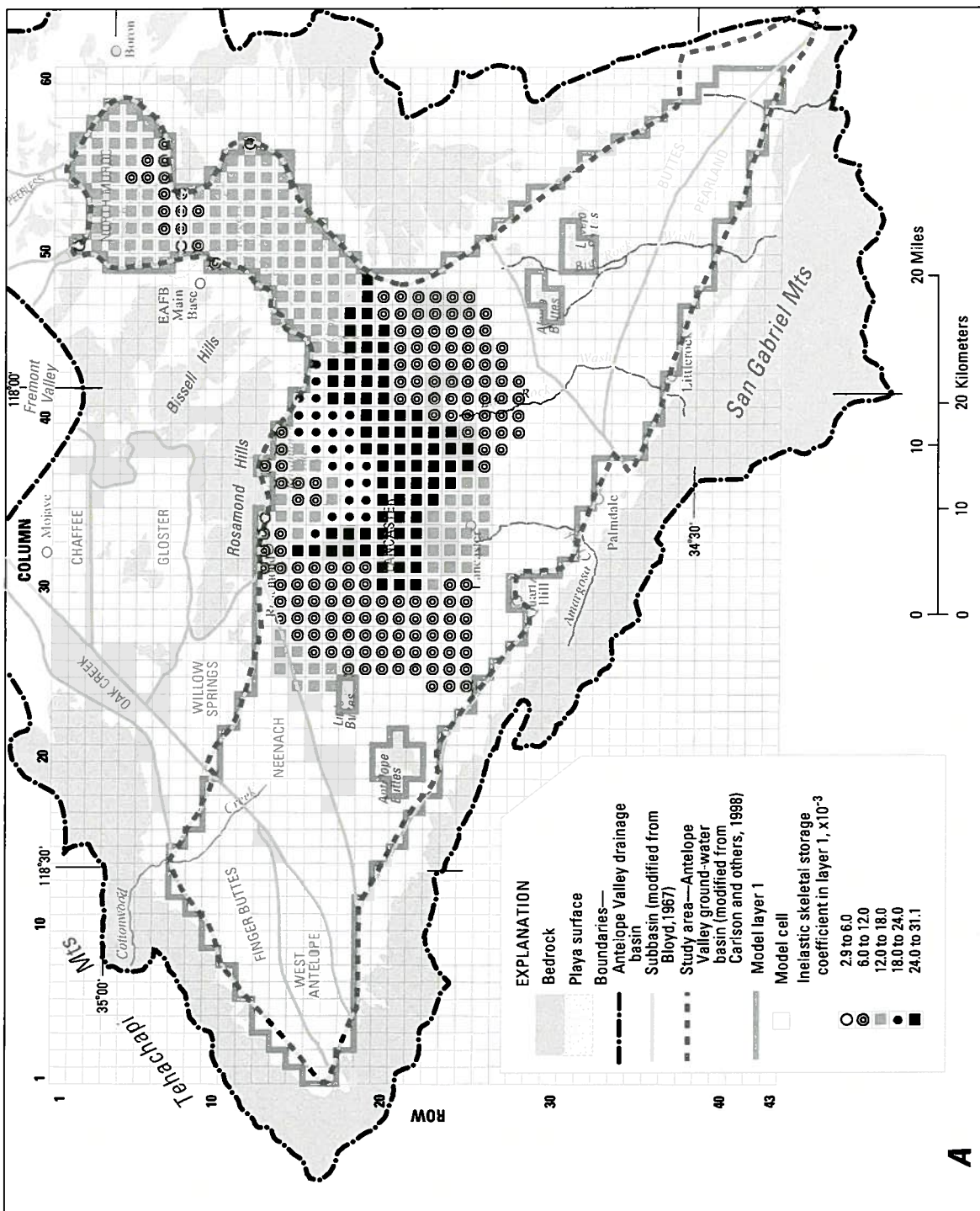


**Figure 23.** Areal distribution of the inelastic skeletal storage coefficient for  $(A)$  layer 1 and  $(B)$  layer 2 in the ground-water flow model of the Antelope Valley ground-water basin, California.





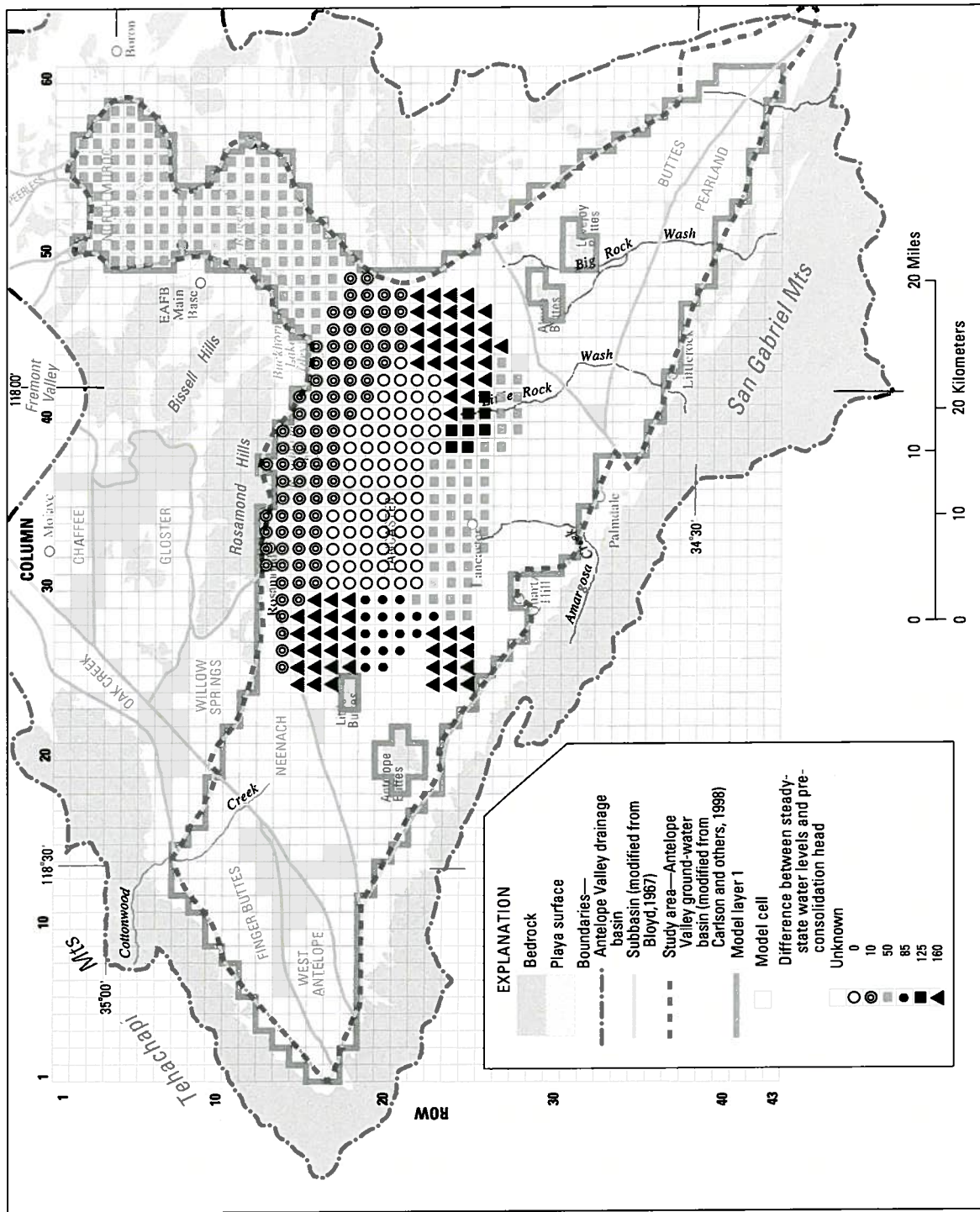


**Figure 24.** Difference between steady-state water levels and preconsolidation head in the ground-water flow model of the Antelope Valley ground-water basin, California.

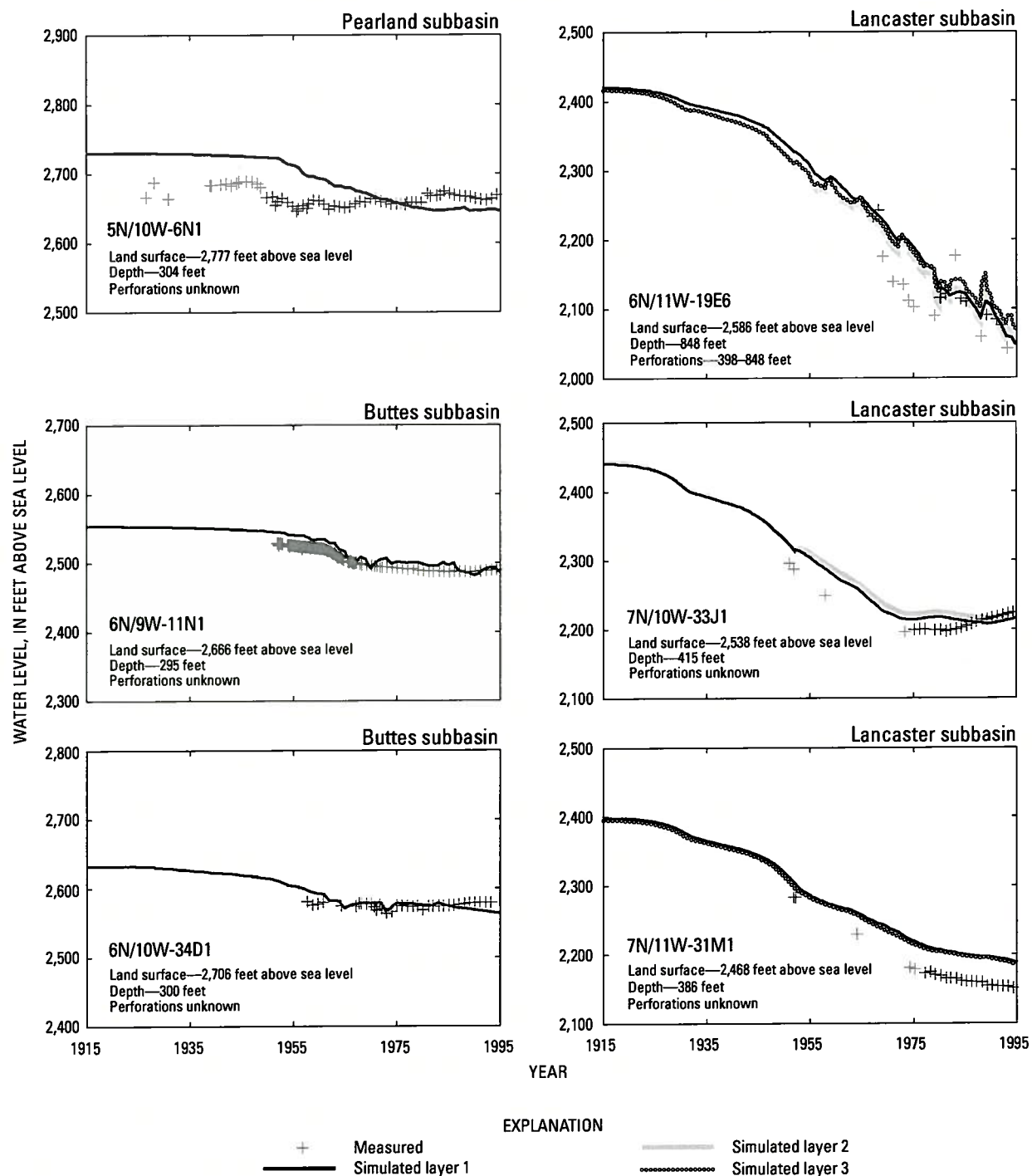


**Figure 25.** Measured and simulated water levels at selected wells in the Antelope Valley ground-water basin, California, 1915–95. (See figure 15 for location of wells.)

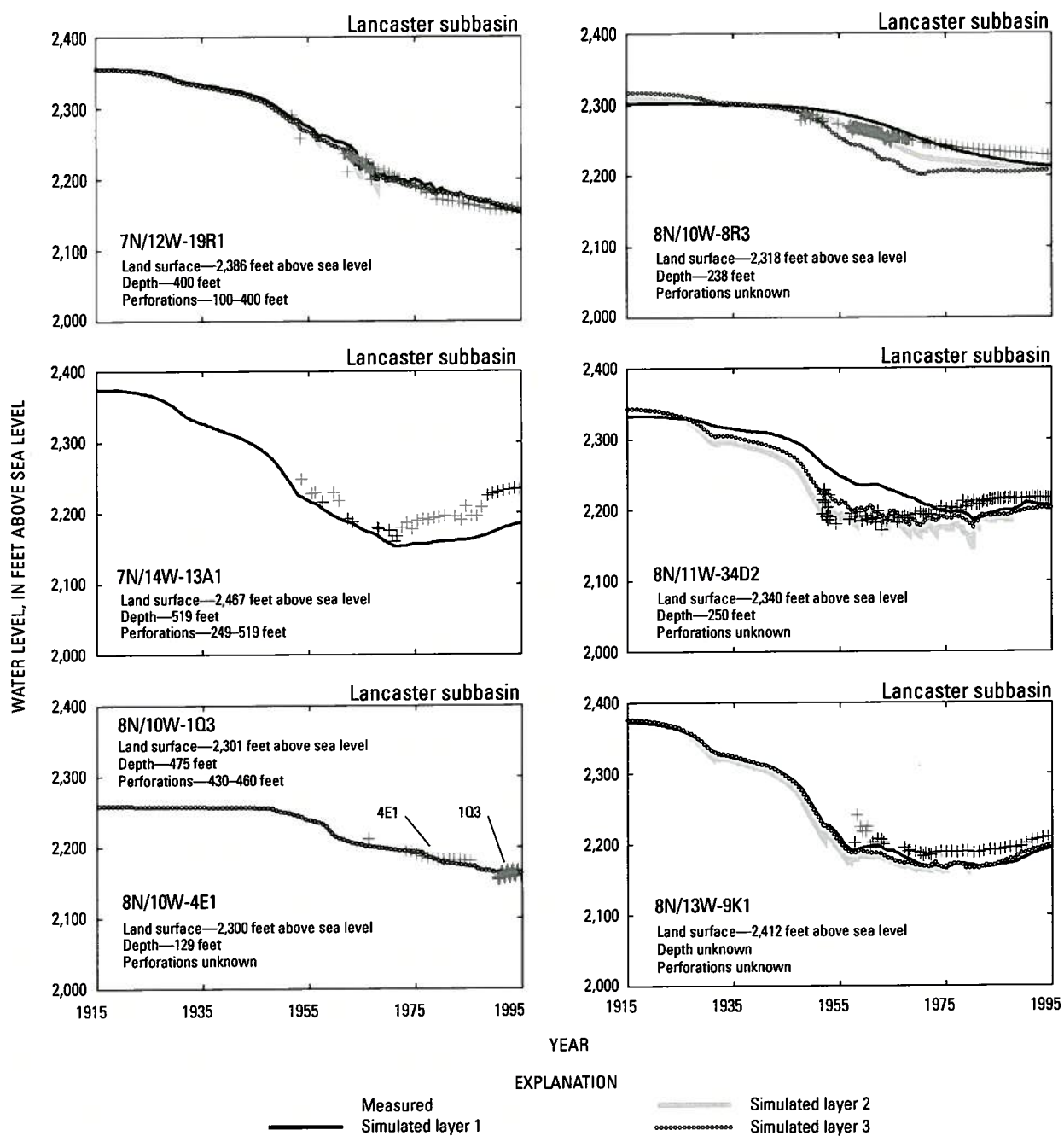


Figure 25.—Continued.

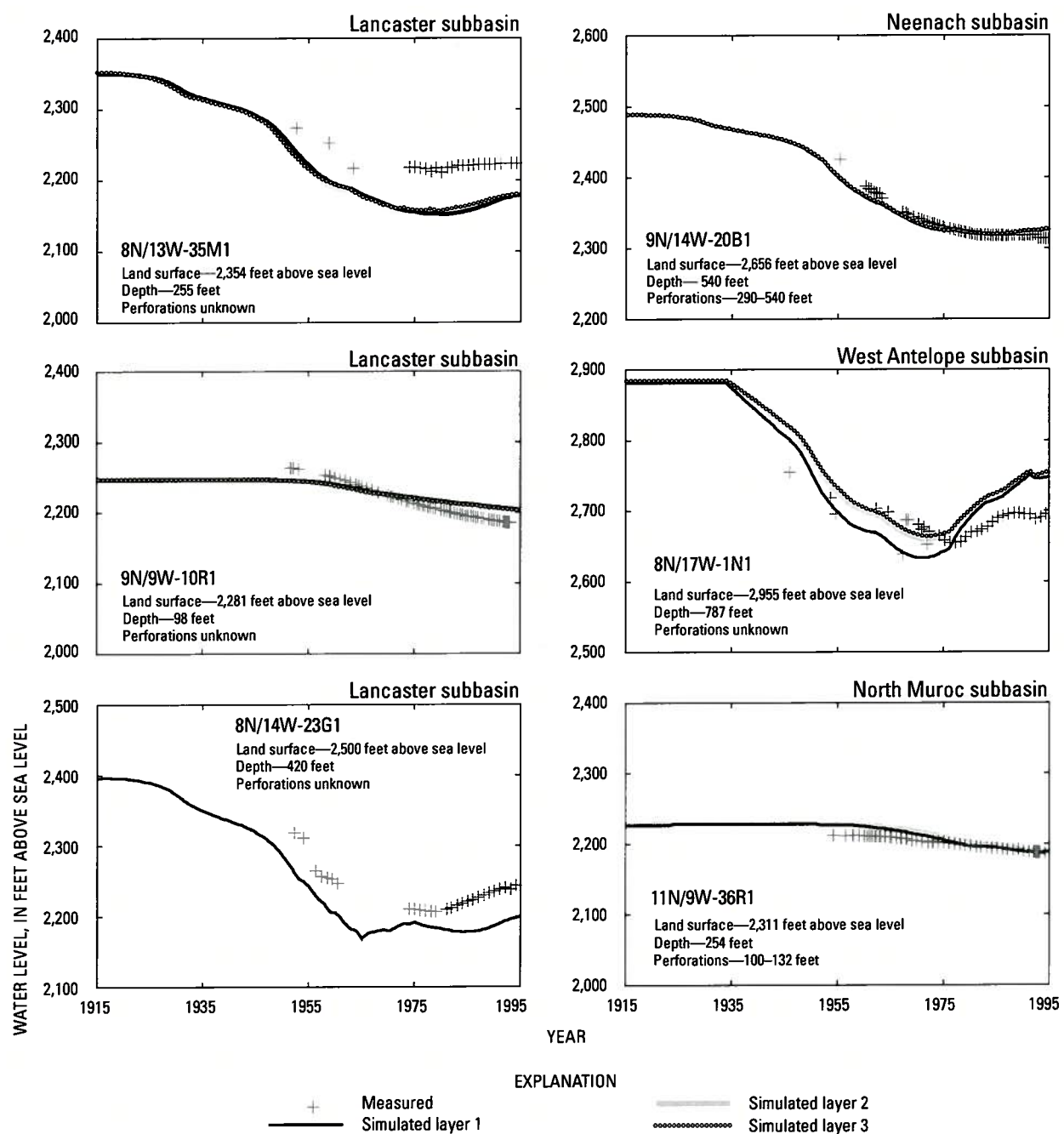


Figure 25—Continued.



In the Buttes subbasin (wells 6N/9W-11N1 and 6N/10W-34D1), measured and simulated water levels matched well. In the Pearland subbasin (well 5N/10W-6N1), the simulated water levels were higher than the measured water levels prior to the 1970s and were lower than the measured water levels after the 1970s. The simulated water level was about 24 ft lower than the measured water level by the end of the simulation period. In the West Antelope subbasin (well 8N/17W-1N1), the simulated water levels matched the measured water levels well through the 1970s, but the simulated water level overestimated the measured water-level rise that occurred from the mid 1970s to 1995 by as much as 65 ft. Because there are virtually no data for this subbasin in the pumpage database, the estimated quantity and distribution of annual pumpage were based only on 1961 land-use data. In addition to the lack of pumpage data for the West Antelope subbasin, there are uncertainties in the estimates of the quantity and distribution of recharge from irrigation-return flows of water delivered by the AVEK Water Agency. It was assumed that water delivered by the AVEK Water Agency was applied to fields near the area where the water was discharged from the aqueduct. In the Neenach subbasin (well 9N/14W-20B1) and the North Muroc subbasin (well 11N/19W-36R1), the simulated and measured water levels matched well.

The simulated water-level gradient between model layers at the end of the model simulation (1995) was compared with the measured February 1996 water-level gradient at nested piezometers 7N/12W-27F5–27F7 in the southern part of the Lancaster subbasin and the measured October 1995 water-level gradient at nested piezometers 8N/10W-1Q1-3 in the northeastern part of the Lancaster subbasin (table 7). In the southern Lancaster subbasin, the measured data indicated that there was an upward water-level gradient, with the largest water-level difference (14 ft) between the middle and lower aquifers (layers 2 and 3). The lacustrine deposits separate the middle and lower aquifers in this part of the subbasin (fig. 3). The model simulated an upward water-level gradient at this site, but the simulated water-level difference between layers 2 and 3 was 11 ft, about 3 ft less than measured water-level difference. In the northeastern Lancaster subbasin, the measured data indicated that there was a small downward water-level gradient; the difference between measured water levels for wells 8N/10W-1Q1-1Q3 was 1–2 ft (table 7). Simulated water levels for the three layers were within 1 ft of each other at this site, indicating little or no vertical ground-water movement at this site. The lacustrine deposits are near land surface in this area (Londquist and others, 1993); these three wells are all perforated below the lacustrine levels.

**Table 7.** Measured and simulated water levels at two sites with nested piezometers completed at multiple depths in the Lancaster subbasin of the Antelope Valley ground-water basin, California.

[State well No.: See well-numbering in text]

Layer	Wells 7N/12W-27F5–7 Land surface altitude: 2,443 feet above sea level				Wells 8N/10W-1Q1–3 Land surface altitude: 2,301 feet above sea level			
	State well No. of nested piezometer	Perforated interval, in feet below land surface	Measured water level, February 1996, in feet above sea level	Simulated water level, 1995, in feet above sea level	State well No. of nested piezometer	Perforated interval, in feet below land surface	Measured water level, October 1995, in feet above sea level	Simulated water level, 1995, in feet above sea level
1	<sup>1</sup> 27F7	505–525	2,138	2,156	<sup>2</sup> 1Q3	430–460	2,154	2,159
2	<sup>1</sup> 27F6	705–725	2,139	2,161	<sup>2</sup> 1Q2	605–635	2,153	2,159
3	<sup>2</sup> 27F5	905–925	2,153	2,172	<sup>2</sup> 1Q1	980–1,010	2,152	2,160

<sup>1</sup> Above the lacustrine clay.

<sup>2</sup> Below the lacustrine clay.

Contours of simulated 1995 and measured 1996 (Carlson and others, 1998) water levels for layer 1 are shown in figure 26. The measured 1996 water-level contours were assumed to be representative of 1995 conditions and were used to qualitatively evaluate the transient-state simulation. The model does a good job of simulating the observed pumping depression near Lancaster and Palmdale, an area of recent extensive pumping for public supply. However, the simulated water levels were lower than measured water levels in the eastern and western parts of the Lancaster subbasin. These areas historically were subject to large amounts of agricultural pumping, which was not metered and therefore difficult to estimate. The simulated flat water-level gradient in the northern part of the Lancaster subbasin and the North Muroc subbasin matched the measured water-level gradient in these areas. The simulated water levels matched the measured water levels throughout most of the Neenach subbasin except in the western part of the subbasin. The simulated and measured water levels matched well in much of the Buttes and Pearland subbasins even though the hydrogeologic and agricultural pumpage data for these subbasins were limited. Because of insufficient water-level data for the Finger Buttes, West Antelope, and parts of the Buttes and Pearland subbasins, comparisons could not be made for these subbasins.

#### Land Subsidence

Simulated land subsidence was compared with periodic surveyed (measured) data collected at 10 bench marks (locations shown in [figure 15](#)) since about 1930 ([fig 27](#)). Simulated land subsidence is the sum of aquifer-system compaction in layers 1 and 2. Recall, compaction was assumed to be minimal in layer 3, and was not simulated in the model. Pumping-induced subsidence is controlled by the thickness of compressible sediments, preconsolidation head, and water-level declines. Where simulated water-level declines are greater than actual water-level declines or where the aquifer contains a smaller thickness of compressible sediments than was represented in the model, simulated subsidence will be larger than measured subsidence. Simulated subsidence will be smaller than measured subsidence where simulated water-level declines are less than actual water-level declines or where the aquifer contains a larger thickness of compressible sediments than was represented in the model. The MODFLOW package,

IBS1, simulates an instantaneous release of water from the compressible interbeds (aquitards) and thus subsidence—and does not account for hydrodynamic lag or residual compaction. This limitation is further discussed in the “Limitations of the Model” section of this report.

Simulated subsidence closely matched measured subsidence at all of the 10 bench marks ([fig. 27](#)). Simulated subsidence began at most locations in the 1930s, but as early as 1928 at bench mark BM 479 and as late as 1950 at bench mark BM 474. Simulated subsidence was greatest (6.3 ft) at bench mark BM 474 near Lancaster; the maximum measured subsidence also was at this bench mark (Ikehara and Phillips, 1994). Large water-level declines have occurred near bench mark BM 474, and the aquifer contains a substantial thickness of compressible sediments. Simulated subsidence was lowest at bench marks BM 2317 (2.0 ft) and BM 823 (2.17 ft). These two sites are located in areas that historically have been subjected to large amounts of pumpage, but the aquifers in the area contain fewer compressible sediments than aquifers in areas that had greater subsidence. Simulated subsidence also was small at bench mark BM 483 (2.2 ft) even though the aquifer in this area consists of a thick layer of compressible sediments. However, there has been minimal pumping and associated water-level declines in this area. The abrupt increase in simulated subsidence at bench marks BM 474, BM 2180, and BM 2317 in about 1977 corresponds to the increase in pumpage for public supply in 1977 ([fig. A2](#)) from the aquifer near these benchmarks.

Although water levels have declined more than 200 ft throughout much of the study area, subsidence greater than 1 ft has been documented only in the central part of the study area ([fig. 8](#)). In the area around Palmdale where water-level declines have been large, no measurable subsidence has occurred (Ikehara and Phillips, 1994). This lack of measurable subsidence suggests that this area may not be susceptible to subsidence even though lacustrine deposits have been mapped in this area ([fig 3](#)). However, it is possible that water levels may not yet have declined below the preconsolidation head in areas where subsidence has not occurred. Subsidence can be simulated in the model only where inelastic storage is specified; inelastic storage was specified only for areas where measurements have shown that subsidence has occurred.

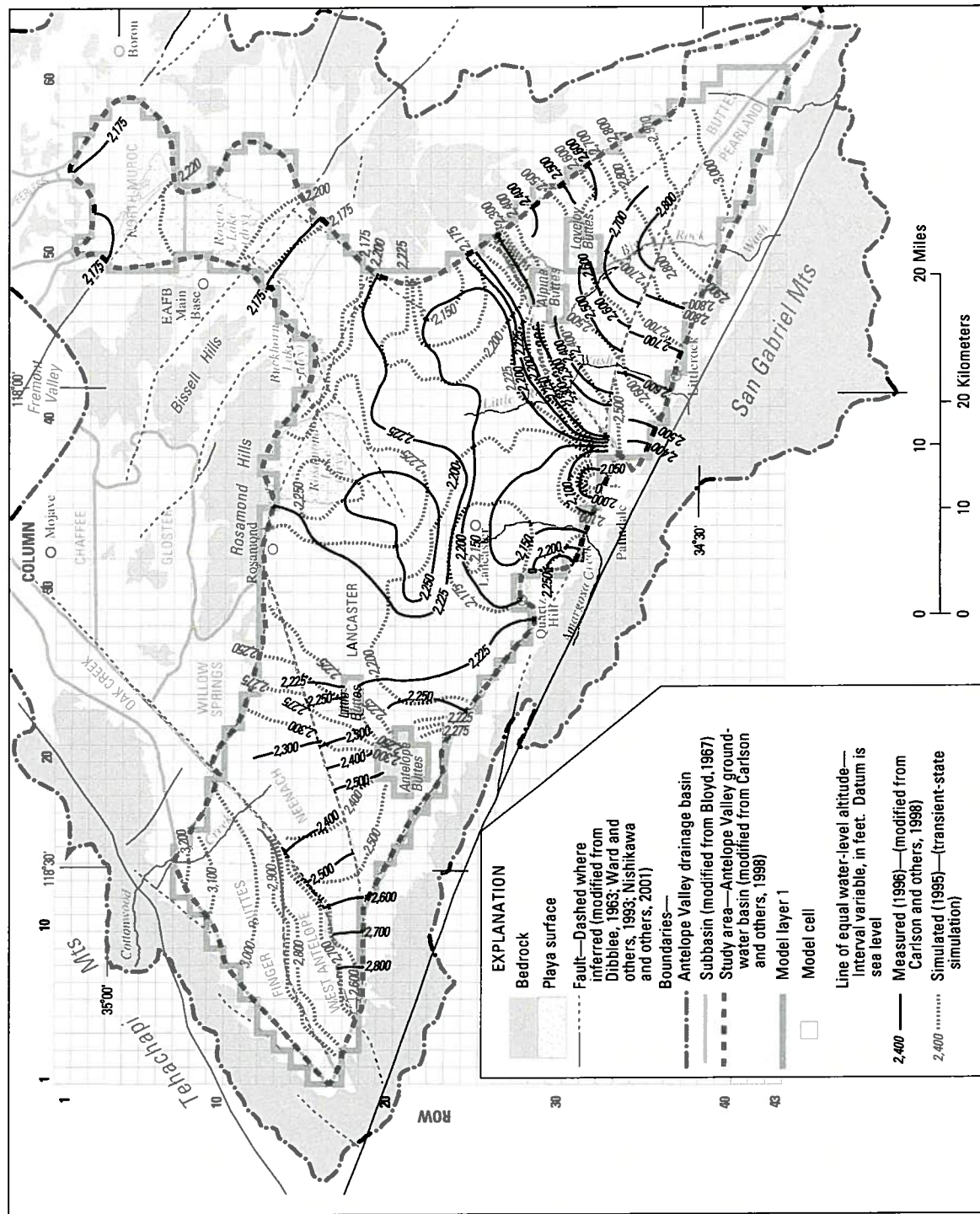


**Figure 26.** Measured (1996) and simulated (1995) water levels from the ground-water flow model of the Antelope Valley ground-water basin, California.

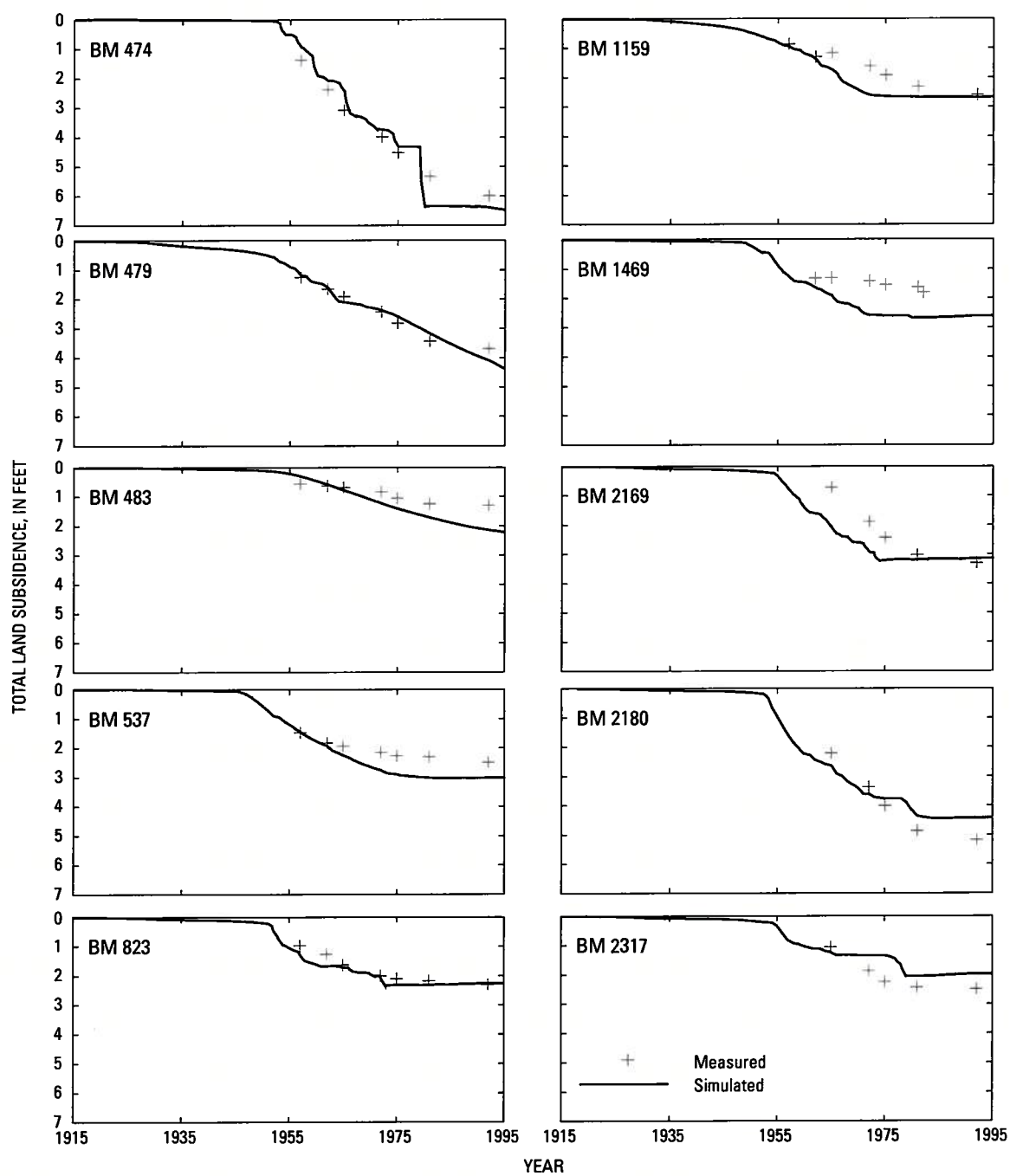


**Figure 27.** Measured and simulated total land subsidence at selected bench marks in the Antelope Valley ground-water basin, California, 1915–95. (See figure 15 for location of bench marks.)



Because of the limitations of the IBS1 Package in the simulation of subsidence, a match between simulated and measured subsidence does not necessarily indicate that the parameters controlling subsidence are accurately represented by the model. The IBS1 Package simulates subsidence instantaneously after a decline in hydraulic head below the preconsolidation head; therefore, there is no time delay in the simulated subsidence to account for the delayed equilibration of hydraulic heads in the thick aquitards. Results from the one-dimensional model developed by Sneed and Galloway (2000) and from a comparison of paired water-level and subsidence data (Ikehara and Phillips, 1994) ([fig. 9](#)) indicate that the delayed drainage of the thick aquitards is an important process in the occurrence of subsidence in Antelope Valley. Therefore, the model developed for this study may simulate subsidence before it actually occurs, owing to hydrodynamic lag and residual compaction and land subsidence. Additionally, simulated subsidence is dependent on simulated drawdown. If simulated drawdown does not match actual drawdown, then simulated subsidence would not be expected to match measured subsidence.

#### Water Budget

The simulated annual volumes of recharge, discharge, and change in storage for Antelope Valley ground-water basin are shown in [table 8](#). Graphs of the simulated recharge and discharge components are shown in [figure 28](#) and a graph of simulated cumulative change in storage for the entire simulation period is shown in [figure 29](#). Results of the transient-state simulation indicate that more than 8.5 million acre-ft of ground water was removed from storage during 1915–95, with most of the storage change occurring between about 1945 and 1975. Ground-water storage changed little during the final 10 years of simulation period because discharge by pumpage had declined sufficiently to be balanced by recharge ([fig. 28C](#)).

Water-budget components for the steady-state simulation and for the 1949–53 and 1991–95 periods of the transient-state simulation are shown in [figure 30](#).

The period 1949–53 was selected to represent hydrologic conditions when agricultural production and associated pumping were at a maximum. The period 1991–95 was selected to represent conditions when pumping for public supply was at a maximum and pumping for agricultural production was at a recent minimum. All components of recharge and the pumpage component of discharge were specified as model input parameters. Evapotranspiration, ground-water underflow, flow between model layers, and changes in aquifer and aquitard storage were simulated by the model.

Under steady-state conditions, recharge from natural sources was balanced by discharge as evapotranspiration and ground-water underflow from the North Muroc subbasin into Fremont Valley, and there were no changes in aquifer storage. The simulated ground-water underflow into Fremont Valley (400 acre-ft/yr) was less than half the amount estimated by Durbin (1978) (1,000 acre-ft/yr). Flow northward across the Willow Springs Fault, southeast of Rogers Lake (barrier 7, [fig. 11](#)), was equal to the ground-water underflow out of the basin. The model simulated that evapotranspiration averaged 29,900 acre-ft/yr; all of the evapotranspiration simulated by the model occurred in the area of alkali soils ([fig. 4](#)) south of barrier 7.

During the 1949–53 period, pumpage reached a maximum of 363,000 acre-ft/yr and recharge averaged 77,800 acre-ft/yr ([fig. 30](#)). Model results indicate that 79 percent of the ground-water pumpage was contributed from aquifer storage (71 percent or 265,100 acre-ft/yr) and aquitard storage (8 percent or 21,600 acre-ft/yr); of that, more than 95 percent (263,000 acre-ft/yr) came from storage in layer 1. Leakage from layer 1 into layer 2 accounted for 86 percent of the ground-water pumpage from layer 2. Recharge from irrigation-return flows was 47,500 acre-ft/yr; about 13 percent of the ground-water pumpage ([fig. 30](#)). As a result of water-level declines ([fig. 25](#)), evapotranspiration was only 1,200 acre-ft/yr, about 4 percent compared to steady-state conditions.

**Table 8.** Simulated recharge, discharge, and change in storage for the Antelope Valley ground-water basin, California, 1915–95

[AVEK, Antelope Valley–East Kern Water Agency: evapotranspiration and ground-water underflow are model computed values; all other values are model inputs: units in thousand acre-feet: positive numbers represent water added to the system, and negative numbers represent water removed from the system]

Year	Recharge				Discharge				Total		Change in storage	
	Irrigation-return flows											
	Pumpage	AVEK deliveries	Natural	Waste-water	Pumpage		Natural		Recharge	Discharge	Annual	Cumulative
					Public supply	Agriculture	Total	Evapotranspiration				
1915	0.0	0.0	30.3	0.0	0.0	0.0	-30.0	-0.4	30.3	-30.4	-0.1	-0.1
1916	.0	.0	30.3	.0	-1.9	-1.9	-29.8	-4	30.3	-32.1	-1.8	-1.9
1917	.0	.0	30.3	.0	-5.8	-5.8	-29.5	-4	30.3	-35.7	-5.4	-7.3
1918	.0	.0	30.3	.0	-10.7	-10.7	-28.9	-4	30.3	-40.0	-9.7	-17.0
1919	.0	.0	30.3	.0	-15.5	-15.5	-28.1	-4	30.3	-44.0	-13.7	-30.7
1920	.0	.0	30.3	.0	-22.3	-22.3	-27.1	-4	30.3	-49.8	-19.5	-50.2
1921	.0	.0	30.3	.0	-29.1	-29.1	-25.8	-4	30.3	-55.3	-25.0	-75.2
1922	.0	.0	30.3	.0	-35.9	-35.9	-24.4	-4	30.3	-60.7	-30.4	-105.6
1923	.0	.0	30.3	.0	-40.7	-40.7	-23.0	-4	30.3	-64.1	-33.8	-139.4
1924	.0	.0	30.3	.0	-50.4	-50.4	-21.4	-4	30.3	-72.2	-41.9	-181.3
1925	.0	.0	30.3	.0	-64.0	-64.0	-19.7	-4	30.3	-84.1	-53.8	-235.1
1926	.6	.0	30.3	.0	-81.4	-81.4	-17.8	-4	30.9	-99.6	-68.7	-303.8
1927	1.7	.0	30.3	.0	-98.9	-98.9	-15.8	-4	32.0	-115.1	-83.1	-386.9
1928	3.2	.0	30.3	.0	-125.1	-125.1	-13.7	-4	33.5	-139.2	-105.7	-492.6
1929	4.7	.0	30.3	.0	-157.1	-157.1	-11.6	-4	35.0	-169.1	-134.1	-626.7
1930	6.7	.0	30.3	.0	-166.8	-166.8	-9.8	-4	37.0	-177.0	-140.0	-766.7
1931	8.7	.0	30.3	.0	-145.4	-145.4	-8.6	-4	39.0	-154.4	-115.4	-882.1
1932	10.8	.0	30.3	.0	-108.6	-108.6	-7.8	-4	41.1	-116.8	-75.7	-957.8
1933	12.2	.0	30.3	.0	-99.9	-99.9	-7.3	-4	42.5	-107.6	-65.1	-1,022.9
1934	15.1	.0	30.3	.0	-111.8	-111.8	-6.7	-4	45.4	-118.9	-73.5	-1,096.4
1935	19.2	.0	30.3	.0	-119.1	-119.1	-6.2	-4	49.5	-125.7	-76.2	-1,172.6
1936	24.4	.0	30.3	.0	-124.3	-124.3	-5.7	-4	54.7	-130.4	-75.7	-1,248.3
1937	29.7	.0	30.3	.0	-132.5	-132.5	-5.3	-4	60.0	-138.2	-78.2	-1,326.5
1938	37.5	.0	30.3	.0	-136.7	-136.7	-4.9	-4	67.8	-142.0	-74.2	-1,400.7
1939	47.1	.0	30.3	.0	-143.9	-143.9	-4.6	-4	77.4	-148.9	-71.5	-1,472.2
1940	50.0	.0	30.3	.0	-149.1	-149.1	-4.2	-4	80.3	-153.7	-73.4	-1,545.6
1941	43.6	.0	30.3	.0	-156.4	-156.4	-3.8	-4	73.9	-160.6	-86.7	-1,632.3
1942	32.6	.0	30.3	.0	-165.7	-165.7	-3.3	-4	62.9	-169.4	-106.5	-1,738.8

**Table 8.** Simulated recharge, discharge, and change in storage for the Antelope Valley ground-water basin, California, 1915–95—Continued

Year	Recharge					Discharge				Total			Change in storage	
	Irrigation-return flows					Natural				Total			Annual	
	Pumpage	AVEK deliveries	Natural	Waste-water	Public supply	Agriculture	Total	Evapotranspiration	Ground-water underflow	Recharge	Discharge	Annual	Cumulative	
1943	30.0	.0	30.3	.0	.0	-176.0	-176.0	-2.9	-.4	60.3	-179.3	-119.0	-1,857.8	
1944	33.5	.0	30.3	.0	.0	-186.4	-186.4	-2.6	-.4	63.8	-189.4	-125.6	-1,983.4	
1945	35.7	.0	30.3	.0	.0	-204.0	-204.0	-2.4	-.4	66.0	-206.8	-140.8	-2,124.2	
1946	37.3	0.0	30.3	0.0	0.0	-226.8	-226.8	-2.1	-0.4	67.6	-229.3	-161.7	-2,285.9	
1947	39.8	.0	30.3	.0	-.6	-269.6	-270.2	-1.9	-.4	70.1	-272.5	-202.4	-2,488.3	
1948	41.0	.0	30.3	.0	-.7	-330.4	-331.1	-1.7	-.4	71.3	-333.2	-261.9	-2,750.2	
1949	43.2	.0	30.3	.0	-.6	-357.0	-357.6	-1.6	-.4	73.5	-359.6	-286.1	-3,036.3	
1950	44.7	.0	30.3	.0	-.7	-373.0	-373.7	-1.4	-.4	75.0	-375.5	-300.5	-3,336.8	
1951	46.9	.0	30.3	.0	-.8	-394.6	-395.4	-1.2	-.5	77.2	-397.1	-319.9	-3,656.7	
1952	49.7	.0	30.3	.0	-6.7	-333.0	-339.7	-1.0	-.5	80.0	-341.2	-261.2	-3,917.9	
1953	52.8	.0	30.3	.0	-9.2	-339.0	-348.2	-.8	-.5	83.1	-349.5	-266.4	-4,184.3	
1954	55.9	.0	30.3	.0	-9.6	-313.0	-322.6	-.6	-.5	86.2	-323.7	-237.5	-4,421.8	
1955	61.2	.0	30.3	.0	-7.0	-324.5	-331.5	-.5	-.5	91.5	-332.5	-241.0	-4,662.8	
1956	68.0	.0	30.3	.0	-13.5	-332.2	-345.7	-.5	-.5	98.3	-346.7	-248.4	-4,911.2	
1957	80.9	.0	30.3	.0	-13.9	-309.4	-323.3	-.4	-.5	111.2	-324.2	-213.0	-5,124.2	
1958	99.1	.0	30.3	.0	-12.7	-293.6	-306.3	-.3	-.5	129.4	-307.1	-177.7	-5,301.9	
1959	107.1	.0	30.3	.0	-15.6	-301.0	-316.6	-.3	-.5	137.4	-317.4	-180.0	-5,481.9	
1960	111.9	.0	30.3	.0	-16.9	-285.5	-302.4	-.3	-.5	142.2	-303.2	-161.0	-5,642.9	
1961	118.4	.0	30.3	.0	-23.3	-278.5	-301.8	-.3	-.5	148.7	-302.6	-153.9	-5,796.8	
1962	100.0	.0	30.3	.0	-28.5	-284.4	-312.9	-.2	-.5	130.3	-313.6	-183.3	-5,980.1	
1963	101.7	.0	30.3	.0	-22.5	-317.5	-340.0	-.2	-.5	132.0	-340.7	-208.7	-6,188.8	
1964	93.9	.0	30.3	.0	-24.7	-332.5	-357.2	-.2	-.5	124.2	-357.9	-233.7	-6,422.5	
1965	97.4	.0	30.3	.0	-26.5	-331.3	-357.8	-.2	-.4	127.7	-358.4	-230.7	-6,653.2	
1966	99.7	.0	30.3	.0	-29.1	-316.3	-345.4	-.1	-.4	130.0	-345.9	-215.9	-6,869.1	
1967	92.8	.0	30.3	.0	-26.0	-297.8	-323.8	-.1	-.4	123.1	-324.3	-201.2	-7,070.3	
1968	88.1	.0	30.3	.0	-28.6	-279.0	-307.6	-.1	-.4	118.4	-308.1	-189.7	-7,259.9	
1969	90.3	.0	30.3	.0	-35.7	-258.3	-294.0	-.1	-.4	120.6	-294.5	-173.9	-7,433.8	
1970	85.6	.0	30.3	.0	-30.1	-240.0	-270.1	-.1	-.4	115.9	-270.6	-154.7	-7,588.5	
1971	83.5	.0	30.3	.0	-32.3	-217.1	-249.4	-.1	-.3	113.8	-249.8	-136.0	-7,724.6	

**Table 8.** Simulated recharge, discharge, and change in storage for the Antelope Valley ground-water basin, California, 1915–95—Continued

Year	Recharge				Discharge				Total		Change in storage	
	Irrigation-return flows			Waste-water	Pumpage		Evapotran-spiration	Ground-water underflow	Recharge	Discharge	Annual	Cumulative
	Pumpage	AVEK deliveries	Natural		Public supply	Agriculture	Total					
1972	85.3	.0	30.3	.0	-32.4	-192.2	-224.6	-1	115.6	-225.0	-109.4	-7,834.0
1973	95.3	.0	30.3	.0	-33.8	-178.6	-212.4	.0	125.6	-212.7	-87.1	-7,921.1
1974	100.8	.0	30.3	.0	-32.2	-164.9	-197.1	.0	131.1	-197.4	-66.3	-7,987.4
1975	99.4	.0	30.3	.0	-30.3	-161.1	-191.4	.0	129.7	-191.7	-62.0	-8,049.4
1976	94.9	.0	30.3	.0	-31.7	-138.0	-169.7	.0	125.2	-170.0	-44.8	-8,094.2
1977	89.3	.0	30.3	.0	-29.0	-166.3	-195.3	.0	119.6	-195.6	-76.0	-8,170.2
1978	83.7	.0	30.3	.0	-36.4	-155.8	-192.2	.0	114.0	-192.5	-78.5	-8,248.7
1979	77.5	0.0	30.3	0.0	-26.0	-135.3	-161.3	0.0	107.8	-161.6	-53.8	-8,302.4
1980	72.0	.0	30.3	.0	-26.1	-128.4	-154.5	.0	102.3	-154.8	-52.5	-8,354.9
1981	65.1	.0	30.3	.0	-26.9	-93.9	-120.8	.0	95.4	-121.1	-25.7	-8,380.6
1982	57.7	.0	30.3	.0	-25.4	-86.1	-111.5	.0	88.0	-111.8	-23.8	-8,404.4
1983	53.6	.0	30.3	.0	-20.9	-91.7	-112.6	.0	83.9	-112.9	-29.0	-8,433.4
1984	49.5	.0	30.3	.5	-27.0	-80.9	-107.9	.0	80.3	-108.1	-27.8	-8,461.1
1985	48.3	.0	30.3	1.4	-26.5	-64.3	-90.8	.0	80.0	-91.0	-11.0	-8,472.1
1986	41.4	7.9	30.3	2.0	-31.5	-55.1	-86.6	.0	81.6	-86.8	-5.2	-8,477.3
1987	44.4	9.1	30.3	2.9	-33.0	-60.6	-93.6	.0	86.7	-93.8	-7.1	-8,484.4
1988	39.8	10.2	30.3	3.2	-23.1	-47.8	-70.9	.0	83.5	-71.1	12.4	-8,472.0
1989	35.8	13.5	30.3	3.4	-39.1	-33.7	-72.8	.0	82.9	-73.0	9.9	-8,462.0
1990	34.8	14.8	30.3	4.9	-36.2	-34.5	-70.7	.0	84.8	-70.9	13.9	-8,448.2
1991	26.0	16.2	30.3	4.5	-56.5	-47.6	-104.1	.0	77.0	-104.3	-27.3	-8,475.5
1992	24.4	9.8	30.3	5.6	-38.3	-42.7	-81.0	.0	70.1	-81.2	-11.1	-8,486.6
1993	25.7	5.1	30.3	6.5	-33.4	-39.7	-73.1	.0	67.6	-73.3	-5.7	-8,492.3
1994	22.7	4.4	30.3	6.9	-40.2	-35.6	-75.8	.0	64.3	-76.0	-11.7	-8,504.0
1995	18.7	5.0	30.3	7.5	-40.4	-34.1	-74.5	.0	61.5	-74.7	-13.2	-8,517.1



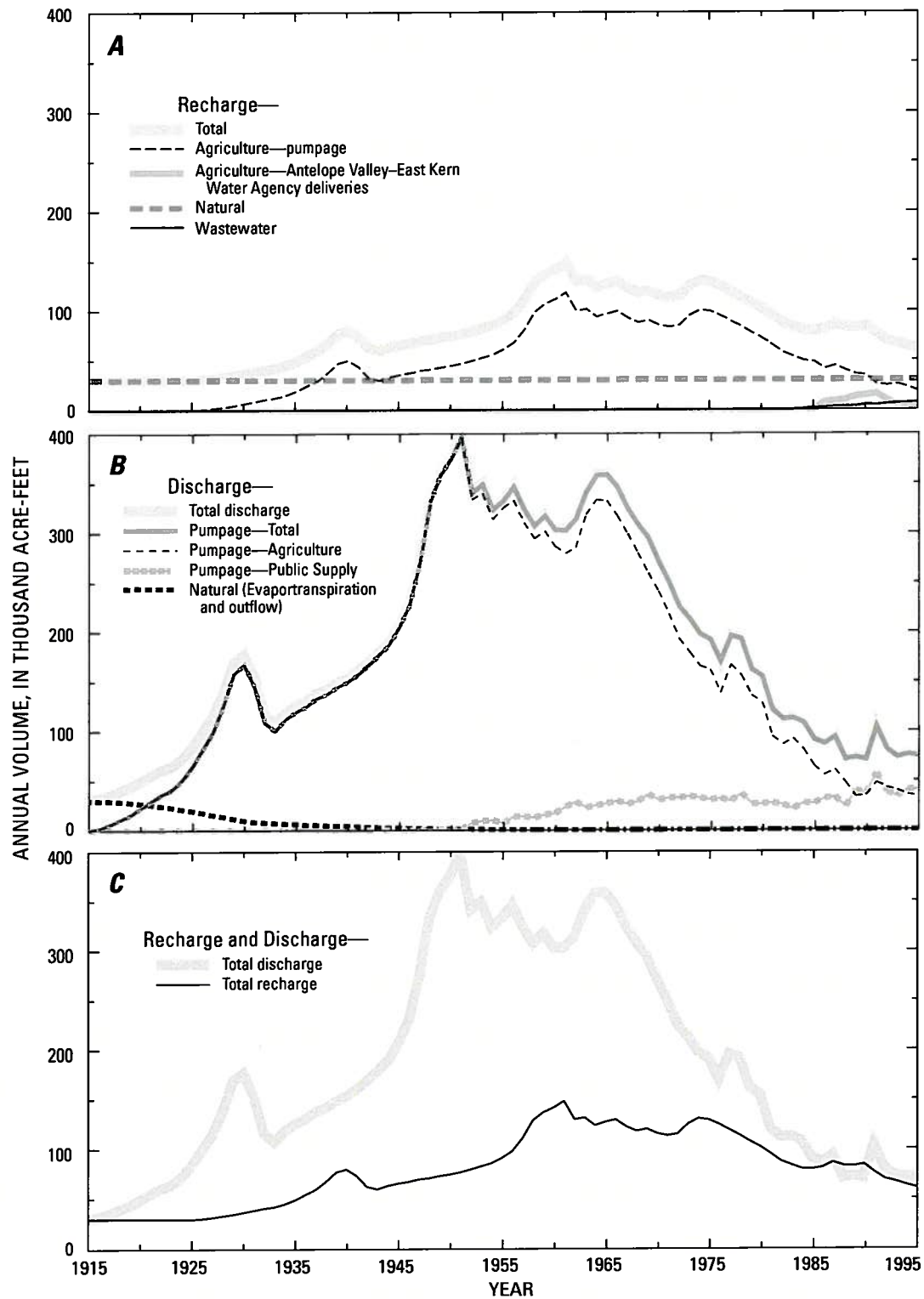


**Figure 28.** Simulated annual volumes of (A) recharge, (B) discharge, and (C) recharge in relation to discharge in the Antelope Valley ground-water basin, California, 1915–95.

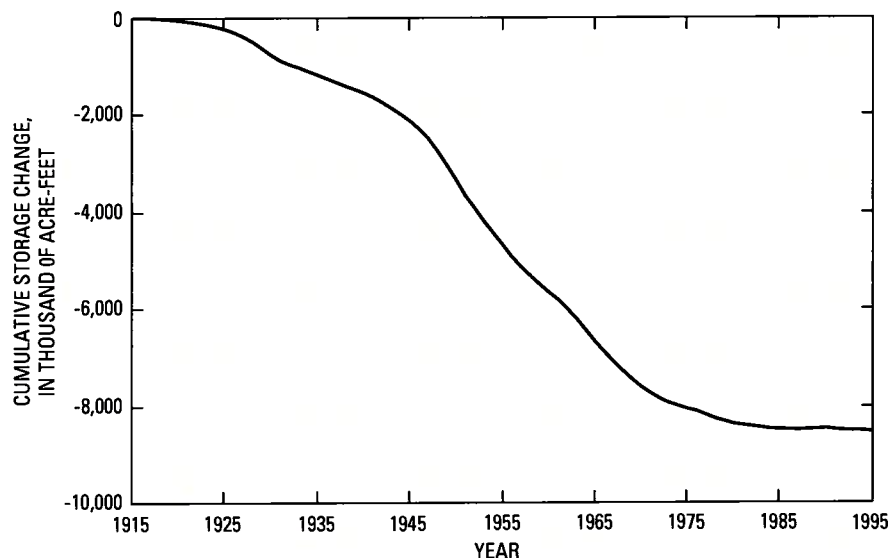


**Figure 29.** Cumulative change in simulated ground-water storage in the Antelope Valley ground-water basin, California, 1915–95.

During the 1991–95 period, pumpage averaged 81,700 acre-ft/yr, which is only 23 percent of the pumpage during the 1949–53 period and total recharge averaged 68,100 acre-ft/yr, which is about 86 percent of the total recharge during the 1949–53 period. Model results indicate that about 13,700 acre-ft/yr of ground water was being removed from aquifer and aquitard storage, which is about 17 percent of the total pumpage. Compaction of the aquitards accounted for 3,800 acre-ft/yr of water being removed from storage, which is 28 percent of the change in storage. Similar to the 1949–53 period, the source of nearly all the ground-water pumpage from layer 2 was leakage from layer 1. Continued water-level declines ([fig. 25](#)), resulted in the cessation of simulated evapotranspiration and a 50-percent reduction of ground-water underflow from the North Muroc subbasin compared to steady-state conditions.

### Model Sensitivity Analysis

A sensitivity analysis was done to determine the sensitivity of the model to changes in model input parameters. Sensitivity analysis can help determine which model parameters have the greatest effect on a model; results of the analysis can guide future data collection efforts that will reduce model errors. The sensitivity simulations were done by changing one input parameter at a time, while holding all others constant. A limitation of this approach is that the effects of simultaneous changes of multiple input parameters are not evaluated. The sensitivity of the model was evaluated by comparing water levels and subsidence from the sensitivity simulations with those from the calibrated transient-state model at the end of the transient period (1995). Sensitivity simulations also were done for the steady-state model; results generally were similar to the results of the transient-state model and therefore are not discussed here.

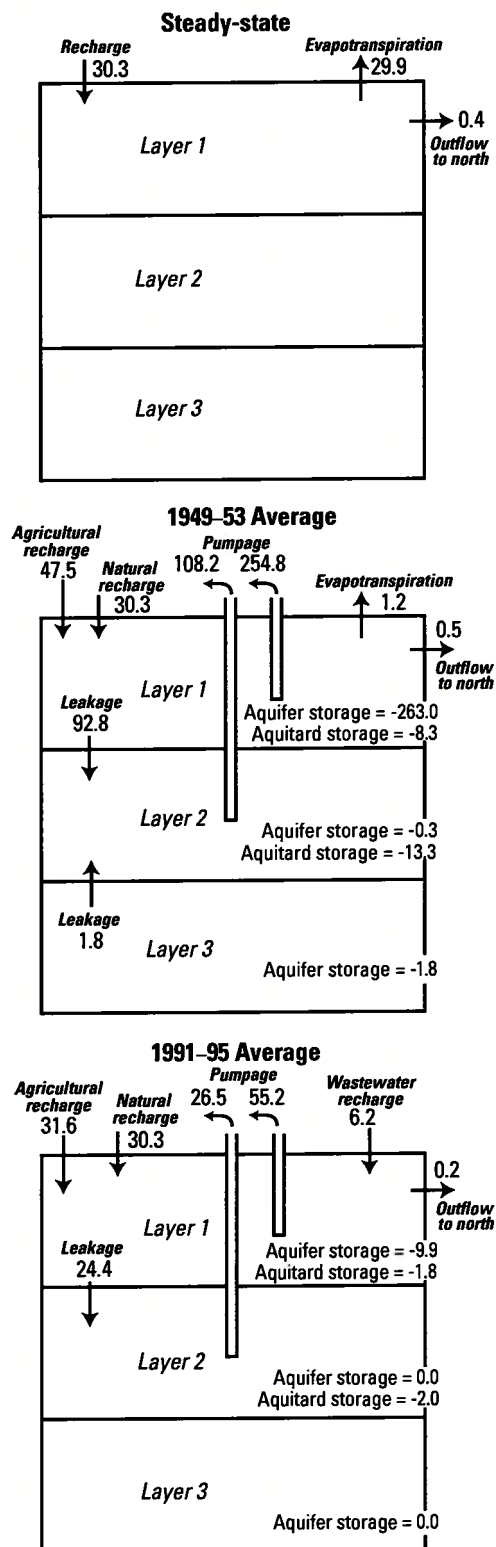


**Figure 30.** Components of the simulated water budget for selected periods from the ground-water flow model of the Antelope Valley ground-water basin, California. (Units are in thousand acre-feet.)

Model sensitivity was determined for variations in hydraulic conductivity (layer 1), transmissivity (layers 2 and 3), confined and unconfined storage coefficients, vertical leakance, pumpage, recharge, and the hydraulic-characteristic values of the flow barriers. The magnitude of these variations was somewhat subjective, but based loosely on the range of reasonable values for each parameter and on the sensitivity observed during the calibration process. Hydraulic conductivity, transmissivity, and specific yield were varied from 0.5 to 2 times calibrated values. Vertical leakance and confined storage coefficients were varied from 0.1 to 10 times calibrated values. Total pumpage, agricultural pumpage, and recharge were increased and decreased by 10 percent. The sensitivity of the model to the effects of the flow barriers was analyzed by removing the barriers (no restriction to flow) and reducing the hydraulic-characteristic values of the barriers to one-half the calibrated values (increased restriction to flow). Sensitivity-analysis results were aggregated into four subareas because the simulated water levels within each subarea showed a similar response to changes in the input parameters. These subareas are (1) the western subarea (the Finger Buttes, Neenach, and West Antelope subbasins); (2) the southeastern subarea (the Buttes and Pearland subbasins); (3) the northern subarea [the North Muroc subbasin and the part of the Lancaster subbasin north of barrier 7 ([figure 11](#))]; and (4) the central subarea (the remainder of the Lancaster subbasin south of barrier 7).

Water-level changes resulting from the sensitivity analysis are shown in [table 9](#). Simulated water levels were most sensitive to changes in the hydraulic characteristic of the flow barrier. The largest water-level changes resulting from changes in the hydraulic characteristic of the flow barriers occurred in the western and southeastern subareas. Water levels in the northern and central subareas were relatively insensitive to changes in the hydraulic characteristics of the flow barriers compared with water levels in the western and southeastern subareas. The western and southern subareas also were sensitive to changes in hydraulic conductivity, transmissivity of layer 2, specific yield, and natural recharge.

Water levels in the northern and central subareas were most sensitive to changes in hydraulic conductivity, specific yield, inelastic skeletal storage

coefficient, and vertical leakance between layers 1 and 2. These subareas also were sensitive to the changes in total pumpage and agricultural pumpage. The insensitivity of the model to changes in transmissivity of layer 3 indicates that defining the base of the model at an altitude of 1,000 ft above sea level was reasonable.

The sensitivity of simulated land subsidence at the end of the transient period (1995) to selected model input parameters is shown in [table 10](#). All the benchmarks used for the subsidence analysis are located in the Lancaster subbasin ([fig. 15](#)), and, therefore, the results of the subsidence sensitivity analysis are for this subbasin only. Pumping-induced subsidence is controlled by the inelastic skeletal storage coefficient and the water-level drawdown below the preconsolidation head. Simulated subsidence, therefore, was most sensitive to the changes in inelastic skeletal storage and specific yield.

In summary, the results of the sensitivity analysis indicate that the model is sensitive to different parameters in different areas. In the northern and central subareas, the model is most sensitive to changes in hydraulic conductivity of layer 1, specific yield, inelastic skeletal storage coefficient, vertical leakance between layers 1 and 2, and pumpage. In the western and southeastern subbasins, the model is most sensitive to changes in hydraulic conductivity of layer 1, transmissivity of layer 2, specific yield, natural recharge, and the hydraulic-characteristic values. Because changes in one model parameter may be offset by changes in another, improving the understanding of one parameter may aid in decreasing the uncertainty of other parameters.

## Limitations of the Model

A ground-water flow model is a valuable tool for testing the conceptualization of the ground-water flow system and for predicting the response of the system to changes in aquifer stresses. However, a model is only an approximation of the actual aquifer system and, therefore, will not exactly simulate the system being modeled. The model relies on estimates of aquifer properties and stresses, which have some degree of uncertainty, and it lacks the small-scale spatial and temporal variability present in the actual system.



**Table 9.** Change in simulated water levels at the end of the transient period (1995) resulting from the sensitivity analysis of the ground-water flow model of the Antelope Valley ground-water basin, California

[Subarea: Western (Finger Buttes, Neenach, and West Antelope subbasins); Southeastern (Buttes and Pearland subbasins); Northern (North Muroc and the part of the Lancaster subbasin north of barrier 7); Central (the part of the Lancaster subbasin south of barrier 7). Order of presentation: from most sensitive (highest median water-level change) to least sensitive (lowest median water-level change)]

Change in parameter or stress		Water-level change, in feet											
		Western subarea				Southeastern subarea				Northern subarea			
		Layer	Range	Mean	Median	Range	Mean	Median	Range	Mean	Median	Range	Mean
Flow barriers not simulated	1		-611/12	-192	-198	-125/73	-44	-48	-25/15	6	11	-52/29	-2
	2		-626/16	-172	-52				-26/18	7	12	-36/27	-2
	3		-628/14	-160	-34				-24/20	7	12	-36/25	-2
Hydraulic characteristics of flow barriers $\times 0.5$	1		2/278	118	128	-62/172	50	38	-12/4	-6	1	-6/52	1
	2		4/273	98	14				-12/2	-6	-7	-5/17	1
	3		4/273	94	11				-12/2	-7	-11	-5/14	1
Hydraulic conductivity of layer 1 $\times 0.5$	1		12/245	104	105	27/340	162	130	-11/12	5	6	-29/126	14
	2		14/142	91	102				-3/9	4	6	-15/113	11
	3		14/138	89	101				-3/9	3	2	-11/112	11
Specific yield of layer 1 $\times 0.5$	1		-26/-116	-76	-68	-119/89	-19	-19	-81/0	-25	-26	-184/131	-108
	2		-36/-113	-82	-84				-86/-22	-25	-26	-177/0	-115
	3		-36/-111	-83	-98				-88/-22	-26	-26	-164/-62	-115
Hydraulic conductivity of layer 1 $\times 2$	1		-177/-9	-82	-87	-186/-8	-105	-94	-12/11	-6	-8	-106/14	-19
	2		-108/-11	-74	-72				-10/0	-6	-8	-101/3	-18
	3		-106/-11	-72	-84				-9/0	-5	-4	-100/2	-17
Specific yield of layer 1 $\times 2$	1		5/75	46	40	2/102	25	22	0/52	17	18	6/166	72
	2		10/75	51	51				12/54	17	18	0/145	75
	3		12/75	53	62				14/56	17	16	29/138	74
Natural recharge $\times 0.9$	1		-56/-8	-34	-40	-36/0	-22	-23	-2/1	0	0	-24/0	-8
	2		-51/-9	-31	-34				-3/1	0	0	-23/0	-8
	3		-50/-9	-31	-29				-3/1	0	0	-23/-2	-8

**Table 9.** Changes in simulated water levels at the end of the transient period (1995) resulting from the sensitivity analysis of the ground-water flow model of the Antelope Valley ground-water basin, California—Continued

Change in parameter or stress		Water-level change, in feet											
		Western subarea				Southeastern subarea				Northern subarea			
		Layer	Range	Mean	Median	Range	Mean	Median	Range	Mean	Median	Range	Mean
Natural recharge $\times$ 1.1	1		9/54	34	40	0/35	21	21	0/2	0	0	-26/23	6
	2		9/49	31	34				0/2	0	0	-19/23	6
	3		9/48	30	29				0/2	0	0	-1/22	7
Inelastic skeletal storage coefficient of layer 2 $\times$ 10	1		0/27	4	1	0/32	2	0	0/59	12	7	0/63	36
	2		0/26	5	1				0/65	16	8	0/89	41
	3		0/26	6	2				0/62	20	25	0/69	42
Inelastic skeletal storage coefficient of layer 1 $\times$ 10	1		0/27	4	1	-1/23	1	0	0/56	12	6	0/56	31
	2		0/26	5	1				0/50	13	7	0/51	32
	3		0/26	5	1				0/49	17	21	2/49	33
Transmissivity of layer 2 $\times$ 2	1		-59/-1	-29	-30	-24/0	-3	-2	-14/3	0	0	-55/17	-8
	2		-64/3	-30	-30				-14/7	0	0	-61/33	-9
	3		-63/2	-29	-29				-5/4	1	1	-59/24	-8
Transmissivity of layer 2 $\times$ 0.5	1		0/39	21	21	0/15	3	2	-3/14	1	0	-26/37	5
	2		-1/41	21	21				-9/16	0	0	-42/43	5
	3		-1/41	21	21				-5/6	0	0	-33/41	5
Vertical leakage between layers 1 and 2 $\times$ 0.1	1		3/27	13	15	0/11	2	2	-2/15	2	2	-5/40	9
	2		-36/26	4	7				-20/-1	-10	-7	-64/13	-10
	3		-34/25	4	7				-19/-4	-11	-14	-60/8	-10
Transmissivity of layer 3 $\times$ 2	1		-28/0	-12	-11	-3/0	-1	-1	-4/1	0	0	-22/4	-2
	2		-30/1	-12	-11				-6/1	0	0	-23/4	-3
	3		-36/3	-12	-11				-6/2	0	0	-28/17	-3

**Table 9.** Changes in simulated water levels at the end of the transient period (1995) resulting from the sensitivity analysis of the ground-water flow model of the Antelope Valley ground-water basin, California—Continued

Change in parameter or stress		Water-level change, in feet											
		Western subarea			Southeastern subarea			Northern subarea			Central subarea		
		Range	Mean	Median	Range	Mean	Median	Range	Mean	Median	Range	Mean	Median
Inelastic skeletal storage coefficient of layer 2 × 0.1	1	-5/0	-1	0	-7/0	0	0	-16/0	-5	-3	-15/0	-8	-8
	2	-4/0	-1	0				-16/0	-6	-3	-15/0	-9	-9
	3	-4/0	-1	0				-15/0	-7	-10	-15/0	-9	-9
Pumpage increased by 10 percent	1	-7/0	-4	-4	-9/0	-2	-1	-8/0	-4	-3	-48/0	-8	-8
	2	-7/0	-4	-5				-7/-2	-4	-4	-39/0	-9	-8
	3	-8/0	-4	-5				-8/-2	-5	-5	-35/0	-9	-9
Agricultural pumpage decreased by 10 percent	1	0/7	3	4	0/3	1	1	0/3	0	0	-10/11	5	6
	2	0/7	4	4				0/3	0	0	-7/10	5	6
	3	0/7	4	5				0/3	0	0	-2/9	6	6
Pumpage decreased by 10 percent	1	0/7	4	4	0/5	2	1	0/8	4	3	-8/40	7	7
	2	0/7	4	5				2/8	4	4	-6/36	7	7
	3	0/8	4	5				2/7	5	5	-1/32	8	8
Transmissivity of layer 3 × 0.5	1	0/16	7	7	0/2	1	1	0/5	0	0	-3/13	2	1
	2	0/17	7	7				-1/6	0	0	-5/14	2	1
	3	-3/20	7	7				-2/7	0	0	-11/16	2	1
Agricultural pumpage increased by 10 percent	1	-7/0	-4	-4	-7/0	-1	-1	-3/0	0	0	-12/0	-6	-7
	2	-7/0	-4	-5				-5/0	0	0	-11/0	-7	-7
	3	-7/0	-4	-5				-4/0	0	0	-9/-3	-7	-7
Storage coefficient of layer 3 × 10	1	0/9	6	6	-2/2	0	0	0/6	2	2	-13/13	5	7
	2	1/9	6	7				1/5	3	3	-10/13	6	7
	3	0/10	6	7				2/6	3	4	-6/17	6	6
Inelastic skeletal storage coefficient of layer 1 × 0.1	1	-4/0	-1	0	-4/1	0	0	-23/1	-4	-2	-18/0	-6	-6
	2	-4/0	-1	0				-18/1	-4	2	-12/0	-6	-6
	3	-4/0	-1	0				-13/1	-5	-7	-11/0	-6	-6

**Table 9.** Changes in simulated water levels at the end of the transient period (1995) resulting from the sensitivity analysis of the ground-water flow model of the Antelope Valley ground-water basin, California—Continued

Change in parameter or stress		Water-level change, in feet											
		Western subarea				Southeastern subarea				Northern subarea			
		Layer	Range	Mean	Median	Range	Mean	Median	Range	Mean	Median	Range	Mean
Vertical leakage between layers 1 and 2 × 10	1		-12/-1	-6	-4	-7/0	-1	0	-3/3	0	0	-21/4	-3
	2		-18/11	-4	-3				-1/6	2	1	-18/15	-1
	3		-17/5	-4	-3				-1/5	2	2	-13/13	-1
Vertical leakage between layers 2 and 3 × 0.1	1		-1/7	2	2	0/1	1	1	-2/13	-1	-1	-12/19	1
	2		-1/7	2	2				-2/15	0	-1	-12/21	1
	3		-37/9	-1	1				-6/6	0	-1	-35/74	3
Elastic storage coefficient of layer 1 × 10	1		-4/5	2	2	-2/2	1	1	0/3	1	2	-17/4	0
	2		-4/5	2	2				0/3	1	2	-15/4	0
	3		-4/5	2	2				0/2	1	2	-8/3	1
Elastic storage coefficient of layer 2 × 10	1		-2/2	1	1	-3/1	0	0	0/3	2	2	-18/2	0
	2		-3/2	1	1				-1/3	2	2	-16/2	-1
	3		-3/2	1	1				-1/3	2	2	-10/2	0
Vertical leakage between layers 2 and 3 × 10	1		-2/1	-1	-1	-1/0	0	0	-7/1	0	0	-13/5	0
	2		-3/1	-1	-1				-9/1	0	0	-13/10	-1
	3		-6/5	0	0				-7/1	0	0	-19/9	-1
Storage coefficient representing the compressibility of water for layer 2 × 10	1		0/2	1	1	-4/1	0	0	0/2	0	0	-18/3	1
	2		0/2	1	1				0/2	1	1	-15/3	1
	3		0/2	1	1				0/2	1	1	-9/2	1
Storage coefficient of layer 3 × 0.1	1		-1/0	-1	-1	-1/1	0	0	-1/0	-1	0	-1/0	-1
	2		-1/0	-1	-1				-1/0	-1	0	-1/0	-1
	3		-1/0	-1	-1				-2/0	-1	0	-2/0	-1



**Table 9.** Changes in simulated water levels at the end of the transient period (1995) resulting from the sensitivity analysis of the ground-water flow model of the Antelope Valley ground-water basin, California—Continued

Change in parameter or stress		Water-level change, in feet											
		Western subarea			Southeastern subarea			Northern subarea			Central subarea		
		Layer	Range	Mean	Median	Range	Mean	Median	Range	Mean	Median	Range	Mean
Wastewater recharge $\times 0.5$	1	0	0	0	0	-3/0	0	0	0/1	0	0	-28/1	-1
	2	0	0	0	0				0/1	0	0	-23/0	-1
	3	0	0	0	0				0/1	0	0	-7/0	-1
Wastewater recharge $\times 2$	1	0	0	0	0	0/6	0	0	0/1	0	0	0/51	1
	2	0	0	0	0				0/1	0	0	0/43	1
	3	0	0	0	0				0/1	0	0	0/14	1
Storage coefficient representing the compressibility of water for layer 1 $\times 0.1$	1	0	0	0	0	0	0	0	-1/0	0	0	0	0
	2	0	0	0	0				-1/0	0	0	-1/0	0
	3	0	0	0	0				-1/0	0	0	0	0
Storage coefficient representing the compressibility of water for layer 1 $\times 10$	1	0	0	0	0	0	0	0	0/1	0	0	0/1	0
	2	0	0	0	0				0/1	0	0	0/1	0
	3	0/1	0	0	0				0/1	0	0	0/1	0
Storage coefficient representing the compressibility of water for layer 2 $\times 0.1$	1	-1/0	0	0	0	-1/0	0	0	-1/0	0	0	-1/0	0
	2	-1/0	0	0	0				-1/0	0	0	-1/0	0
	3	-1/0	0	0	0				-1/0	0	0	-1/0	0
Elastic skeletal storage coefficient of layer 1 $\times 0.1$	1	-1/1	0	0	0	-1/0	0	0	-1/0	0	0	-1/0	0
	2	-1/1	0	0	0				-1/0	0	0	-1/0	0
	3	-1/1	0	0	0				-1/0	0	0	-1/0	0
Elastic skeletal storage coefficient of layer 2 $\times 0.1$	1	-1/1	0	0	0	-1/0	0	0	-1/0	0	0	-1/1	0
	2	-1/0	0	0	0				-1/0	0	0	-1/1	0
	3	-1/1	0	0	0				-1/0	0	0	-1/0	0

**Table 10.** Change in simulated land subsidence at the end of the transient period (1995) resulting from changes in selected model input parameters and stresses during the sensitivity analysis of the ground-water flow model of the Antelope Valley ground-water basin, California

[Order of presentation: from most sensitive (highest median subsidence change) to least sensitive (lowest median subsidence change)]

Change in parameter or stress	Change in simulated subsidence, in feet		
	Range	Mean	Median
Layer 2 inelastic skeletal storage coefficient $\times 10$	1.65/14.20	6.08	5.94
Layer 1 inelastic skeletal storage coefficient $\times 10$	2.81/8.47	5.25	5.24
Layer 1 specific yield $\times 0.5$	1.90/7.98	4.08	3.40
Layer 1 specific yield $\times 2$	-3.99/-1.37	-2.29	-1.93
Layer 2 inelastic skeletal storage coefficient $\times 0.1$	-4.03/-.61	-1.54	-1.39
Layer 1 inelastic skeletal storage coefficient $\times 0.1$	.21/1.53	1.53	.42
Pumpage increased by 10 percent	-.01/.95	.38	.29
Agricultural pumpage increased by 10 percent	-.01/.73	.31	.28
Layer 1 elastic skeletal storage coefficient $\times 10$	-.09/.73	.31	.23
Layer 2 elastic skeletal storage coefficient $\times 10$	-.06/.65	.28	.23
Layer 3 storage coefficient $\times 10$	-.41/-.15	-.25	-.20
Pumpage decreased by 10 percent	-.49/-.09	-.21	-.20
Natural recharge $\times 1.1$	-.41/-.05	-.18	-.17
Natural recharge $\times 0.9$	.04/.46	.18	.16
Agricultural pumpage decreased by 10 percent	-.24/-.04	-.14	-.15
Hydraulic conductivity of layer 1 $\times 2$	-.32/1.05	.33	.14
Vertical leakance between layers 1 and 2 $\times 0.1$	-.26/.42	.08	.06
Hydraulic conductivity of layer 1 $\times 0.5$	-.56/.38	-.08	-.06
Vertical leakance between layers 1 and 2 $\times 10$	-.72/.12	-.12	-.05
Transmissivity of layer 3 $\times 2$	-.07/.29	.06	.04
Layer 2 storage coefficient representing the compressibility of water $\times 10$	-.09/-.03	.05	.04
Vertical leakance between layers 2 and 3 $\times 0.1$	-.54/.12	-.07	.03
Layer 1 elastic skeletal storage coefficient $\times 0.1$	-.07/.0	-.03	-.02
Transmissivity of layer 2 $\times 2$	-.33/.62	.05	-.02
Layer 2 elastic skeletal storage coefficient $\times 0.1$	-.06/.0	-.03	-.02
Layer 3 storage coefficient $\times 0.1$	.01/.05	.03	.02
Vertical leakance between layers 2 and 3 $\times 10$	-.29/.19	-.01	-.02
Transmissivity of layer 2 $\times 0.5$	-.57/.54	-.01	.02
Layer 2 storage coefficient representing the compressibility of water $\times 0.1$	-.01/.0	-.01	-.01
Hydraulic characteristics of low barriers $\times 0.5$	-.04/.09	.00	.01
Wastewater recharge $\times 0.5$	.0/.01	.00	.00
Wastewater recharge $\times 2$	-.01/.0	.00	.00
Flow barriers not simulated	-.34/.53	.04	.00
Transmissivity of layer 3 $\times 0.5$	-.30/.04	-.05	.00
Layer 1 storage coefficient representing the compressibility of water $\times 0.1$	-.03/.08	.00	.00
Layer 1 storage coefficient representing the compressibility of water $\times 10$	.0/.01	.00	.00

Water levels and land subsidence calculated by the model are average values for the area represented by each model cell. Simulated water levels can vary considerably from measured water levels because of well location, depth, and construction. For example, wells may be screened over a depth represented by more than one model layer, whereas, measured water levels may be a composite of the actual water levels in each layer. The size of the model cell and the length of the stress period of the model are appropriate for the resolution of available data and for simulations on a regional scale. Because model uncertainty increases significantly with the decreasing size of the area of interest, the model generally should not be used to address local-scale problems.

Little is known about the geohydrology of the Finger Buttes, West Antelope, Neenach, Pearland, and Buttes subbasins. Consequently, hydraulic properties specified in the model for these subbasins were based on limited data. Available data indicate that hydraulic conductivity of the aquifer material is lower in the upslope areas adjacent to the mountain fronts than in the downslope areas, which is contrary to what would be expected for areas with typical alluvial fan development, where coarse-grained material is deposited at the fan heads (higher hydraulic conductivity) and fine-grained material is deposited at the fan margins (lower conductivity). In these five subbasins, which have depths to water greater than the other subbasins, the water table may be below the more transmissive coarse-grained material. Tectonic processes, such as uplift and erosion, also may affect the hydrologic properties of the aquifers. The water-level data for these subbasins used to calibrate the model also were limited; consequently, the differences between the simulated and the measured water levels were greatest in these subbasins. Although the simulated water levels for Finger Buttes, West Antelope, Neenach, Pearland, and Buttes subbasins provide reasonable boundary conditions for simulating the water levels in the Lancaster subbasin for the calibration period, the high degree of uncertainty in the model input for these subbasins greatly reduces the potential for accurate predictions of ground-water conditions in these subbasins. Additional geohydrologic data would improve the accuracy of the model for these subbasins.

The model is sensitive to the location and simulated barrier effect of faults. It is likely that there are additional concealed faults crossing the study area

that have not yet been identified in areas that are not currently being stressed. The barrier effect of these faults may become apparent in the future, if pumping or recharge occurs near unknown faults. If these faults significantly affect ground-water flow, the faults should be added to the model.

The quantity and distribution of agricultural pumpage is uncertain. As shown in the sensitivity analysis, the variability in estimates of pumpage can significantly affect model results. More accurate estimates of agricultural pumpage would improve the model results. Results from simulations of future conditions that include pumpage for areas where pumping had not previously occurred should be interpreted carefully because the stresses from pumping were not simulated during the calibration process of the model.

Natural and agricultural recharge are difficult to measure and, therefore, the recharge rates and temporal distribution of recharge were based on the model calibration results. The calibration process resulted in a lower rate of natural recharge than had been estimated for previous studies. Additional geohydrologic data are needed to confirm that the natural recharge rates used in the model are accurate; however, collection of additional data was beyond the scope of this study. The travel time for irrigation-return flows to reach the water table was simulated as a constant (10 years) for the entire model area. Model results probably could be improved by more accurately specifying the travel time for each area on the basis of the depth-to-water and aquifer material.

The approach taken in this study to simulate aquifer-system compaction in unconfined portions of the model layer 1 using the IBS1 package will tend to overestimate compaction in that layer, where the water table declines, and underlying model layers. IBS1 does not account for changes in the total stress that occur when the water table rises and lowers, as it may in model layer 1. Changes in the position of the water table cause changes in the total stress exerted on the underlying sediment owing to the overlying weight of water that changes when the water table fluctuates. These effects are relatively small and the overestimated subsidence in the model simulation is expected to be in the range of 1.18 to 1.33 percent, and is primarily dependent upon the porosity of the sediments in model layer 1 in the zone of water-table fluctuation.

Although the model does a relatively good job of simulating the measured quantity of land subsidence, the IBS1 Package used to simulate aquifer compaction does not accurately simulate the delayed drainage in the thick aquitards or the timing of subsidence in areas where thick aquitards are a major contributor to subsidence. IBS1 simulates the instantaneous release of water from storage from fine-grained, compressible interbeds for a head decline in the surrounding aquifer. As such, the heads in the interbeds are assumed to equilibrate instantaneously with head changes in the aquifers. This treatment ignores the delayed equilibration of head associated with the low permeability interbeds and aquitards which is further exacerbated by their thickness—the time constants governing head equilibration in these units is proportional to their squared thickness. Additionally, the model does not simulate subsidence throughout the modeled area because values of inelastic storage only were specified in areas where subsidence previously had been measured. In areas where inelastic skeletal storage was not specified, future water-level declines below preconsolidation heads could cause subsidence where compressible sediments exist in these areas. Subsidence cannot be simulated for these areas unless inelastic skeletal storage coefficients and preconsolidation heads are specified for these areas.

Owing to uncertainty in some parameters used in the model, especially in the agricultural component of pumpage, model results from the predictive simulation should be used with caution. The model, like most models, is not ideally suited for predicting absolute changes in water levels or subsidence. The most appropriate application of the model is comparing the relative effects of different water-management scenarios on the aquifer system.

### **Simulation of Aquifer-System Response to Pumping Scenarios**

A calibrated flow model can be used as a tool to evaluate and compare the responses of an aquifer system to potential future stresses. Management actions involving changes in the quantity and distribution of pumpage or recharge can be simulated

and the aquifer-system responses compared to evaluate the effectiveness of these actions satisfying management goals. Although water levels and subsidence simulated for a given scenario may not accurately represent the values in the real system, the relative differences in water levels and subsidence over time can be compared to provide managers with useful information for planning and decision making.

For this study, the model was used to simulate the aquifer-system response to two potential pumping scenarios for 1995–2025. For both scenarios, all model parameters were unchanged from those specified in the transient-state simulation. Natural recharge and artificial recharge from irrigation-return flows and from reclaimed wastewater were specified equal to the quantities specified for those sources for 1995. For both scenarios, recharge from irrigation-return flows was calculated as 30 percent of the water used for irrigation and was assumed to recharge the water table 10 years after the irrigation water was applied. For scenario 1, total annual pumpage for 1995–2025 was specified equal to total annual pumpage in 1995. For scenario 2, public-supply pumpage was increased 3.3 percent annually and agricultural pumpage was assumed to be 75 percent greater than agricultural pumpage in 1995 for the simulated period 1995–2025. Recharge from irrigation-return flows was correspondingly increased by 75 percent. The annual increase in public-supply pumpage was based on population growth projections for Palmdale and Lancaster from the Southern California Association of Governments (2001). The increase in agricultural pumpage was based on crop-acreage data from the Los Angeles County Agricultural Commissioner which indicated that agricultural production in the study area increased as much as 75 percent during 1995–98. The spatial distribution of pumpage for both scenarios was the same as was specified for 1995.

The simulated water-level (layer 1) and land-subsidence values for both scenarios are shown in [figures 31](#) and [32](#), respectively. Recall that the simulated water-level and land-subsidence values are averages for the entire model cell and, therefore, may be different from the measurements for specific wells and bench marks.

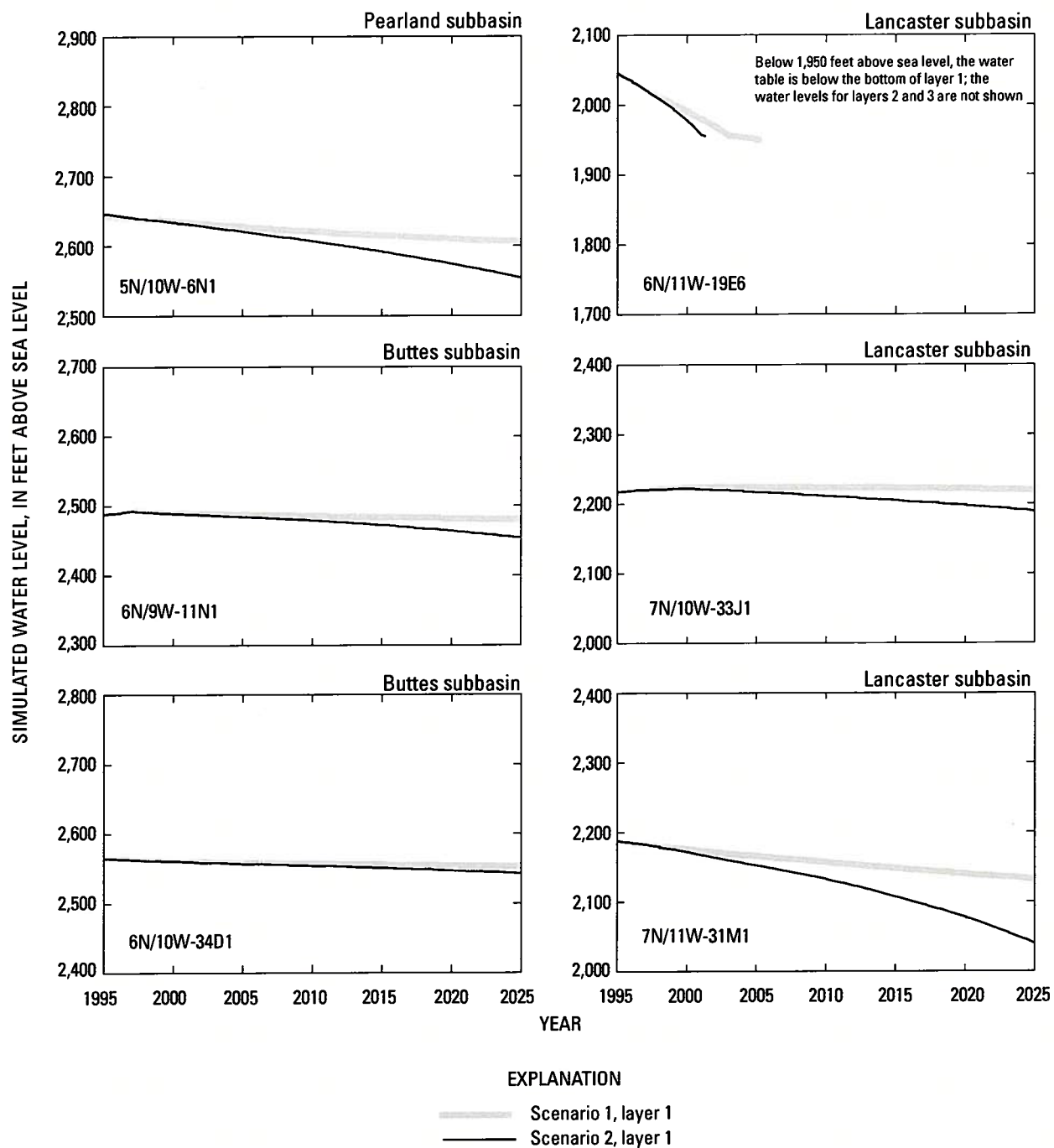


**Figure 31.** Simulated water levels for two pumping scenarios for the Antelope Valley ground-water basin, California, 1995–2025.



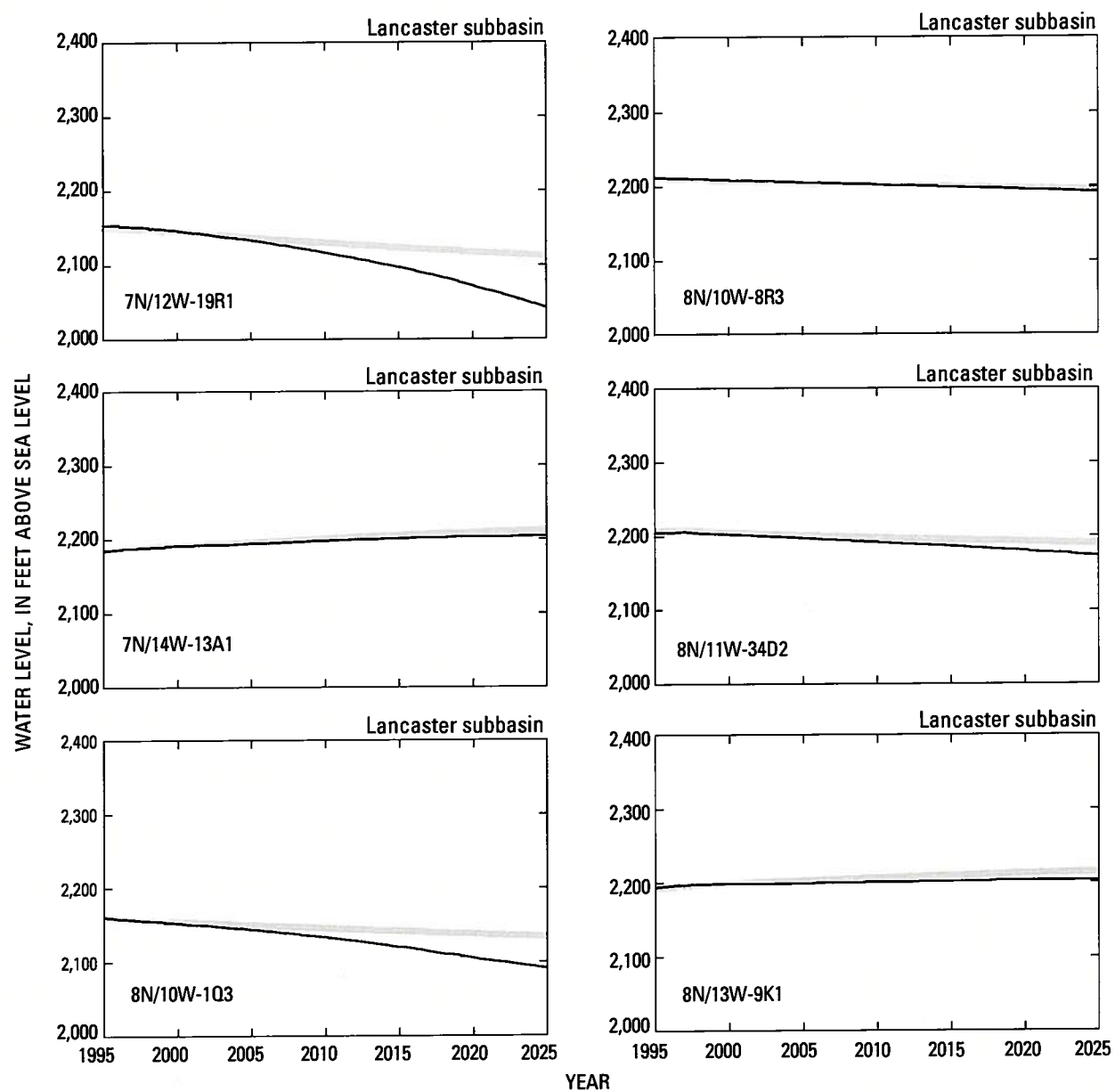


**Figure 31.**—Continued.

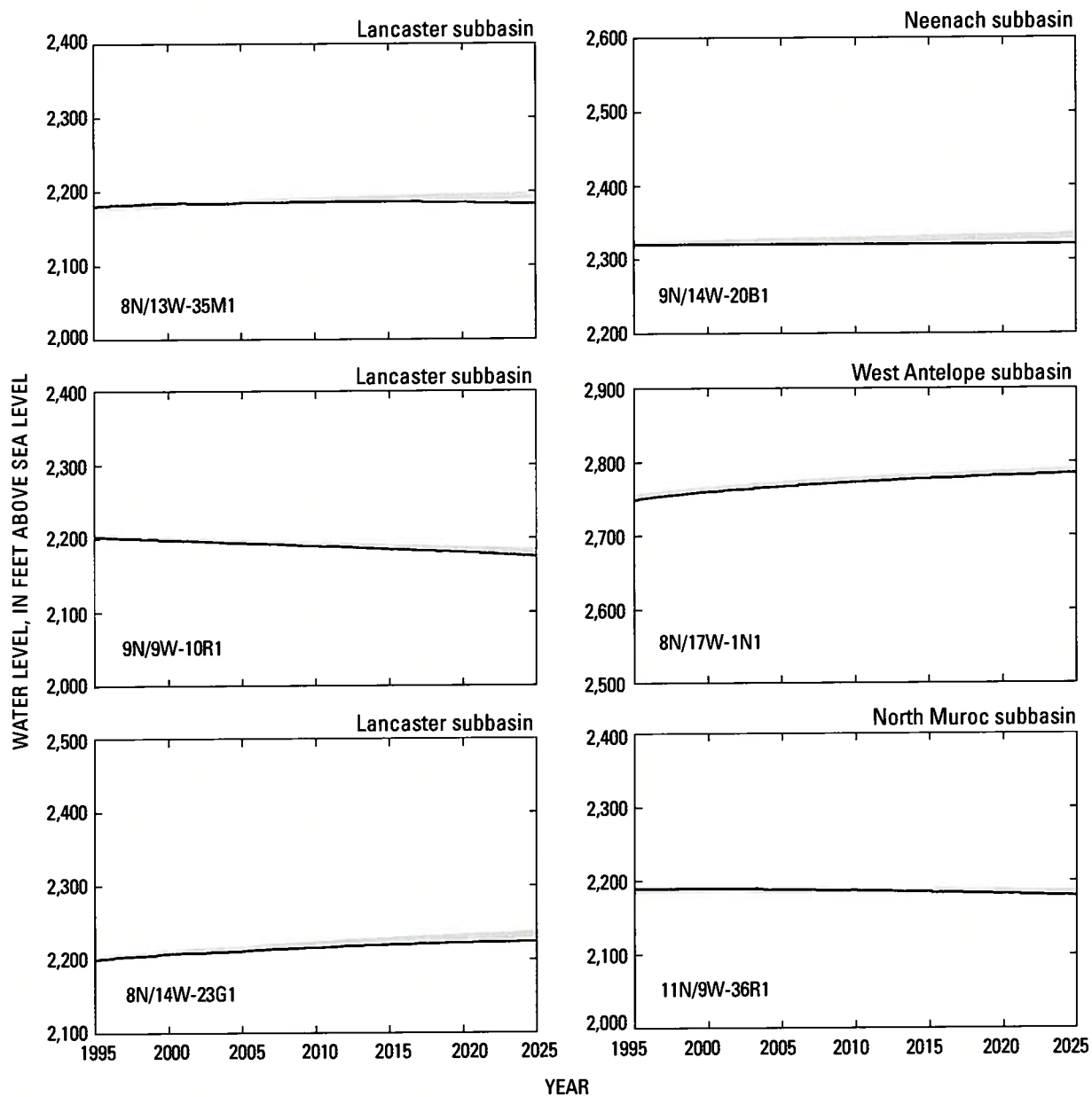


**Figure 31.**—Continued.

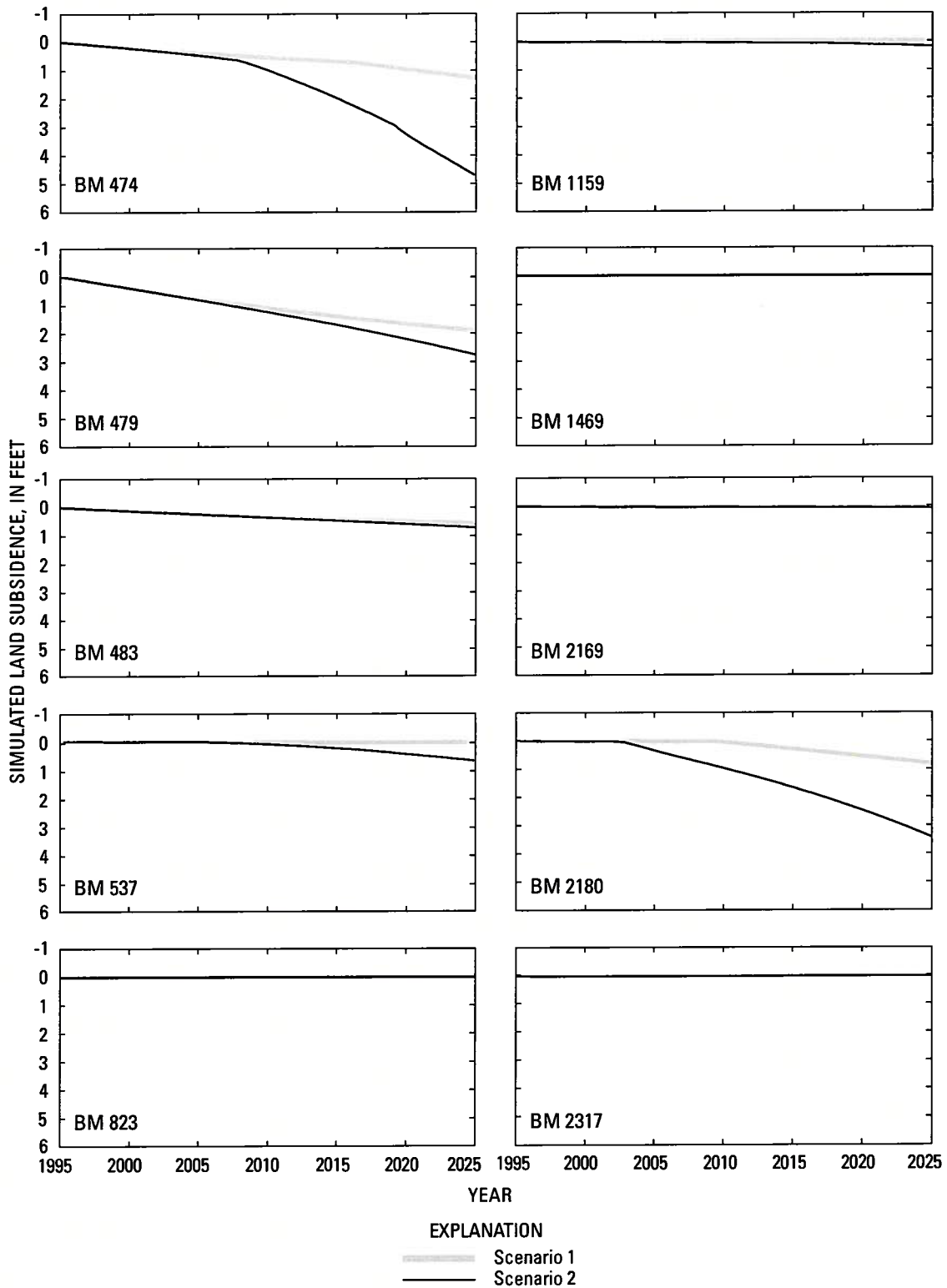


**Figure 32.** Simulated land subsidence near indicated bench marks for two pumping scenarios for the Antelope Valley ground-water basin, California, 1995–2025.

For scenario 1, water levels rose in the western Lancaster subbasin and in the Neenach and West Antelope subbasins, continuing the long-term recovery from drawdown caused by the much greater historical agricultural pumpage (Carlson and others, 1998; Carlson and Phillips, 1998). Water levels rose as much as 11 ft at well 9N/14W-20B1 in the Neenach subbasin and as much as 36 ft at well 8N/17W-1N1 in the West Antelope subbasin; however, the rate of the water-level rise declined over time (fig. 31). The decline in the rate of water-level rise was caused, in part, by the 10-year delay in recharge from irrigation-return flows. Even though the simulated annual pumpage was constant from 1995 to 2025, recharge from irrigation-return flows was based on agricultural pumpage prior to 1995, which was higher than in 1995. From 1996 to 2004, the annual quantity of recharge from irrigation-return flows gradually declined; in 2005, recharge from irrigation-return flows remained constant for the remainder of the simulation period. In the southern, eastern, and northern part of the Lancaster subbasin and in the Buttes, Pearland, and North Muroc subbasins, water levels generally declined as a result of the scenario 1 pumpage, except at well 7N/10W-33J1 in the eastern part of the Lancaster subbasin where water levels did not decline. The largest decline in the simulated water levels (more than 100 ft) was at well 6N/11W-19E6, where the water level declined below the bottom of model layer 1 into layer 2 in 2006. The water level in layer 2 continued to decline after 2006 (water levels for layer 2 are not shown in fig. 31). Simulated water-level declines were greatest at this well because most of the pumping for public supply occurs in this area. Further land subsidence was simulated in the central part of the Lancaster subbasin north and east of the city of Lancaster. The maximum simulated subsidence for scenario 1 occurred at bench mark BM 479 (1.9 ft). These model results indicate that pumpage for public

supply at 1995 rates in the Lancaster and Palmdale areas will result in significant water-level declines and land subsidence, indicating that future pumpage may have to be redistributed or augmented by artificial recharge.

For scenario 2, public supply pumpage was increased 3.3 percent annually and annual agricultural pumpage and irrigation-return flows were 75 percent greater than the values simulated for scenario 1. Similar to scenario 1, water levels rose in the western Lancaster subbasin; however, the water-level rise was not as great. In the Neenach subbasin, the water levels for well 9N/14W-20B1 remained unchanged from 1995 to 2025. In the southern, eastern, and northern part of the Lancaster subbasin and in the Buttes and Pearland subbasins, water levels declined more than the water levels for scenario 1. Pumpage increases for scenario 2 resulted in significant water-level declines in the southern and northeastern part of the Lancaster subbasin (wells 6N/11W-19E6, 7N/12W-19R1, and 8N/10W-1Q3) because most pumping for public supply occurs in these areas. Water-level declines were as great as 150 ft in the south-central part of the Lancaster subbasin. Simulated subsidence at bench marks BM 474, BM 479, BM 537, and BM 2180 was greater for scenario 2 than for scenario 1, and the maximum simulated subsidence for 1995–2025 was about 5 ft at bench mark BM 474. The simulated subsidence was the greatest in the central Lancaster subbasin north and east of the city of Lancaster, near bench marks BM 474, BM 479, and BM 2180, where combined public supply and agricultural pumping are greatest. Because inelastic storage coefficients were specified only for areas where subsidence has previously been measured, neither scenario 1 nor 2 is able to predict subsidence from future water-level declines outside this area.

## SUMMARY

Ground-water pumpage has provided from 50 percent to more than 90 percent of the water supply in Antelope Valley since the early 1900s. This long-term ground-water pumpage has caused water-level declines and associated increased pumping lifts; it also has reduced well efficiencies and caused land subsidence. Urban growth and limited available surface-water supply are likely to continue to increase reliance on ground water. A numerical ground-water flow and land-subsidence model of the Antelope Valley ground-water basin was developed to improve the understanding of the ground-water flow system. The model can be used as a tool in making informed water-management decisions.

The Antelope Valley ground-water basin consists of unconsolidated alluvial and lacustrine deposits, more than 5,000 ft thick in places. The alluvium consists of poorly sorted gravels, sands, silts, and clays. Older, deep alluvial deposits are more compacted and indurated than the younger, shallow deposits. The lacustrine deposits are as much as 300 ft thick and are composed mostly of clay and silty clay with some layers of sand and silt. The lacustrine deposits are as much as 800 ft below land surface near Palmdale, become progressively shallower northward, and are exposed at the surface near the southern edge of Rogers Lake.

The study area was conceptually divided into seven ground-water subbasins on the basis of faults, bedrock outcrops, ground-water divides, and arbitrary boundaries. Some faults seem to act as barriers to ground-water flow. Geophysical logs from previous studies show that induration of the alluvial material increases with depth, which suggests a decrease in the ability to transmit and store water with depth. Data from test wells drilled in the Lancaster area and at Edwards Air Force Base indicate that there is a change in the properties of the aquifer materials at altitudes of about 1,950 ft and 1,550 ft above sea level. Unconsolidated material at altitudes of 1,950 ft above sea level and greater was designated as the upper aquifer, unconsolidated material between 1,950 and 1,550 ft above sea level was designated as the middle aquifer, and unconsolidated material below 1,550 ft above sea level was designated as the lower aquifer. The lacustrine deposits are contained within the upper aquifer in the northern part of the Lancaster subbasin

and primarily within the middle aquifer in the southern part of the Lancaster subbasin. The upper aquifer is unconfined to confined and the middle and lower aquifers are confined.

Prior to ground-water development in Antelope Valley, recharge to the ground-water system was primarily from the infiltration of precipitation runoff near the valley margins. Precipitation over the valley floor generally is less than 10 in./yr and probably contributes little, if any, recharging to the aquifer system owing to the high evapotranspiration rates in the study area. In the lowland parts of the valley, discharge from the aquifer system was primarily from evapotranspiration. A small amount of ground water is discharged from the valley north into the Fremont Valley Basin.

Development of the ground-water system began around 1915 and increased rapidly into the 1950s. Ground-water pumping has caused large water-level declines in the ground-water basin; as a result, evapotranspiration has decreased to an insignificant amount. The water-level declines from pumping also have caused land subsidence owing to the compaction of compressible sediments. The major source of discharge in the valley has changed from evapotranspiration to ground-water pumping; ground water now flows from areas of recharge toward the major pumping centers rather than to natural discharge areas where evapotranspiration had occurred. Recharge from the infiltration of irrigation-return flows is a major contributor of recharge to the aquifer system.

A numerical ground-water flow model was developed and calibrated for steady-state pre-development (1915) and transient-state (1915–95) conditions. The model aggregates old and new geohydrologic information to aid in better understanding the ground-water flow system and to aid in making informed water-management decisions. The model was vertically discretized into three layers. Layer 1 (upper aquifer) extends from the water table to an altitude of 1,950 ft above sea level or to bedrock, whichever is higher; layer 2 (middle aquifer) extends from 1,950 to 1,550 ft above sea level or to bedrock, whichever is higher; layer 3 (lower aquifer) extends from 1,550 to 1,000 ft above sea level or to bedrock, whichever is higher. The bottom of layer 3 was set to an altitude of 1,000 ft because it was assumed that the alluvial material below this depth was not a significant part of the flow system owing to compaction and induration of this older material.



The model was calibrated by adjusting hydraulic conductivity, transmissivity, specific yield, natural recharge, aquitard thickness, hydraulic characteristic of flow barriers, and preconsolidation head within reasonable limits to obtain reasonable agreement between simulated and measured water levels and subsidence. The model did well in simulating water levels in the Lancaster, Neenach, Pearland, and Buttes subbasins where the geohydrology is well known. In the North Muroc Subbasin, measured and simulated horizontal and vertical water-level gradients match well; however, the simulated water levels were higher than the measured water levels. In the Finger Buttes and West Antelope subbasins, where few geohydrologic data are available, the match between the simulated and the measured water levels was not as good. Measured and simulated land subsidence data also were compared and matched well at all the bench marks used for calibration.

During model calibration, natural recharge was reduced from an initial estimate of 40,700 acre-ft/yr to 30,300 acre-ft/yr. Results of the transient-state simulation indicate that more than 8.5 million acre-ft of ground water was removed from storage during 1915–95, with most of the storage change occurring between about 1945 and 1975. Ground-water storage changed little during the final 10 years of simulation period because discharge by pumpage had declined sufficiently to be balanced by recharge. Model results show that during the period of peak pumping (1949–53) 79 percent of the ground water withdrawn from the aquifer came from storage. Water released from compaction of the aquitards accounted for about 21,600 acre-ft/yr of the ground water removed from storage. Pumpage from layer 2 induced leakage of ground water from layer 1, which accounted for about 86 percent of the total pumpage in layer 2. During the last 5 years of the simulation (1991–95), only 17 percent of pumpage came from storage.

Results of the sensitivity analysis showed that the model was most sensitive to changes in the hydraulic characteristic of flow barriers, specific yield, hydraulic conductivity of layer 1, natural recharge, inelastic skeletal storage coefficient, transmissivity of layer 2, and pumpage. The sensitivity of the model varied spatially. The model was not sensitive to the

transmissivity of layer 3, which indicates that specifying the bottom of the model at 1,000 ft above sea level was a reasonable assumption.

The calibrated model was used to test the aquifer response to two future pumping scenarios for 1995 to 2025. For scenario 1, annual pumpage remained the same as pumpage specified for 1995. Water levels rose in the western Lancaster subbasin and in the Neenach and West Antelope subbasins, continuing the long-term recovery from drawdown caused by the much greater historical agricultural pumpage. In areas where pumping for public supply is concentrated, water levels continued to decline and subsidence continued in the central part of the Lancaster subbasin. Water-level declines were greatest (more than 100 ft) in the south-central part of the basin because most of the public supply pumpage occurs in this area; as much as 1.9 ft of additional subsidence was simulated in the central part of the ground-water basin for 1995 through 2025. For scenario 2, public supply pumpage was increased 3.3 percent annually compared with that specified for 1995 and agricultural pumpage was increased 75 percent. This scenario resulted in significant water-level declines in the southern and eastern part of the Lancaster subbasin because most of the public supply and agricultural pumping occurs in these areas. Results of this simulation showed that water levels declined more than 150 feet in the south-central part of the ground-water basin and that an additional 5 feet of subsidence was simulated in the central part of the basin.

## REFERENCES CITED

- Benda, W.K., Erd, R.C., and Smith, W.C., 1960, Core logs from five test holes near Kramer, California: U.S. Geological Survey Bulletin 1045-F, p. 319–393.
- Bloyd, R.M., Jr., 1967, Water resources of the Antelope Valley–East Kern Water Agency area, California: U.S. Geological Survey Open-File Report, 73 p.
- Bouwer, Herman, 1982, Physical principles of vadose zone flow, in *Deep Percolation Symposium*, Scottsdale, Arizona, October 26, 1982, Proceedings: [Phoenix, Ariz.], Arizona Department of Water Resources Report 4, p. 7–15.

- California Department of Finance, 1998, City/county population and housing estimates, 1990–98: Sacramento, Calif., California Department of Finance, Demographics Research Unit.
- California Department of Public Works, 1955, Memorandum report on water conditions in Antelope Valley in Kern, Los Angeles, and San Bernardino Counties: [Sacramento, Calif.], California Department of Public Works, 27 p.
- California Department of Water Resources, 1947, Report to the Assembly of the State Legislature on water supply in Antelope Valley in Los Angeles and Kern counties pursuant to House Resolution number 101 of February 16, 1946: [Sacramento, Calif.], California Department of Water Resources, 22 p.
- 1980, Planned utilization of water resources in Antelope Valley: District report: Los Angeles, Calif., California Department of Water Resources, Southern District, 70 p.
- 1990, 1988 Annual water use—Additional information for Bulletin 160-87, 85 p.
- 1991, 1989 Annual water use—Water supply balances: Memorandum Report, 28 p.
- Cande, S.C. and Kent, D.V., 1995, Revised calibration of the geomagnetic polarity time scale for the Late Cretaceous and Cenozoic, *Journal of Geophysical Research*, v. B100, no. 4, p. 6093–6095.
- Carlson, C.S., Leighton, D.A., Phillips, S.P., and Metzger, L.F., 1998, Regional water table (1996) and water-table changes in the Antelope Valley ground-water basin, California: U.S. Geological Survey Water-Resources Investigations Report 98-4022, 2 plates.
- Carlson, C.S., Phillips, S.P., 1998, Water-level changes (1975–98) in the Antelope Valley, California: U.S. Geological Survey Open File Report 98-561, 2 plates.
- Dibblee, T.W., Jr., 1952, Geology of the Saltdale quadrangle, California: California Division of Mines Bulletin 160, 66 p., scale 1:62,500.
- 1957, Simplified geologic map of the western Mojave Desert: U.S. Geological Survey Open-File Report, scale 1:250,000.
- 1958a, Geologic map of the Boron quadrangle, Kern and San Bernardino Counties, California: U.S. Geological Survey Mineral Investigations Field Studies Map MF-204, scale 1:62,500.
- 1958b, Geologic map of the Castle Butte quadrangle, Kern County, California: U.S. Geological Survey Mineral Investigations Field Studies MF-170, scale 1:62,500.
- 1959a, Geologic map of the Rosamond quadrangle, California: U.S. Geological Survey Open-File Report, Scale 1:62,500.
- 1959b, Geologic map of the Rogers Lake quadrangle, California: U.S. Geological Survey Open-File Map, scale 1:48,000.
- 1959c, Geologic map of the Alpine Butte quadrangle, California: U.S. Geological Survey Mineral Investigations Field Studies Map MF-222, scale 1:62,500.
- 1959d, Preliminary geologic map of the Mojave quadrangle, California: U.S. Geological Survey Mineral Investigations Field Studies Map MF-219, scale 1:62,500.
- 1960a [1961], Geologic map of the Lancaster quadrangle, Los Angeles County, California: U.S. Geological Survey Mineral Investigations Field Studies Map MF-76, scale 1:62,500.
- 1960b [1961], Geology of the Rogers Lake and Kramer quadrangles, California: U.S. Geological Survey Bulletin 1089-B, p. 73–139.
- 1963, Geology of the Willow Springs and Rosamond quadrangles, California: U.S. Geological Survey Bulletin 1089-C, p. 141–253.
- 1967, Areal geology of the western Mojave Desert, California: U.S. Geological Survey Professional Paper 522, 153 p.
- 1981, Regional structure of the Mojave Desert, *in* Howard, K.A., Carr, D.M., Miller, D.M., eds., *Tectonic framework of the Mojave and Sonoran deserts*, California and Arizona: Abstracts from a conference held by the U.S. Geological Survey in Menlo Park, California: U.S. Geological Survey Open-File Report 81-0503, p. 26–28.
- Duell, L.F.W., Jr., 1987, Geohydrology of the Antelope Valley area, California, and design for a ground-water-quality monitoring network: U.S. Geological Survey Water-Resources Investigations Report 84-4081, 72 p.
- Durbin, T.J., 1978, Calibration of a mathematical model of the Antelope Valley ground-water basin, California: U.S. Geological Survey Water-Supply Paper 2046, 51 p.
- Dutcher, L.C., and Worts, G.F., 1963, Geology, hydrology, and water supply of Edwards Air Force Base, Kern County, California: U.S. Geological Survey Open-File Report, 225 p.
- Fram, M.S., Bergouse, J.K., Bergamaschi, B.A., Fujii, Roger, Goodwin, K.D., and Clark, J.F., 2002, Water-quality monitoring and studies of the formation and fate of trihalomethanes during the third Injection, storage, and recovery test at Lancaster, Antelope Valley, California, March 1998 through April 1999: U.S. Geological Survey Open-File Report 02-102, 48 p.
- Freeze, R.A. and Cherry, J.A., *Groundwater*: Prentice-Hall, Inc., Englewood Cliffs, New Jersey, 604 p.

- Galloway, D.L., Hudnut, K.W., Ingebritsen, S.E., Phillips, S.P., Peltzer, G., Rogez, F., and Rosen, P.A., 1998, Detection of aquifer system compaction and land subsidence using interferometric synthetic aperture radar, Antelope Valley, Mojave Desert, California: *Water Resources Research*, v. 34, n. 10, October 1998, p. 2573–2585.
- Galloway, Devin, Jones, David R., and Ingebritsen, S.E., eds., 1999, Land subsidence in the United States: U.S. Geological Survey Circular No. 1182, 175 p.
- Hewett, D.F., 1954, General geology of the Mojave Desert region California, *in* Jahns, R.H., Baily T.L., eds., *Geology of southern California*: Department of Mines and Geology Bulletin 170, Chapter 2, p. 5–20.
- Holzer, T.L., 1981, Preconsolidation stress of aquifer systems in areas of induced land subsidence: *American Geophysical Union, Water Resources Research*, v. 17, n. 3, p. 693–704.
- Howle, J.F., Phillips, S.P., Denlinger, R.P., and Metzger, L.F., 2003, Determination of specific yield and water-table changes using temporal microgravity surveys collected during the second injection storage and recovery test at Lancaster, Antelope Valley, California, November 1996 through April 1997: U.S. Geological Survey Water-Resources Investigations Report 03-4019, 28 p.
- Hsieh, P.A., and Freckleton, J.R., 1993, Documentation of a computer program to simulate horizontal-flow barriers using the U.S. Geological Survey's modular three-dimensional finite-difference ground-water flow model: U.S. Geological Survey Open-file Report 92-477, 32 p.
- Ikehara, M.E., and Phillips, S.P., 1994, Determination of land subsidence related to ground-water-level declines using Global Positioning System and leveling surveys in Antelope Valley, Los Angeles and Kern Counties, California, 1992: U.S. Geological Survey Water-Resources Investigations Report 94-4184, 101 p.
- Ireland, R.L., Poland, J.F., and Riley, F.S., 1984, Land subsidence in the San Joaquin Valley, California, as of 1980: U.S. Geological Survey Professional Paper 437-I, 93 p.
- Izbicki, J.A., Martin, Peter, and Michel, R.L., 1995, Source, movement and age of ground water *in* the upper part of the Mojave River Basin, California, USA, *in* Adar, E.M., and Leibundgut, Christian, eds., *Application of tracers in arid zone hydrology*: International Association of Hydrological Sciences (IAHS) Proceedings and Report series, no. 232, p. 43–56.
- Johnson, H.R., 1911, Water resources of Antelope Valley, California: U.S. Geological Survey Water-Supply Paper 278, 92 p.
- Kennedy/Jenks Consultants, 1995, Antelope Valley water resources study, final report: Kennedy/Jenks Consultants report prepared for the Antelope Valley Water Group, November 1995.
- Law Environmental, 1991, Water supply evaluation, Antelope Valley, California: Palmdale Water District, 49 p., 4 appendices.
- Leake, S.A., and Prudic, D.E., 1991, Documentation of a computer program to simulate aquifer-system compaction using the modular finite-difference ground-water flow model: *Techniques of Water-Resources Investigations of the U.S. Geological Survey*, book 6, chap. A2, 68 p.
- Lee, C.H., 1912, An intensive study of the water resources of a part of Owens Valley, California: U.S. Geological Survey Water-Supply Paper 294, 135 p.
- Lines, G.C., and Bilhorn, T.W., 1996, Riparian vegetation and its water use during 1995 along the Mojave River, Southern California: U.S. Geological Survey Water-Resources Investigations Report 96-4241, 10 p.
- Londquist, C.J., Rewis, D.L., Galloway, D.L., and McCaffrey, W.F., 1993, Hydrogeology and land subsidence, Edwards Air Force Base, Antelope Valley, California, January 1989–December 1991: U.S. Geological Survey Water-Resources Investigations Report 93-4114, 74 p.
- McDonald, M.G., and Harbaugh, A.W., 1988, A modular three-dimensional finite-difference ground-water flow model: U.S. Geological Survey Techniques of Water-Resources Investigations, book 6, chap. A1, 484 p.
- Mabey, D.R., 1960, Gravity survey of the western Mojave Desert, California: U.S. Geological Survey Professional Paper 316-D, p. 51–73.
- Metzger, L.F., Ikehara, M.E., and Howle, J.F., 2002, Vertical-deformation, water-level, microgravity, geodetic, water-chemistry, flow-rate data collected during injection, storage, and recovery tests at Lancaster, Antelope Valley, California, September 1995 through September 1998: U.S. Geological Survey Open-File Report 01-414, 149 p.
- Nishikawa, Tracy, Rewis, D.L., and Martin, Peter, 2001, Numerical model of ground-water flow and land subsidence for Edwards Air Force Base, Antelope Valley, California: U.S. Geological Survey Water-Resources Investigations Report 01-4038.
- Noble, L.F., 1953, Geology of the Pearland quadrangle, California: U.S. Geological Survey Geologic Quadrangle Map GQ-24, scale 1:24,000.

- Orloff, S.B., Hanson, B., and Lanphier, T., 1989, High Desert Irrigation Study, Water application rates for maximum profits: University of California Cooperative Extension, High Desert Research Results, 1989, 7 p.
- Phillips, S.P., Carlson, C.S., Metzger, L.F., Howle, J.F., Galloway, D.L., Sneed, Michelle, Ikehara, M.E., Hudnut, K.W., and King, N.E., in press, Analysis of tests of subsurface injection, storage, and recovery of freshwater in Lancaster, Antelope Valley, California: U.S. Geological Survey Water-Resources Investigations Report 03-4061.
- Ponti, D.J., 1985, The Quaternary alluvial sequence of the Antelope Valley, California: Geological Society of America Special Paper 203, p. 79–96.
- Rantz, S.E., compiler, 1969, Mean annual precipitation in the California region: U.S. Geological Survey Basic-Data Compilation, scale 1:1,000,000, 11 sheets, 5 p.
- Rewis, D.L., 1993, Drilling, construction, and subsurface data for piezometers on Edwards Air Force Base, Antelope Valley, California, 1991–92: U.S. Geological Survey Open-File Report 93-148, 35 p.
- , 1995, Ground-water-level monitoring, basin boundaries, and potentiometric surfaces of the aquifer system at Edwards Air Force Base, California, 1992: U.S. Geological Survey Water-Resources Investigations Report 95-4131, 61 p.
- Sneed, M.R., and Galloway, D.L., 2000, Aquifer-system compaction and land subsidence: measurements, analyses, and simulations—the Holly site, Edwards Air Force Base, Antelope Valley, California: U.S. Geological Survey Water-Resources Investigations Report 00-4015, 65 p.
- Snyder, J.H., 1955, Ground water in California—The experience of Antelope Valley: Berkeley, California, University of California, Division of Agriculture Science, Giannini Foundation Ground-Water Studies No. 2, 171 p.
- Southern California Association of Governments, 2001, Regional transportation plan 2001 growth forecast: accessed May 23, 2001, at URL <http://www.scag.ca.gov/subregion1.pdf/>
- Templin, W.E., Phillips, S.P., Cherry, D.E., DeBortoli, M.L., and others, 1995, Land use and water use in Antelope Valley, California: U.S. Geological Survey Water-Resources Investigations Report 94-4208, 97 p.
- Terzaghi, K., 1925, *Erdbaumechanik auf bodenphysikalischer Grundlage*: Wien, Austria, Deuticke, 399 p.
- Thayer, W.N., 1946, Geologic features of Antelope Valley, California: Los Angeles County Flood Control District Report, 20 p.
- Thomasson, H.G., Jr., Olmsted, F.H., and Le Roux, E.F., 1960, Geology, water resources, and usable ground-water storage capacity of part of Solano County, California: U.S. Geological Survey Water-Supply Paper 1464, 693 p.
- Thompson, D.G., 1929, The Mojave Desert region, California, a geographic, geologic, and hydrologic reconnaissance: U.S. Geological Survey Water-Supply Paper 578, 759 p.
- University of California Cooperative Extension, 1994, Using reference evapotranspiration ( $ET_0$ ) and crop coefficients to estimate crop evapotranspiration for agronomic crops, grasses, and vegetable crops: University of California Cooperative Extension, Division of Agriculture and Natural Resources Leaflet 21427, 12 p.
- Ward, A.W., Dixon, G.L., and Jachens, R.C., 1993, Geologic setting of the East Antelope Basin, with emphasis on fissuring on Rogers Lake, Edwards AFB, Mojave Desert, California: U.S. Geological Survey Open-File Report 93-263, 9p.
- Weir, J.E., Jr., Crippen, J.R., and Dutcher, L.C., 1965, A progress report and proposed test-well drilling program for the water-resources investigation of the Antelope Valley–East Kern Water Agency area, California: U.S. Geological Survey Open-File Report, 134 p.

## APPENDIX: WATER USE 1992–95

Water managers and planners require comprehensive and accurate water-use data to make informed water-management decisions. Templin and others (1995) compiled available water-use data for Antelope Valley for 1919–92 (1992 data were incomplete). For the purpose of this study, annual water-use data for 1992–95 were compiled to extend the period of record reported by Templin and others (1995) for use in the ground-water flow and subsidence model developed for this study.

The methodology, sources, and areal extent [Antelope Valley drainage basin ([fig. 1](#))] used to obtain the water-use data for 1992–95 were consistent with those used by Templin and others (1995) so that data for all years could be compared and analyzed. As a part of their work, Templin and others (1995) developed a database of ground-water pumpage for 1947–92; during this current study, pumpage data for 1992–95 were collected and added to the 1947–92 database.

Some additional data for 1947–91 also were obtained and added to the database. The tables in this appendix include data only for 1992–95, but the graphs show data for the entire period of the pumpage database (1947–95) and, therefore, can show trends in water use over time.

Water supply for Antelope Valley was obtained from four sources; (1) ground-water pumping, (2) local surface-water diversions, (3) imported water, and (4) reclaimed wastewater. Each of these components and total annual water supply for 1947–95 are shown in [figure A1](#). Total water supply increased during 1992–95 because of increases in imported surface water in 1992 and 1993, increases in ground-water pumping in 1994 and 1995, and increased use of reclaimed wastewater. Historically, ground-water pumping has been the primary source of water supply in the valley, and remained the primary source during 1992–95. Supply from local surface-water sources was small and generally remained steady during 1992–95.

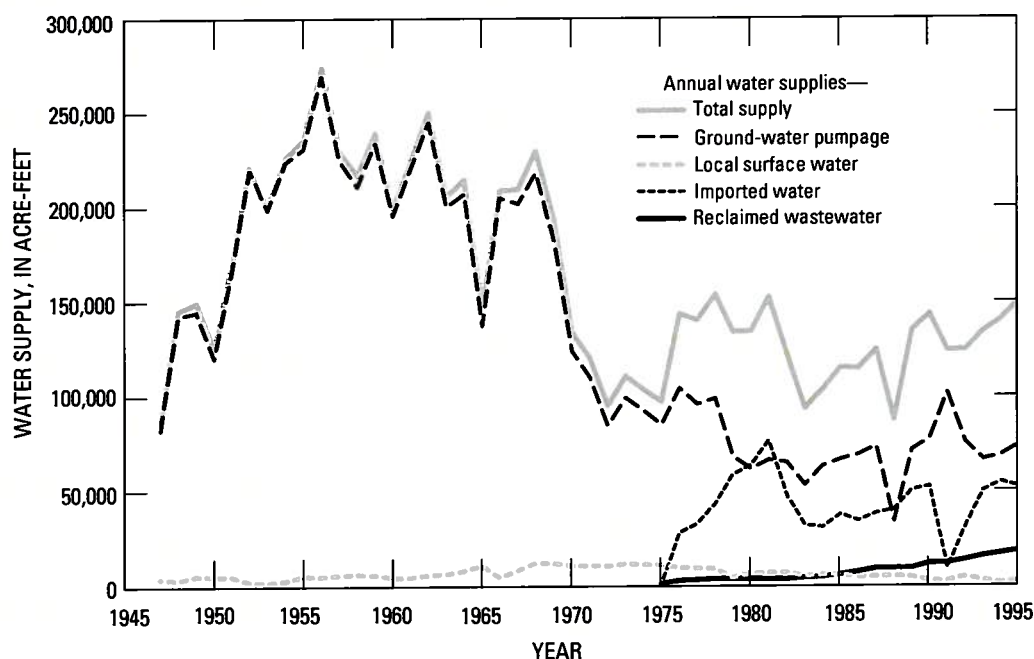


**Figure A1.** Sources of water supply in the Antelope Valley ground-water basin, California, 1947–95.



## Ground Water

Templin and others (1995) divided ground-water use into two categories, public supply and self supply. Ground-water pumpage for public supply represents ground water that is withdrawn by public or private entities for sale and delivery to customers, usually for domestic, commercial, and industrial uses. Ground-water pumpage for self supply represents ground water that is withdrawn by private entities for use by that entity. In Antelope Valley, most ground-water pumpage for self supply is used for agriculture and in this report is referred to as agricultural pumpage. Most of the ground-water-use data for public supply was obtained by contacting the suppliers directly; however, some of the data were obtained from pumpage records maintained by the California State Water Resources Control Board (SWRCB). Agricultural-pumpage data were obtained primarily from the records of the SWRCB, but these records are limited to wells in the Los Angeles County and San Bernardino County parts of Antelope Valley. Because the SWRCB does not

require that agricultural pumpage in Kern County be reported, data for that part of Antelope Valley are nonexistent.

Ground-water pumpage by user is shown in [tables A1](#) (public supply) and [A2](#) (agricultural supply). [Figure A2](#) shows annual ground-water pumpage for the entire period of record (1947–95) in the pumpage database. Note that the agricultural pumping presented in the data base ([figure A2](#)) is less than the agricultural pumpage estimated for this study ([table 8](#)). Templin and others (1995) noted that ground-water pumpage reported to the SWRCB may not accurately reflect actual pumpage in the valley because of evidence of underreporting and overreporting of annual pumpage, reporting of identical amounts of pumpage year after year, and inaccurate methods of estimating pumpage. Also, although agricultural-pumpage data for the Kern County part of the study areas does not exist, the data reported in [table A2](#) are the best available data at the time of this current study. Additional work is needed to improve estimates of the quantity and spatial distribution of agricultural pumpage.

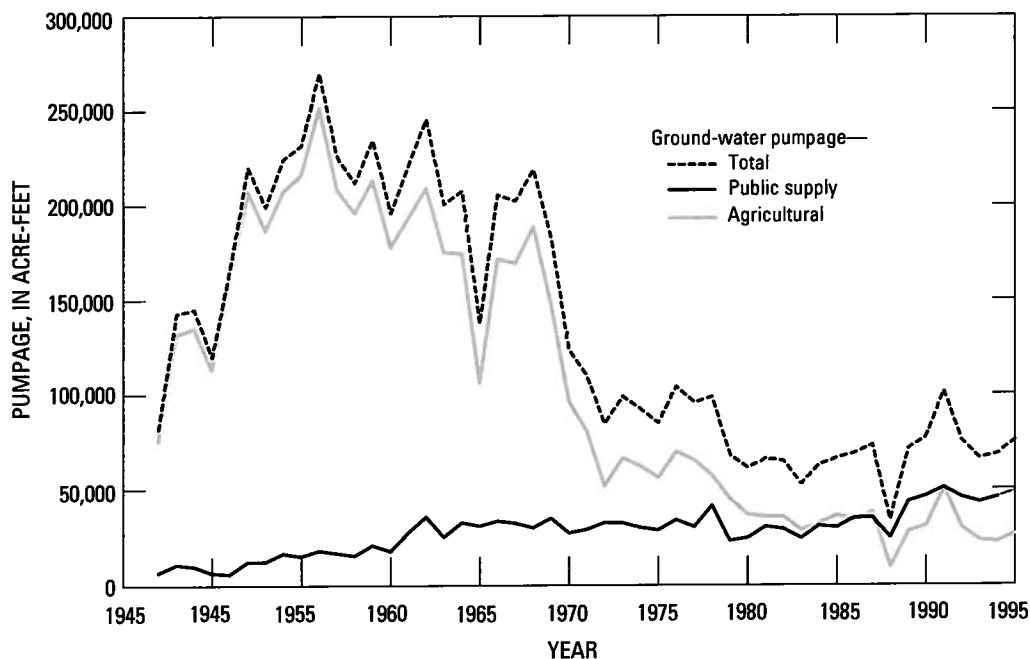


**Figure A2.** Ground-water pumpage recorded in the pumpage database for Antelope Valley, California, 1947–95.

## Surface Water

Water supply from surface water comes from local surface-water diversions and from imported water by way of the California Aqueduct. Imported water provides a much larger proportion of surface-water supply than local surface-water diversions. The availability of imported water is controlled primarily by rainfall conditions in northern California. Minimal local rainfall and limited storage facilities prevent local surface water from becoming a significant component of water supply in Antelope Valley.

### Local Surface Water

Local surface-water diversions are used for public supply and agriculture. Data on local surface-water diversions for public supply were obtained directly from the public supply entities ([table A1](#)). Palmdale Water District was the only user of local surface water for public supply for which data were available during 1992–95 ([table A1](#)).

Data on local surface-water diversions for agricultural supply ([table A2](#)) were obtained from the SWRCB, Division of Water Rights. These data and the self-supplied surface-water data reported by Templin and others (1995) indicate that, for many users, the quantity of reported local surface-water use often is constant over a period of several years. These constant values probably are due to users reporting their water-rights entitlement rather than their actual usage.

### Imported Water

Data on the annual quantity of imported water was obtained directly from the public entities that distribute the water ([table A3](#)). The annual quantity of water imported by the Antelope Valley–East Kern Water Agency (AVEK) represents only those deliveries

made within the study area defined in this report. Imported water averaged about 48,900 acre-ft/yr for 1992–95 ([table A3](#)), which is less than one-third of the annual entitlement of 158,000 acre-ft reported by Templin and others (1995). Imported water is used for both public supply and agriculture.

## Reclaimed Wastewater

Data on water supply from reclaimed wastewater from the Lancaster and Palmdale Water Reclamation Plants (David Lambert, County Sanitations Districts of Los Angeles County, written commun., 1996) are shown in [table A4](#). These two facilities are the largest treatment plants in the study area; there are about 10 additional treatment plants that treat much smaller quantities of wastewater. Templin and others (1995) reported that the Lancaster and Palmdale facilities accounted for 84 percent of the treated wastewater in Antelope Valley in 1990 (a year when data were available for all treatment plants). Discharge of treated wastewater from the Lancaster Water Reclamation Plant used for wetlands ([table A4](#)) is slightly higher than the wastewater discharge shown in [table 1](#) because a small amount of the treated wastewater discharge from the Lancaster Water Reclamation Plant is diverted to a wildlife pond.

The quantity of reclaimed wastewater available for water supply has increased almost every year since 1975 ([fig. A3](#)) due to increases in population and in treatment capacities. In 1995, reclaimed wastewater represented about 12 percent of the total available supply in Antelope Valley. Treated wastewater disposed to land surfaces is subject to evapotranspiration and infiltration to the ground-water system. There is potential for identifying more beneficial uses for this component of reclaimed wastewater.

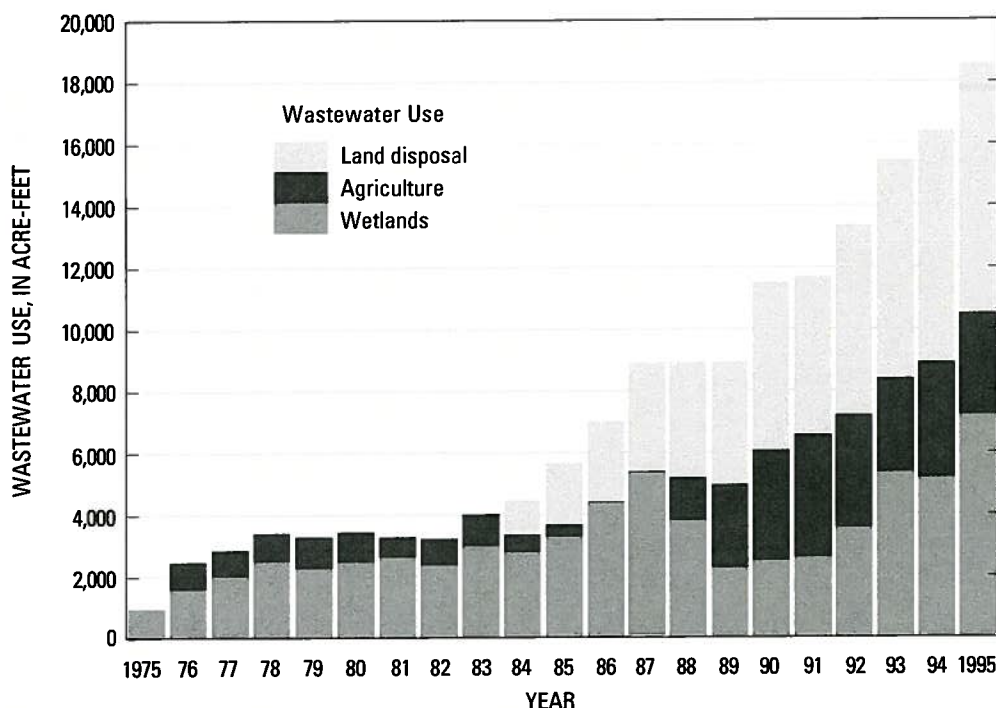


**Figure A3.** Wastewater use in Antelope Valley ground-water basin, California, 1975–95.

Owing to the depth to the water table and the existence of thin aquitards, a time delay is likely between the onset of irrigation and the recharge of this water to the regional water table. Snyder (1955) stated that agricultural recharge probably had reached the water table by the early 1950s, but Durbin (1978) assumed that no irrigation water had reached the water table by 1961. Durbin (1978) based this assumption on water-chemistry data collected from wells in agricultural areas that showed little change in dissolved solids over time. However, it is likely that water had reached the water table much sooner than estimated by Snyder (1955) or Durbin (1978). Results from a simple model of the unsaturated zone indicate that, in a silt loam, recharge will infiltrate to a depth of about 120 ft approximately 10 years after the water is applied at land surface (Alan Flint, U.S. Geological Survey, written commun., 1999).

The largest producers of reclaimed wastewater in the study area are the Palmdale Water Reclamation Plant and the Lancaster Water Reclamation Plant (Templin and others, 1995). Beginning in 1975, reclaimed wastewater has been disposed of in ponds or

on spreading grounds where the water is spread over land surface to evaporate or infiltrate below land surface. A small amount of reclaimed wastewater is reused primarily for agriculture (Templin and others, 1995). The quantity of disposed wastewater to reach the regional water table as recharge was estimated by subtracting the estimated evaporation from the quantity of reclaimed water that is disposed of in the ponds or on spreading grounds. At the Palmdale Water Reclamation Plant, reclaimed wastewater is spread on approximately 60 acres of land. On the basis of a pan evaporation rate of 114 in./yr for Antelope Valley (Bloyd, 1967), it was estimated for this study that about 570 acre-ft/yr is lost to evaporation. At the Lancaster Water Reclamation Plant, wastewater is disposed of in ponds with an area of approximately 430 acres and evaporation was estimated to be about 4,080 acre-ft/yr. The estimated evaporation was subtracted from the quantity of reclaimed wastewater (David Lambert, County Sanitation Districts of Los Angeles County, written commun., 1996) to estimate the recharge to the water table at these sites ([table 1](#)) ([fig. 12](#)).

**Table A1.** Water-use information for public water suppliers in Antelope Valley, California, by water-supply sources, 1992–955

[Units are in acre-feet. USAF, United States Air Force. —, no data]

Year	Antelope Park Mutual Water Company		Antelope Valley Indian Museum		Antelope Valley Union High School District		Antelope Valley Water Company		Aqua J Mutual Water Company Inc.		Averydale Mutual Water Company	
	Ground water	Purchased water	Ground water	Purchased water	Ground water	Purchased water	Ground water	Total	Ground water	Total	Ground water	Total
1992	161.1	0.5	—	569.7	207.0	776.7	53.6	287.8	53.6	287.8	53.6	287.8
1993	149.5	.5	236.0	616.3	176.0	792.3	58.2	296.1	58.2	296.1	58.2	296.1
1994	162.5	.5	238.0	—	171.0	317.6	59.0	317.6	59.0	317.6	59.0	317.6
1995	162.0	.5	—	—	171.0	312.2	64.2	312.2	64.2	312.2	64.2	312.2

Year	Bleiche Flat Mutual Water Company		Boeing (Rockwell) USAF Plant 42		Boron Community Service District		California Poppy Reserve	
	Ground water	Purchased water	Ground water	Purchased water	Ground water	Purchased water	Ground water	Total
1992	17.2	149.6	253.0	253.0	506.0	16.0	16.5	16.5
1993	16.3	80.9	305.0	305.0	610.0	.0	.5	.5
1994	16.9	129.3	—	548.0	548.0	.0	.8	.8
1995	21.0	120.5	—	569.0	569.0	.0	.7	.7

Year	Desert Lake Community Services District		Edgemont Acres Mutual Water Company		Edwards Air Force Base (Main Base)		Edwards Air Force Base (Rocket Site)	
	Ground water	Purchased water	Ground water	Purchased water	Ground water	Purchased water	Ground water	Total
1992	348.0	24.0	372.0	70.0	4,794.2	0.0	4,794.2	431.8
1993	353.0	43.0	396.0	53.0	3,498.8	1,345.0	4,843.8	415.0
1994	—	174.0	174.0	27.0	3,162.3	2,103.0	5,265.3	419.4
1995	—	314.0	314.0	45.0	3,803.8	1,171.0	4,974.8	435.1

Year	El Dorado Mutual Water Company		Evergreen Mutual Water Company		Landale Mutual Water Company		Land Projects Mutual Water Company		Little Baldy Water Company	
	Ground water	Purchased water	Ground water	Purchased water	Ground water	Purchased water	Ground water	Total	Ground water	Total
1992	117.4	186.6	304.0	80.0	0.0	1.0	795.5	21.7	795.5	21.7
1993	195.3	114.8	210.1	81.0	220.7	15.0	782.6	21.7	782.6	21.7
1994	39.6	302.0	341.6	82.0	—	.0	915.4	21.7	915.4	21.7
1995	47.5	297.7	345.2	81.0	—	.0	869.7	—	869.7	—

**Table A1.** Water-use information for public water suppliers in Antelope Valley, California, by water-supply sources, 1992–95—Continued

Year	Littlerock Creek Irrigation District				Lockhead Martin USAF Plant 42			Los Angeles County		Los Angeles County Sheriff Mira Loma Facility	
	Ground water	Surface water	Purchased water	Total	Ground water	Purchased water	Total	Surface water	Ground water		
1992	1,212.0	1,420	251.0	2,882	—	12.0	12.0	8.7	188.7		
1993	1,270.0	1,105	735.0	3,110	74.4	14.3	88.7	8.7	.0		
1994	1,615.0	1,100	1,100.0	3,815	9.3	1.2	10.5	8.7	81.2		
1995	1,630.0	6	480.0	2,116	7.1	.6	7.7	8.7	235.0		

Year	Los Angeles County Waterworks District No. 4				Los Angeles County Waterworks District No. 24			Los Angeles County Waterworks District No. 27	
	Ground water	Surface water	Purchased water	Total	Ground water	Purchased water	Total	Ground water	Surface water
1992	13,771.8		12,691.0	26,462.8	117.3	219.0	336.3	366.8	
1993	13,368.8		16,765.0	30,133.8	66.3	513.0	579.3	196.1	
1994	14,942.9		16,757.0	31,699.9	4.5	579.0	583.5	426.9	
1995	17,782.6		13,850.0	31,632.6	42.8	495.0	537.8	835.6	

Year	Los Angeles County Waterworks District No. 33				Los Angeles County Waterworks District No. 34			Los Angeles County Waterworks District No. 35	
	Ground water	Surface water	Purchased water	Total	Ground water	Purchased water	Total	Ground water	Surface water
1992	0.0	823.0	823.0	823.0	258.5	2,738.0	2,996.5	86.8	161.7
1993	.0	991.0	991.0	991.0	199.3	3,649.0	3,848.3	26.0	240.7
1994	.0	1,049.0	1,049.0	1,049.0	224.0	4,035.0	4,259.0	79.0	217.1
1995	.0	776.0	776.0	776.0	438.3	4,023.0	4,461.3	82.2	219.4

Year	Los Angeles County Waterworks District No. 38				Los Angeles County Waterworks District No. 39			Mojave Public Utility District	
	Ground water	Surface water	Purchased water	Total	Ground water	Purchased water	Total	Ground water	Surface water
1992	200.5	2,068.7	2,269.2	2,269.2	239.0	0.0	239.0	433.0	433.0
1993	264.2	2,248.2	2,512.4	2,512.4	267.1	.0	267.1	78.0	78.0
1994	1,059.5	1,689.0	2,748.5	2,748.5	228.2	20.5	248.7	380.0	380.0
1995	478.8	2,327.8	2,806.6	2,806.6	208.4	.0	208.4	118.0	118.0



**Table A1.** Water-use information for public water suppliers in Antelope Valley, California, by water-supply sources, 1992–95—Continued

Year	North Edwards Water District		Northrop Corporation B-2 Division		Oak Springs Valley Water Company		Palmdale Water District			
	Ground water	Purchased water	Ground water	Purchased water	Ground water	Purchased water	Ground water	Surface water	Purchased water	Total
1992	0.0		138.6		0.0		10,295.0	3,449.0	3,845.0	17,589.0
1993	—		136.9		—		8,209.0	2,538.0	10,136.0	20,883.0
1994	—		128.2		—		11,458.0	1,123.0	8,037.0	20,618.0
1995	—		117.8		—		11,277.0	3,771.0	6,613.0	21,661.0

Year	Palm Ranch Irrigation District			Quartz Hill Water District			Rosamond Community Service District			
	Ground water	Purchased water	Total	Ground water	Purchased water	Total	Ground water	Purchased water	Total	Total
1992	682.0	679.0	1,361.0	1,028.0	1,646.0	2,674.0	1,090.0	877.7	1,967.7	1,967.7
1993	1,151.0	175.0	1,326.0	811.8	1,833.0	2,644.8	1,025.0	1,295.1	2,320.1	2,320.1
1994	962.0	515.0	1,477.0	1,044.6	2,485.0	3,529.6	1,025.0	1,457.7	2,482.7	2,482.7
1995	758.0	736.0	1,494.0	—	2,098.0	2,098.0	826.0	1,632.6	2,458.6	2,458.6

Year	Saddleback Butte State Park		Saint Andrews Priory		San Bernardino County Service Area No. 70L			Shadow Acres Mutual Water Company		
	Purchased water	Ground water	Purchased water	Ground water	Ground water	Surface water	Total	Ground water	Purchased water	Total
1992	0.9	—	—	874.3	874.3	0.0	874.3	3.7	133.0	136.7
1993	.9	—	—	934.9	934.9	.0	934.9	4.0	160.0	164.0
1994	.9	—	—	678.2	678.2	.0	678.2	4.3	154.0	158.3
1995	.9	321.0	321.0	906.8	906.8	.0	906.8	4.6	163.0	167.6

Year	Sunnyside Farms Mutual Water Company			Tierra Bonita Mutual Water Company			U.S. Borax and Chemical Corporation			
	Ground water	Purchased water	Total	Ground water	Purchased water	Total	Ground water	Purchased water	Total	Total
1992	4.6	226.0	230.6	16.9	16.9	1,436.3	1,436.3	595.4	2,031.7	2,031.7
1993	4.6	219.0	223.6	16.9	16.9	1,289.0	1,289.0	705.9	1,994.9	1,994.9
1994	4.6	236.0	240.6	16.9	16.9	386.7	386.7	1,556.0	1,942.7	1,942.7
1995	4.6	242.0	246.6	16.9	16.9	21.5	21.5	2,538.1	2,559.6	2,559.6

**Table A1.** Water-use information for public water suppliers in Antelope Valley, California, by water-supply sources, 1992–95—Continued

Year	West Side Park Mutual Water Company			West Valley County Water District		White Fence Farms Mutual Water Company 2			White Fence Farms Mutual Water Company 3	
	Ground water	Purchased water	Total	Ground water	Ground water	Ground water	Purchased water	Total	Purchased water	Purchased water
1992	230.0	0.0	230.0	141.2	590.4	21.8	612.2	391.0		
1993	176.0	47.0	223.0	141.2	257.5	398.2	655.7	382.0		
1994	96.7	131.2	227.9	165.7	304.9	319.6	624.5	425.0		
1995	238.0	24.0	262.0	153.4	583.5	119.7	703.2	414.0		
<b>Total</b>										
Year	Total			Grand total		Grand total		Grand total		
	Ground water	Purchased water	Surface water	Grand total	Grand total	Grand total	Grand total	Grand total	Grand total	Grand total
1992	46,129.8	3,575.0	28,319.8	78,024.6						
1993	43,571.7	2,664.0	41,903.1	88,138.8						
1994	46,212.6	1,249.0	43,370.1	90,831.6						
1995	49,333.1	3,897.0	38,958.8	92,188.8						

**Table A2.** Water-use information for self-supplied water users in Antelope Valley, California, by water supply sources, 1992-95

[Units are in acre-feet. —, no data]

Year	No owner recorded		Alesso Farms		Almondale Farms		Antelope Valley Country Club			Association of Irrigation Water Users			Bailey, John (Rumar)		
	Ground water	Surface water	Ground water	Surface water	Purchased water	Ground water	Purchased water	Ground water	Total	Purchased water	Ground water	Total	Ground water	Purchased water	Total
1992	84.0	—	0.0	—	725.0	208.0	277.0	488.0	485.0	27.0	488.0	—488.0	—	—	—
1993	160.0	—	—	—	1,102.0	14.6	402.0	—	416.6	31.0	—	—	—	—	—
1994	62.6	—	—	—	1,156.0	—	473.0	—	473.0	27.0	—	—	—	—	—
1995	—	—	—	—	925.0	—	417.0	—	417.0	31.0	—	—	—	—	—

Year	Ball, William and Mildred		Beery Ranch		Bell, Louis and Sandra		Bio Gro Systems, Inc.		Biscaichipy Ranch		Blalock-Eddy Ranch Co.		Blua, Andrew	
	Surface water	Ground water	Purchased water	Total	Surface water	Purchased water	Purchased water	Surface water	Purchased water	Surface water	Ground water	Surface water	Ground water	Surface water
1992	22.4	—	0.0	0.0	63.9	—	—	63.9	—	—	—	312	—	—
1993	22.4	—	845.0	845.0	63.9	—	—	63.9	—	—	—	368	—	—
1994	22.4	—	509.0	509.0	63.9	—	—	63.9	—	—	—	578	—	—
1995	22.4	—	509.0	509.0	63.9	—	—	63.9	—	—	—	916	—	—

Year	Bonnie AC Ranch			Bozgian Ranch			Bryden, Lloyd W.			Buchanan, Virginia			Calandri Ranch		
	Ground water	Surface water	Total	Ground water	Purchased water	Total	Ground water	Surface water	Total	Ground water	Surface water	Total	Ground water	Surface water	Total
1992	0.0	—	0.0	90.0	—90.0	0.0	0.0	0.0	0.0	—	14.5	—	—	—	—
1993	—	—	—	—	—	—	—	—	—	—	—	—	—	—	—
1994	—	—	—	—	—	—	—	—	—	—	—	—	—	—	—
1995	—	—	—	—	972.0	972.0	—	—	—	—	—	—	—	—	—

Year	California Portland Cement Company			California Resources Enterprises, Inc.			Calmat Co.			Cameo Ranching Co.			Carter, Maurice R.			Castronova, Daniel			Caton, Robert and Richard		
	Ground water	Surface water	Total	Ground water	Purchased water	Total	Ground water	Surface water	Total	Ground water	Surface water	Total	Ground water	Surface water	Total	Ground water	Surface water	Total	Ground water	Surface water	Total
1992	0.0	—	0.0	—	—	—	—	—	—	—	—	—	—	—	—	—	—	—	—	—	—
1993	—	166.4	166.4	—	—	—	—	—	—	—	—	—	—	—	—	—	—	—	—	—	—
1994	—	155.6	155.6	—	—	—	—	—	—	—	—	—	—	—	—	—	—	—	—	—	—
1995	—	159.0	159.0	—	—	—	—	—	—	—	—	—	—	—	—	—	—	—	—	—	—

**Table A2.** Water-use information for self-supplied water users in Antelope Valley, California, by water-supply sources, 1992–95—Continued

Year	Christoff, Chris A.	Church of Latter Day Saints	Circle JM Ranch	City Ranch	Clark, Dick	Clayton, Richard, M.	Cole, J.G., and Sons	Coor-Pender, R.L. and Ruth B.	Compton, Alan and Carol (previously Jerome Thompson)
	Ground water	Ground water	Ground water	Purchased water	Purchased water	Ground water	Ground water	Ground water	Surface water
1992	128.0	0.0	0.0	0.0	6.0	0.0	0.0	0.0	3.1
1993	110.0	—	—	.0	6.0	—	—	—	3.1
1994	129.0	—	—	.0	6.0	—	—	—	3.1
1995	129.0	—	—	.0	6.0	—	—	—	3.1

Year	Corpus Canon, and Regina	Davis, Shelton	Delia, Joseph, E.	Derosier, Lionel P. and Particia	Derrick, Olin E.	Dustin, Doug	DVM	EPIC/Smith Development Company	Fabe
	Ground water	Ground water	Ground water	Ground water	Ground water	Ground water	Ground water	Ground water	Purchased water
1992	0.0	0.0	34.3	0.0	0.0	0.0	0.0	0.0	0.0
1993	—	—	45.5	—	—	—	—	—	.0
1994	—	—	65.0	—	—	—	—	—	.0
1995	—	—	45.5	—	—	—	—	—	.0

Year	Freund, Jerry	Frisella, Josef	Fuson	Gagik Galstian, Trustee	Gallin, Leo and Ruth Morton	Gonzales, Avelino and Hazel	Graham, John and others	Grainger, Donald L.	Greco, Connie Marie
	Purchased water	Ground water	Purchased water	Ground water	Ground water	Surface water	Surface water	Ground water	Surface water
1992	1.0	0.0	-230.0	0.0	0.0	0.3	1.1	0.0	0.8
1993	.0	—	.0	—	—	.3	1.1	—	.8
1994	5.0	—	.0	—	—	.3	1.1	—	.8
1995	6.0	—	.0	—	—	.4	1.1	—	.8

Year	Griffen, Laura	Groven, Dennis L.	Harter, Leo A.	Hathaway Ranch	Healy Enterprises Inc.	Hecht, Nathaniel	Hee, Thornton, and Patti	Heiner, David R.
	Ground water	Ground water	Ground water	Ground water	Ground water	Surface water	Ground water	Ground water
1992	0.0	600.0	0.0	0.0	0.0	—	0.0	0.0
1993	—	600.0	—	—	—	—	—	—
1994	—	600.0	—	—	—	—	—	—
1995	—	360.0	—	—	—	0.8	—	—

**Table A2.** Water-use information for self-supplied water users in Antelope Valley, California, by water-supply sources, 1992–95—Continued

Year	Hicks, Lucius B.	Hines, Robert G.	Hughes	Hughes Development Corporation	Hughes, Rodger	Iarussi, Armando	Johnson, Malachi S.	Johnston, Arch D.	Kadivar, Steve
	Ground water	Ground water	Purchased water	Purchased water	Purchased water	Purchased water	Ground water	Ground water	Ground water
1992	0.0	0.0	-99.0	0.0	7.0	2.0	0.0	84.9	0.0
1993	.0	—	.0	.0	21.0	7.0	—	84.9	—
1994	.0	—	.0	.0	23.0	9.0	—	84.9	—
1995	20.0	—	.0	.0	17.0	57.0	—	94.9	—

Year	Kaufman and Broad Land Company			Kellerman, Pat	Kelly Ranch	Kindig, George B.	Kindig, Paul S.	Kirby, James and Robert	Kleksted Tree Farm
	Ground water	Purchased water	Total	Purchased water	Purchased water	Ground water	Ground water	Surface water	Purchased water
1992	0.0	0.0	0.0	6.0	0.0	0.0	0.0	2.9	0.0
1993	—	.0	.0	6.0	.0	.0	.0	2.9	.0
1994	—	.0	.0	6.0	.0	.0	.0	1.0	.0
1995	—	16.0	16.0	7.0	525.0	.0	.0	1.0	.0

Year	Larsen Brothers			Lane, Frank A.			Lowe, John and Becky			Montemayer, Abel and others		
	Purchased water	Ground water	Total	Ground water	Purchased water	Total	Ground water	Purchased water	Total	Ground water	Purchased water	Total
1992	6.0	15.0	6,639.0	0.0	12.0	397.0	31.0	0.0	428.0	0.0	0.0	0.0
1993	6.0	15.0	6,359.8	—	686.0	397.0	43.0	—	440.0	—	.0	.0
1994	6.0	.0	5,343.0	—	15.0	300.0	58.0	—	358.0	—	.0	.0
1995	6.0	.1	7,108.0	—	2,744.0	300.0	39.0	—	339.0	—	.0	.0

Year	Leona Valley Estates Ltd.			Leviste Management Systems	Littlerock Aggregate Company			Llarena, Albert	Los Angeles Department of Airports			Los Angeles Firemen's Relief Assoc.			Margaretten, Joel			Montemayer, Abel and others		
	Purchased water	Ground water	Total	Ground water	Ground water	Ground water	Ground water	Ground water	Ground water	Ground water	Ground water	Ground water	Ground water	Ground water	Ground water	Ground water	Ground water	Ground water	Ground water	Ground water
1992	4.0	0.0	305.0	0.0	0.0	5,097.5	0.0	0.0	0.0	0.0	0.0	0.0	0.0	0.0	0.0	0.0	0.0	0.0	0.0	0.0
1993	.0	.0	305.0	.0	.0	6,376.0	.0	.0	.0	.0	.0	.0	.0	.0	.0	.0	.0	.0	.0	.0
1994	.0	.0	270.0	.0	.0	5,723.0	.0	.0	.0	.0	.0	.0	.0	.0	.0	.0	.0	.0	.0	.0
1995	.0	.0	270.0	.0	.0	6,445.0	.0	.0	.0	.0	.0	.0	.0	.0	.0	.0	.0	.0	.0	.0



**Table A2.** Water-use information for self-supplied water users in Antelope Valley, California, by water-supply sources, 1992–95—Continued

Year	McCormick, Raymond W.	Mescal Creek Water, Inc.	Miccolis, F.P. Adele Bruno	Millford, Terry	Miller, Keith	Mitchel and Gunning	Monsello, Andrew	Morgan, Carlos, Estate of	Morris, Wayne F. and Annetto L.
	Ground water	Surface water	Ground water	Purchased water	Purchased water	Purchased water	Ground water	Ground water	Surface water
1992	0.0	915.8	0.0	6.0	11.0	46.0	0.0	5.0	1.6
1993	—	915.8	—	6.0	10.0	482.0	—	2.0	—
1994	—	1,220.7	—	6.0	11.0	826.0	—	.0	—
1995	—	1,220.7	—	6.0	9.0	851.0	—	.0	—

Year	Mountain Glen Ranch	Mountain High—Holiday Hill Company	Nakasone Development Company	Nebeker Ranch		Nishimoto, Jimmie M.	Nishimoto, Roy	Oakwood Enterprises	Ordway, Ben
	Ground water	Ground water	Ground water	Ground water	Reclaimed water	Total	Ground water	Surface water	Surface water
1992	0.0	0.0	0.0	323.0	3,640.0	3,963.0	0.0	0.0	6.1
1993	—	0.0	—	259.0	2,997.0	3,256.0	—	—	6.1
1994	—	0.0	—	286.0	3,711.0	3,997.0	—	—	6.1
1995	—	0.0	—	240.0	3,226.0	3,466.0	—	—	6.1

Year	Pablo, Mr. and Mrs. Pastor	Peachland Farms	Piani, Gino	Poncedeleon, Modesto	Portanova	Pratt, Dr. W.H.	Proctor, Carl	Pulsipher Enterprises
	Ground water	Purchased water	Ground water	Purchased water	Purchased water	Ground water	Ground water	Purchased water
1992	0.0	288.0	0.0	6.0	0.0	0.0	0.0	8.0
1993	—	264.0	—	6.0	.0	—	.0	9.0
1994	—	436.0	—	7.0	.0	—	.0	12.0
1995	—	339.0	—	9.0	.0	—	.0	11.0

Year	Punchbowl Canyon Water Association	R and M Ranch, Inc.	RR Ranch	Rabinov, David MD	Rancho Corona Del Valle Corporation	Rancho Vista Development	Reca, Dominique	Retlaw Enterprises Incorporated
	Surface water	Ground water	Purchased water	Ground water	Surface water	Purchased water	Ground water	Ground water
1992	27.5	3,950.0	479.0	0.0	31.5	0.0	0.0	6,914.0
1993	27.5	3,567.0	1,194.0	—	31.5	.0	—	1,500.0
1994	27.5	2,837.0	1,357.0	—	31.5	.0	—	2,250.0
1995	27.5	3,674.0	919.0	—	31.5	.0	—	1,800.0

**Table A2.** Water-use information for self-supplied water users in Antelope Valley, California, by water-supply sources, 1992–95—Continued

Year	Ritter and Godde			Robbins, David	Robinson, F. Willard and others	Rosen, Santee	S&D	Sasland Farms Spivak-Brown
	Ground water	Purchased water	Total					
1992	2,275.1	1,124.0	3,399.1	8.0	—	6.0	0.0	0.0
1993	1,139.3	2,316.0	3,455.3	7.0	—	6.0	.0	—
1994	415.6	2,841.0	3,256.6	6.0	—	1.0	.0	—
1995	1,993.0	2,611.0	4,604.0	8.0	—	4.0	.0	—

Year	Schnaidt, Harold			Searcy, Travis	Seiki Investment Corporation	Silva, Don	Simi, Roy	Southern California Edison Company
	Ground water	Purchased water	Total					
1992	—	65.0	65.0	6.0	0.0	10.0	0.0	10.1
1993	—	56.0	56.0	7.0	—	11.0	.0	11.2
1994	—	81.0	81.0	13.0	—	11.0	.0	12.7
1995	—	68.0	68.0	8.0	—	10.0	.0	.0

Year	Stevens, William E.		Sundown Ranch Company		Tapia Brothers	Taunton, Windsor P.	Tejon Ranch		Traweck, S.V.
	Ground water	Purchased water	Ground water	Purchased water			Ground water	Purchased water	
1992	0.0	0.0	0.0	402.0	0.0	0.0	1,006.0	–230.0	776.0
1993	—	.0	—	238.0	—	—	—	.0	.0
1994	—	.0	—	205.0	—	—	—	.0	.0
1995	—	.0	—	795.0	—	—	—	.0	.0

Year	U.S. Forest Service, Angeles National Forest			Union Wilshire Incorporated		Unnamed spring group	Vandereyk	Vaught, Amelia	Wade, Thomas H.	Ward, J.W./Lyman Champlain
	Ground water	Surface water	Total	Ground water	Purchased water					
1992	0.0	24	24	0.0	0.0	18.1	0.0	6.0	0.0	0.0
1993	—	24	24	—	—	18.1	.0	6.0	.0	—
1994	—	24	24	—	—	18.1	.0	7.0	.0	—
1995	—	2.5	2.5	—	—	18.1	.0	6.0	3.3	—

**Table A2.** Water-use information for self-supplied water users in Antelope Valley, California, by water-supply sources, 1992–95—Continued

Year	Weaver	White, J.F. Jr., H.B., and D.B.	White, James B. or Dee Ann	White, Michael G.	White, Richard A.	Williams, Claude	Wilmar Farms	Zamzla, Johnny
	Purchased water	Surface water	Ground water	Ground water	Ground water	Ground water	Purchased water	Ground water
1992	0.0	0.8	0.0	0.0	0.0	0.0	0.0	0.0
1993	.0	—	.0	—	.0	—	1,157.6	—
1994	.0	—	.0	—	.0	—	2,139.0	—
1995	.0	—	24.0	—	5.7	—	2,119.0	—
<b>Total</b>								
Year	Grand total		Grand total		Grand total		Grand total	
	Ground water	Surface water	Purchased water	Grand total	Ground water	Surface water	Purchased water	Grand total
1992	29,925.7	888.5	2,692.0	33,506.2				
1993	23,015.1	.0	8,690.6	31,705.7				
1994	22,437.3	.0	12,833.0	35,270.3				
1995	26,613.7	.0	13,447.0	40,060.7				

**Table A3.** Deliveries of imported water to Antelope Valley from the California Aqueduct, 1992–95

[Units are in acre-feet per year]

Year	Antelope Valley– East Kern Water Agency <sup>1</sup>	Littlerock Creek Irrigation District <sup>2</sup>	Palmdale Water District <sup>3</sup>	Total
1992	27,663	251	3,845	31,759
1993	40,928	735	10,136	51,799
1994	49,536	1,100	8,037	58,673
1995	46,091	480	6,613	53,184

<sup>1</sup>Russell Fuller, Antelope Valley–East Kern Water Agency, written commun., 1998.<sup>2</sup>Brad Jones, Littlerock Creek Irrigation District, written commun., 1996.<sup>3</sup>Matt Knudson, Palmdale Water District, written commun., 1996.**Table A4.** Use of reclaimed wastewater in Antelope Valley, California, 1992–95

[Units are in acre-feet. Data from David Lambert (County Sanitation Districts of Los Angeles County, written commun., 1996)]

Year	Lancaster Water Reclamation Plant			Palmdale Water Reclamation Plant		
	Wetlands	Irrigation	Total	Land disposal	Irrigation	Total
1992	3,520	3,640	7,160	6,150	21	6,170
1993	5,280	3,000	8,280	7,080	42	7,120
1994	5,110	3,700	8,810	7,480	51	7,530
1995	7,140	3,225	10,360	8,070	67	8,140